



UNIVERSIDADE D  
**COIMBRA**

Laura Alexandrina Sequeira Neves

**LINKING MITOCHONDRIAL SRC AND  
HIPPOCAMPAL DENDRITIC CHANGES IN  
ALZHEIMER'S DISEASE**

**Dissertação no âmbito do Mestrado Integrado em Engenharia Biomédica,  
no ramo de Neurociências, orientada pela Professora Doutora Ana  
Cristina Rego e Doutora Sandra Mota**

Fevereiro de 2021



Laura Alexandrina Sequeira Neves

# **LINKING MITOCHONDRIAL SRC AND HIPPOCAMPAL DENDRITIC CHANGES IN ALZHEIMER'S DISEASE**

Thesis submitted to the University of Coimbra  
for the degree of Master in Biomedical Engineering

**Orientador(es):**

Professora Doutora Ana Cristina Carvalho Rego (Faculdade de Medicina da  
Universidade de Coimbra, Centro de Neurociências e Biologia Celular de Coimbra)

Doutora Sandra Mota (Centro de Neurociências e Biologia Celular de Coimbra)

Coimbra, 2021



This work was developed in collaboration with:





Esta cópia da tese é fornecida na condição de que quem a consulta reconhece que os direitos de autor são pertença do autor da tese e que nenhuma citação ou informação obtida a partir dela pode ser publicada sem a referência apropriada.

This copy of the thesis has been supplied on condition that anyone who consults it is understood to recognize that its copyright rests with its author and that no quotation from the thesis and no information derived from it may be published without proper acknowledgement



## **AGRADECIMENTOS**

Agradeço em primeiro lugar às minhas orientadoras. À Professora Doutora Ana Cristina Rego, que sempre foi uma excelente professora e pela oportunidade que me proporcionou ao poder realizar a minha tese no seu grupo de investigação, bem como todo o apoio que demonstrou durante a elaboração da mesma. À Doutora Sandra Mota, por toda a paciência, todo o conhecimento que transmitiu, aprendi imenso, e sobretudo, todo o apoio e ajuda que me deu desde o início deste projecto.

À minha família, à minha mãe por toda a dedicação e amor incondicional, pai por ter sempre uma atitude otimista perante a vida, avó por todos os miminhos. Ao meu avô, deixo um agradecimento com especial saudade pois sempre me inspirou pela sua enorme força de vontade e sábios conselhos, ele sempre dizia “A Laurinha tem que ir estudar para Coimbra” e tinha razão.

Às amigas que me acompanharam neste meu percurso académico em Coimbra. Às mais antigas, que conheço desde o meu ano de calbira, Adriana e a Natália que sempre estiveram comigo a apoiar-me, a rir, a chorar.... Às minha amigas mais recentes, Filipa e Gabriela pelos seus bons conselhos e enorme companheirismo.

A todos os que foram aqui mencionados reitero o meu sincero agradecimento e retribuo a minha amizade e carinho.



## **Abstract**

Alzheimer's disease (AD) is a neurodegenerative disease for which the main histological hallmarks are senile plaques composed of beta-amyloid peptide (A $\beta$ ) and neurofibrillary tangles (NFTs) resulting from hyperphosphorylated tau. A $\beta$ <sub>1-42</sub> oligomers (A $\beta$ O<sub>1-42</sub>) constitute the most synaptotoxic form of A $\beta$ . Previous studies suggest that both mitochondrial and synaptic dysfunction precede A $\beta$  and NTF deposition. Thus, the decline in mitochondrial function and dynamics may affect Ca<sup>2+</sup> homeostasis, therefore, glutamatergic synapses and spine dynamics. The protein Src, a tyrosine kinase, is located in mitochondria and regulates their activity. In this study, using primary mouse hippocampal neuron cultures, we evaluated the role of Src in A $\beta$ O<sub>1-42</sub>-induced changes in dendritic mitochondrial function and dynamics and the correlation with synaptic plasticity by evaluating spine dynamics.

We evidenced that acute treatment with A $\beta$ O<sub>1-42</sub> affected mitochondrial movement by decreasing the percentage of time of mitochondria in pause, increasing the retrograde and anterograde movement and increasing mitochondrial switch. Interestingly, acute treatment with A $\beta$ O<sub>1-42</sub> promoted mitochondrial fragmentation, an effect prevented by pre-treatment with SU6656, a Src inhibitor, and MK-801, a selective inhibitor of N-methyl-D-aspartate receptors (NMDAR), suggesting that A $\beta$ -induced mitochondrial fragmentation occurs in a Src- and NMDAR-dependent manner. Interestingly, A $\beta$ O<sub>1-42</sub>-induced changes in mitochondrial movement and morphology were accompanied by an increase in mitochondrial Ca<sup>2+</sup>, also prevented by SU6656. In addition, acute and prolonged treatment with A $\beta$ O<sub>1-42</sub> induced a reduction in spine length and an increase in the width/length ratio of spines suggesting spine enlargement and maturation, prevented by Src inhibition.

Altogether, data suggest that Src is a potential candidate to slow down the progression of AD due to its effect on mitochondrial morphology and function, rather than modulation of mitochondrial movement.

**Keywords:** Alzheimer's disease, A $\beta$ O<sub>1-42</sub>, Src, Ca<sup>2+</sup> homeostasis, dendritic spines



## **Resumo**

A doença de Alzheimer (DA) é uma doença neurodegenerativa cujas principais marcas histológicas são placas senis compostas pelo peptídeo beta-amilóide (A $\beta$ ) e emaranhados neurofibrilares (NFTs) resultantes de tau hiperfosforilada. Os oligómeros A $\beta$ O<sub>1-42</sub> (A $\beta$ O<sub>1-42</sub>) constituem a forma mais sinaptotóxica de A $\beta$ . Estudos anteriores sugerem que as disfunções mitocondrial e sináptica precedem a deposição de A $\beta$  e NTF. Assim, o declínio da função e dinâmica mitocondrial pode afetar a homeostasia do Ca<sup>2+</sup>, portanto, das sinapses glutamatérgicas e a dinâmica da espícula. A proteína Src, uma tirosina quinase, está localizada na mitocôndria e regula a sua atividade. Neste estudo, usando culturas primárias de neurónios de hipocampo de murganho, avaliamos o papel da Src nas alterações induzidas pelo A $\beta$ O<sub>1-42</sub> na função e dinâmica mitocondrial dendrítica e a correlação com a plasticidade sináptica avaliando a dinâmica da espícula.

Evidenciamos que o tratamento agudo com A $\beta$ O<sub>1-42</sub> afetou o movimento mitocondrial, diminuindo a percentagem de tempo das mitocôndrias em pausa, aumentando o movimento retrógrado e anterógrado e aumentando switch mitocondrial. Curiosamente, o tratamento agudo com A $\beta$ O<sub>1-42</sub> promoveu a fragmentação mitocondrial, efeito prevenido pelo pré-tratamento com SU6656, um inibidor da Src, e MK-801, um inibidor seletivo dos receptores N-metil-D-aspartato (NMDAR), sugerindo que a fragmentação mitocondrial induzida pelo A $\beta$  ocorre de maneira dependente da Src e NMDAR. Curiosamente, as alterações induzidas pelo A $\beta$ O<sub>1-42</sub> no movimento mitocondrial e na morfologia foram acompanhadas por um aumento no Ca<sup>2+</sup> mitocondrial, também evitado pelo SU6656. Além disso, o tratamento agudo e prolongado com A $\beta$ O<sub>1-42</sub> induziu uma redução no comprimento da espícula e um aumento na proporção largura / comprimento das espículas, sugerindo aumento e maturação da espícula, evitado pela inibição da Src.

De um modo geral, os dados sugerem que a Src é um potencial candidato a desacelerar a progressão da AD devido ao seu efeito na morfologia e função mitocondrial, ao invés da modulação do movimento mitocondrial.

**Palavras-Chave:** Doença de Alzheimer, A $\beta$ O<sub>1-42</sub>, Src, homeostasia do Ca<sup>2+</sup>, espículas dendríticas



## **ABBREVIATIONS and ACRONYMS**

**a. a.** - Amino acids

**AD**- Alzheimer's disease

**AICD** – APP intracellular domain

**AKAP121** - Kinase Anchor Proteins 121

**AMPA** -  $\alpha$ -Amino-3-hydroxy-5-methyl-4-isoxazolepropionic acid receptor

**apo-CaM** -  $\text{Ca}^{2+}$ -free-calmodulin form

**APOE** -Apolipoprotein E

**APP** -  $\beta$ -Amyloid precursor protein

**A $\beta$**  –  $\beta$ -Amyloid peptide

**A $\beta$ O** - A $\beta$  oligomers

**BACE1** -  $\beta$ -Site APP cleaving enzyme 1( $\beta$  -secretase)

**CaM** - Calmodulin

**CaMKII** - Calcium/calmodulin-dependent kinase II

**cAMP**- Cyclic adenosine monophosphate

**CAM** - Cell adhesion molecule

**CCCP**- Carbonyl cyanide m-chlorophenylhydrazone

**CNS** - Central nervous system

**Cof1**- Cofilin-1

**COX**- Cytochrome c oxidase

**CREB** - cAMP response element-binding protein

**CSF** - Cerebrospinal fluid

**Dok-4** -Downstream of tyrosine kinase 4

**DRPs** - Dynamin-related proteins

**ECM** - Extracellular matrix

**EM** - Electron microscope

**ER** - Endoplasmic reticulum

**FAD**- Familial forms of AD

**fMRI** - Functional magnetic resonance imaging

**GRIP1** - Glutamate receptor interaction protein 1

**GSK3 $\beta$**  - Glycogen synthase kinase-3  $\beta$

**IMM**- Inner mitochondrial membrane

**iRNA** – Interference RNA

**IP3** - Inositol-1,4,5-trisphosphate

**K(ATP) channel** - ATP-sensitive potassium channel

**KIFs** - Kinesins gene family

**LTP** - Long Term Potentiation

**MCU**- Mitochondrial calcium uniporter

**mGluRs**- Metabotropic glutamate receptors

**MAM**- Mitochondrial associated membrane

**Mfn** - Mitofusins

**mPTP** - Mitochondrial permeability transition pore

**mtDNA**- Mitochondrial DNA

**MTs** - Microtubules

**NDUFV2** - NADH dehydrogenase [ubiquinone] flavoprotein 2, mitochondrial

**NFTs** - Neurofibrillary tangles

**Ng**- Neurogranin

**NL** - Neuroligin

**NMDAR** - N-methyl-D-aspartate receptor

**OMM** - Outer mitochondrial membrane

**OPA1** - Optic atrophy protein 1

**OXPHOS** - Oxidative phosphorylation

**p-Cof1** –Phosphorylated Cofilin

**PET** - Positron emission tomography

**PKC** - Protein kinase C

**PLC $\gamma$**  - Phospholipase C $\gamma$

**PS1** - Presenilin-1

**PS2** - Presenilin-2

**PSD** - Postsynaptic density

**PTPD1** - Protein tyrosine phosphatase D1

**sAPP $\alpha$**  - Secreted APP $\alpha$

**SKF** - Src kinase family

**TGN** - Trans-Golgi-network

**VDAC**- Voltage-dependent anion channel

**$\Delta\Psi$**  - Electrical transmembrane potential

**$\Delta\Psi_m$**  - Mitochondrial transmembrane potential

**$\Delta pH$**  – Proton gradient

## **MOLECULAR FORMULA and SYMBOLS**

**$^{18}F$ -fluorodeoxyglucose** -FDG

**C11-PiB** - Pittsburgh compound B (PiB) [ $^{11}C$ ] N-methyl [ $^{11}C$ ] 2-4'methylaminophenyl)-6-hydroxy-benzothiazole

**Ca $^{2+}$**  - Calcium ion

**H $^{+}$**  - Proton

**Mg $^{2+}$**  - Magnesium ion

**Na $^{+}$**  - Sodium ion

**Ser**- Serine

**Tyr**- Tyrosine

**P-tau181** - Tau phosphorylated at threonine 181

**T-tau**- Total Tau



# **TABLE OF CONTENTS**

AGRADECIMENTOS.....	i
Abstract .....	iii
Resumo .....	v
ABBREVIATIONS and ACRONYMS.....	vii
MOLECULAR FORMULA and SYMBOLS .....	ix
TABLE OF CONTENTS.....	xi
LIST OF FIGURES .....	xiii
CHAPTER I – INTRODUCTION .....	1
1.1.1 General Features.....	2
1.1.2 Histopathology of AD .....	3
1.2.Synaptic plasticity.....	7
1.2.1 General Features.....	7
1.2.2 Dendritic spine changes in synaptic plasticity.....	9
1.2.3 Impaired synaptic plasticity in AD.....	12
1.3. Mitochondria.....	14
1.3.1 General features .....	14
1.3.2 Mitochondrial transport and dynamics.....	16
1.3.3 A $\beta$ induced mitochondrial dysfunction in AD .....	21
1.4 The tyrosine kinase protein Src .....	23
1.4.1 General features .....	23
1.4.2 Src and mitochondria .....	26
1.4.3 Src at glutamatergic synapses .....	27
1.4.4 Src kinase in AD .....	29
1.5 Objectives .....	30
CHAPTER II – MATERIALS AND METHODS.....	33
2.1 Materials.....	34

2.2 Primary Hippocampal Cultures .....	34
2.3 A $\beta$ O <sub>1-42</sub> Preparation .....	35
2.4 Cell Transfection .....	35
2.5 Live-Cell Imaging-Calcium Fluorescence.....	36
2.6 Mitochondrial Movement Analysis .....	37
2.7 Morphology Analysis .....	37
2.8 Spine Morphology Analysis .....	39
2.9 Statistical Analysis.....	39
CHAPTER III – RESULTS .....	41
3.1 A $\beta$ O <sub>1-42</sub> alters neurite mitochondrial movement in mature hippocampal neurons – influence of Src .....	42
3.2 A $\beta$ O <sub>1-42</sub> impact on neurite mitochondrial morphology in a Src dependent manner .....	46
3.3.A $\beta$ O <sub>1-42</sub> induce decrease mitochondrial Ca <sup>2+</sup> retention in hippocampal neurites	48
3.4 A $\beta$ O <sub>1-42</sub> seem to induce a fast increase in mushroom spine content in hippocampal dendrites dependent on Src .....	50
CHAPTER IV – DISCUSSION AND CONCLUSIONS .....	53
4.1 Discussion.....	54
4.2 Conclusions.....	57
REFERENCES .....	59

## **LIST OF FIGURES**

Figure 1-Pathway of APP through non-amyloidogenic and amyloidogenic pathways. ....	4
Figure 2-Model for LTP induction.....	9
Figure 3-Dendritic spine structure. ....	10
Figure 4-ATP formation through mitochondrial OXPHOS.....	15
Figure 5-Two models of Ca <sup>2+</sup> recruitment of mitochondria in a Miro adaptor-dependent manner. ....	19
Figure 6-Representation of main mitochondrial mechanisms potentially affected in AD onset.....	22
Figure 7-c-Src activation mechanism. ....	25
Figure 8- Src kinase is an up regulator of NMDAR activity enhancing LTP induction ..	28
Figure 9-Main steps of MitoProtAnalyser a macro for FIJI/imageJ. ....	38
Figure 10-Mitochondrial distribution parameters and respective kymographs following exposure to A $\beta$ O <sub>1-42</sub> . in hippocampal neurons.....	43
Figure 11-Mitochondrial movement parameters in hippocampal neurons treated with A $\beta$ O <sub>1-42</sub> .....	45
Figure 12-Mitochondrial morphology evaluation in mature hippocampal neurons exposed to A $\beta$ O <sub>1-42</sub> . ....	47
Figure 13-Mitochondrial Ca <sup>2+</sup> levels assessed using CEPIA3mt plasmid in mature hippocampal neurons treated with A $\beta$ O <sub>1-42</sub> .....	49
Figure 14-Dendritic spines morphology in mature hippocampal neurons treated with A $\beta$ O <sub>1-42</sub> .....	51

## **List of Tables**

Table 1-Spine classification according to the head, length and width.....	39
---	----



# **CHAPTER I – INTRODUCTION**

## **1.1 Alzheimer's Disease**

### **1.1.1 General Features**

In 1906, Doctor Alois Alzheimer reported the autopsy results of Auguste Deter, a 55-year-old woman, struggling with severe memory loss, disorientation, hallucinations, and aggressive behaviour. This was the first described case of what years later would be known as AD. AD is a neurodegenerative disease and one of the most common causes of dementia worldwide, accounting to 60% to 80% of cases and affecting 47 million people worldwide. In 2030 it is estimated that the population affected with AD will be around 74.7 million and in 2050 around 131.5 million (Du et al., 2018). Moreover, women present a higher susceptibility of developing the disease, which can be explained by their longer average lifespan and the hormonal influence (Janicki and Schupf. 2010). AD is characterized by a decline in a vast number of domains such as memory, language, personality, and behaviour (Crous-Bou et al., 2017). Mild memory impairment or mild cognitive impairment is commonly the first early symptom detected in AD patients (pre-AD), frequently associated with neurodegeneration in the hippocampus, a structure strongly involved in memory formation (Gold, Carl A, and Andrew 2008). Spreading of the disease throughout the cortex and the rest of the brain, symptoms worsen (e.g. speaking difficulty, swallowing, and walking) and the typical life expectancy following diagnosis is three to nine years. Importantly, AD onset is thought to start in the brain 20 years or more before appearing the first clinical symptoms of AD (Bateman et al., 2012), defined as hippocampal atrophy and memory impairment (Villemagne et al. 2010). Furthermore, decreases in synaptic density, activity, and function appear in the earliest stages of the disease, preceding neurodegeneration (Boisvert et al., 2018), although the molecular pathways involved are not fully understood.

AD cases may be divided in two groups: familial forms of the disease (FAD, standing for 'Familial AD), also named early-onset AD (onset before 65 years of age), accounting for only 2 to 5% of total cases (Blennow, et al., 2006), and the non-hereditary form or sporadic form of AD. FAD have been associated with almost 270 mutations in three genes codifying for  $\beta$ -amyloid precursor protein (APP), presenilin-1 and presenilin-2 (PS1, PS2) (Giau et al., 2019). Cleavage of APP through the amyloidogenic pathway (described in section 1.1.2) leads to the formation of  $\beta$  amyloid protein ( $A\beta$ ), while PS1 and PS2 are both subunits of the  $\gamma$ -secretases (part of the APP cleavage machinery), being PS1 associated with plasma membrane targeting and PS2 with trans-Golgi network targeting (Meckler and Checler, 2016). The causes of sporadic or late AD are poorly understood; however, environmental, and genetic factors have been identified as

major risk factors for developing AD. Late-onset AD is strongly linked to aging and apolipoprotein E4 (*APOE4*) polymorphism. APOE is a 299 amino acid protein (~34 kDa) encoded by the *APOE* gene, located in chromosome 19 (Mahley, 1988). This protein is responsible for cholesterol transport in the bloodstream, which is extremely abundant in the Lipid Rafts and it influences membrane's fluidity, protein trafficking and, synaptic transmission (Korade and Kenworthy, 2008). Lipid Rafts constitute a fundamental platform for APP to find its cleaving enzymes and to form the A $\beta$  peptide, thus a depletion of cholesterol affects A $\beta$  production and has also been associated with impaired synaptic transmission (Jeong et al., 2019). In this sense, *APOE* is particularly important in the central nervous system (CNS) to sustain the neuronal circuit health. The *APOE* gene possesses three alleles, namely  $\epsilon$ 2,  $\epsilon$ 3, and  $\epsilon$ 4, being the later correlated with a higher risk of developing AD (Stocker, et al., 2018), whereas  $\epsilon$ 2 allele appears to have a "protective" effect against AD onset (Holtzman et al., 2012). All three isoforms interact with A $\beta$  peptide, promoting its fibrillation, although this interaction is notably amplified by  $\epsilon$ 4 allele (Ma et al., 1994), which stimulates the rate of A $\beta$  aggregation (Castano et al., 1995; Wisniewski et al., 1994) and, therefore, formation of senile plaques, being one of the greatest risk factors in AD onset. Beyond genetics, epigenetics also plays a key role in AD onset, particularly, changes in DNA methylation, chromatin remodelling, histone modifications, and non-coding RNA regulation (Liu et al., 2018). Finally, aging and particularly brain aging is an important risk factor for sporadic AD. Thus, age-associated molecular modifications, including reduced proteostasis, mitochondrial dysfunction, cellular senescence, stem cell exhaustion and/or lack of cellular communication contribute for increasing brain susceptibility to AD (Hou et al., 2019).

### **1.1.2 Histopathology of AD**

The autopsy of Auguste Deter evidenced the presence of two distinctive hallmarks in patient's brain: intracellular NFTs and extracellular amyloid plaques. NFTs are mainly composed of aggregated hyperphosphorylated Tau (Anand et al., 2014; Weller et al., 2017), while extracellular amyloid plaques, or senile plaques, and are mainly composed of aggregated A $\beta$  peptide (Crane et al., 1991). Both proteinaceous accumulations are considered as the two main histological hallmarks of AD.

A $\beta$  is a peptide composed by 38 to 43 amino acids (a. a.) derived from APP proteolysis, an important transmembrane protein. Previous studies in transiently transfected cell lines showed that APP plays a fundamental physiological role as a modulator of cell growth,

motility and neurite outgrowth (O'Brien and Wong, 2011; Tiwari et al., 2019). This protein is mainly localized in postsynaptic densities (PSDs) being critical for neural survival, neurite growth, synaptogenesis, and synaptic plasticity. There are multiple alternative pathways for APP proteolysis, not all leading to A $\beta$  generation. Briefly, full-length APP (Selkoe et al., 1988) is synthesized in the endoplasmic reticulum (ER) and then transported through the Golgi apparatus towards the trans-Golgi-network (TGN). APP is then transported to the cell surface or internalized via an endosomal compartment. On the cell surface, APP is proteolytically cleaved by an  $\alpha$ -secretase followed by a  $\gamma$ -secretase, generating a secreted APP $\alpha$  (sAPP $\alpha$ ), the P3 fragment and the APP intracellular domain (AICD) (Zhang et al., 2011), through the non-amyloidogenic pathway (Sisodia, 1992). When the first cleavage is processed, after APP endocytosis, in the amyloidogenic pathway by  $\beta$ -secretase, also known  $\beta$ -site APP cleaving enzyme 1 (BACE1) it generates sAPP $\beta$  and C99. Then, C99 is cleaved by  $\gamma$ -secretases forming AICD peptide and A $\beta$  peptide (Xu et al., 1997; Kuentzel et al., 1993; Chen et al 2017). At the end, A $\beta$  may be either degraded in the lysosome or transported into the extracellular space (Wang et al., 2016). **(Figure 1).**

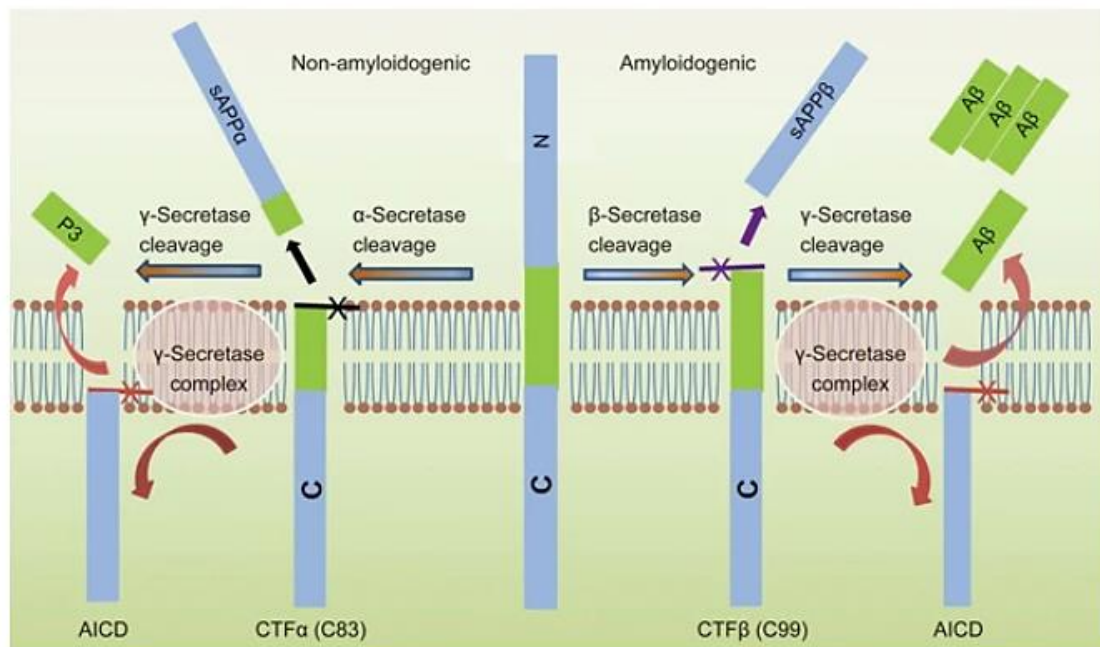


**Figure 1-Pathway of APP through non-amyloidogenic and amyloidogenic pathways.** In the non-amyloidogenic pathway, APP is cleaved by  $\alpha$ - and  $\gamma$ -secretases forming sAPP $\alpha$ , P3 and AICD. In contrast, in the amyloidogenic pathway, APP is sequentially cleaved by  $\beta$ - and  $\gamma$ -secretases, forming sAPP $\beta$ , AICD peptide and A $\beta$  monomers which tend to aggregate into oligomers and fibrils forming the A $\beta$  plaques (Chen et al., 2017)

Interestingly, synaptic activity promotes APP processing and generation of A $\beta$ , which may sustain long-term potentiation (LTP) in healthy brain conditions (Benarroch, 2018). A $\beta$  variants are determined by the peptide cleavage site, being A $\beta$ 40 the preponderant species, accounting for about 90% of peptide species (Citron et.al, 1996). Conformation, self-assembly, and aggregation of A $\beta$  peptide is influenced by the sequence of its a.a. (Lovas and Lyubchenko 2013). Thus, A $\beta$ 42 is significantly more amyloidogenic than A $\beta$ 40 due to the presence of two extra hydrophobic a.a. located at the C-terminus, being preferentially deposited in extracellular space (Gu and Guo, 2013). Peptide aggregation is a result of protein misfolding, where the conformational changes from random coil or  $\alpha$ -helix to  $\beta$ -strands are maximized by hydrophobic conformation (Tycko, 2003). A $\beta$  monomers suffer aggregation, forming soluble structures called A $\beta$  oligomers (A $\beta$ O), consisting of misfolded A $\beta$  (ranging from dimers to dodecamers) that rapidly spread throughout the brain (Wu et al., 2010). Furthermore, A $\beta$  aggregation can also result in A $\beta$  fibrils, which are elongated protofibrils resulting from the polymerization of either A $\beta$ 42 or A $\beta$ 40, in a process that is regulated by the temperature and ionic strength, (Harper et al., 1999) and that further mature to form insoluble fibril aggregates or amyloid plaques, that widely accumulate in areas of the brain dedicated to cognitive function, such as the hippocampus.

The Amyloidogenic Hypothesis was firstly proposed by John Hardy and David Allsop in 1992, postulating that large A $\beta$  aggregates constitute the main triggers of neurotoxicity and dementia in AD (Hardy and Allsop, 1992). Importantly, several studies have demonstrated that A $\beta$ -derived toxins in the form of soluble A $\beta$ O appear to have more neurotoxic effects than the insoluble plaque structure itself. Thus, in mouse brain slices cultures exposure to A $\beta$ O for 45 min is induced a complete blockage of LTP (Lambert et al., 1998). Moreover, data obtained in the mouse model Tg2576 that develops plaque pathology and behavioural deficits at 9 months of age evidenced that A $\beta$ O are responsible for memory impairments and not the larger insoluble aggregates (Larson ME and Lesné, 2012). Similar observations have been done in APP transgenic mice model brains showing abnormal alterations in synaptic proteins correlated with cognitive impairment and A $\beta$ O accumulation (Pham, 2010). Thus, a more recent hypothesis, the A $\beta$ O hypothesis, has suppressed the Amyloidogenic Hypothesis (Selkoe and Hardy, 2016), focusing on the oligomer-induced rupture in synaptic plasticity as the main trigger of memory impairment observed in AD.

Tau is a microtubule-associated protein that acts as strengthening lateral interactions between protofilaments, regulating their dynamics and stability (Daun et al. 2017), and

that also participates in dendritic and axonal transport. This protein is abnormally phosphorylated in approximately 30 sites in AD, mainly through the intervention of glycogen synthase kinase-3 $\beta$  (GSK3 $\beta$ ) (Avila, 2018). Although not all phosphorylation sites are involved in the formation of toxic forms of tau protein, the Ser-199/202/205, Thr-212, Thr-231/Ser-235, Ser-262/356, and Ser-404 sites seem to be especially critical for AD onset (Alonso et al., 2004). Evidences obtained in the mouse model P301S of Tau pathology and in the brain of AD patients evidences that Tau protein spreads throughout the brain in a prion-like way (Laurent, et al., 2018). Importantly, the injection of Tau oligomers into the brain of wild-type mice is enough to induce cognitive, synaptic, and mitochondrial impairment (Shafiei et al., 2017). Interestingly, the ratio A $\beta$ <sub>42/40</sub> rather than total A $\beta$  levels, seems to be more impacting in Tau aggregation, where a higher ratio A $\beta$ <sub>42/40</sub> triggers Tau pathology (Kwak et al., 2020). Furthermore, A $\beta$  and Tau appear to cooperate synergistically in particular, localized A $\beta$  deposits can cause long-distance effects on grey matter, namely volume reduction, which seems to be mediated by tau protein spreading (Iaccarino, et al., 2017).

The levels of A $\beta$  and Tau content in the brain of AD patients used in combination with neurological evaluation and neuroimaging techniques are commonly used to diagnose and follow up AD patients. Levels of A $\beta$ <sub>1-42</sub>, total Tau (T-Tau), and Tau phosphorylated at threonine 181 (P-Tau181) in the cerebrospinal fluid (CSF) are used as AD biomarkers. Interestingly, levels of tau protein are two to three times higher in CSF from AD patients than in healthy controls, while A $\beta$  levels are 40% lower (Shaw et al., 2007). In this sense, CSF A $\beta$ <sub>1-42</sub> levels inversely correlate with total A $\beta$  load in the brain, while CSF tau correlates with results of immunohistochemistry for hyperphosphorylated tau in the brain of patients with AD (Tapiola et al., 2009), implicating an undergoing cell death process. CSF A $\beta$ <sub>1-42</sub>/A $\beta$ <sub>1-40</sub> ratio appears to be more efficient in AD prediction than the total A $\beta$  content only (Niemantsverdriet et.al, 2017). Using Positron emission tomography (PET) imaging, it is possible to access AD-associated metabolic patterns and key proteins in the brain. Thus, 18F-fluorodeoxyglucose (FDG) tracer is used to collect information regarding brain metabolism since glucose metabolism has been correlated with A $\beta$  deposits in AD (Mao et al., 2011). AD neuroinflammation is an important process related to the deposition of A $\beta$  plaques process, which can occur in both the grey matter and the white matter. Interestingly, when assessing white matter glucose metabolism significantly higher levels are observed in AD patients than in healthy subjects (Jeong et al., 2017). Furthermore, <sup>18</sup>F-flortaucipir (conventionally [<sup>18</sup>F] AV1451 or [<sup>18</sup>F] T807) is used to evaluate hyperphosphorylated Tau filaments and C11-PiB to assess A $\beta$  plaques, providing a link between amyloid plaques and modifications in brain structure and

function in AD (Laforce et al., 2018; Cohen and Rabinovici, 2012). Moreover, using multimodal neuroimaging, combining PET with functional magnetic resonance (fMRI), it is possible to establish a relationship between protein deposits in AD patients' brains (A $\beta$  and Tau proteins) and brain activity. Thus, this combined approach has evidenced that cortical A $\beta$  load is associated with disruption of functional connectivity in the brain (Song et al., 2015) and that Tau spreads across synaptic connections in an activity-dependent manner, where AD subjects show faster Tau accumulation than controls (Franzmeier et al., 2020).

## **1.2. Synaptic plasticity**

### **1.2.1 General Features**

Santiago Ramón y Cajal was the first to discover the existence of a discontinuity between neurons (Cajal, 1904); later, other investigators reported that neurons were able to communicate through these discontinuities (specialized junctions) and classified it as synapses. Tripartite synaptic structures constitute the fundamental units of neurotransmission, being composed of two separated pre- and postsynaptic components (which can be either an axon, dendrite, or soma) and adjacent astrocytes. Synapses hold chemical and electrical transmission signals, being classified as either excitatory or inhibitory. Most inhibitory synapses take place in cell bodies and dendritic shafts and excitatory synapses take place in dendritic spines (Arikath, 2012).

Synaptic plasticity is defined as the ability of the nervous system to change its neural activity, therefore transmission, as a response to experience, in this sense it plays a fundamental role in memory formation. Postsynaptic plasticity is a result of changes in the number and properties of postsynaptic receptors, whereas presynaptic plasticity occurs after an increase or decrease in the release of neurotransmitters. Moreover, postsynaptic plasticity is strongly associated with the activity of glutamatergic synapses in different brain regions (Pinky and Parsons, 2018), being highly abundant in the hippocampus. Glutamate is the main excitatory neurotransmitter in the nervous system and glutamatergic receptors are classified as either metabotropic (G protein-coupled) or ionotropic (ion channel-associated). Ionotropic receptors play a crucial role in glutamatergic synapses since they are faster in neurotransmission due to the flux of calcium (Ca<sup>2+</sup>) and sodium (Na<sup>+</sup>) ions. There are three types of ionotropic receptors:  $\alpha$ -

amino-3-hydroxy-5-methyl-4-isoxazolepropionic acid receptor (AMPA), kainate receptor, and NMDAR. NMDAR are in the postsynaptic membrane of excitatory synapses and are highly permeable to  $\text{Ca}^{2+}$ . Indeed, these constitute the main type of receptors responsible for modulating synaptic plasticity (Collingridge, 1987). NMDARs display a heterotetrameric complex, composed of a mandatory subunit, GluN1, which can combine with other 6 types of subunits. Interestingly, GluN2A and GluN2B are the most expressed subunit types in the hippocampus. Importantly, NMDAR is blocked in a voltage-dependent manner by magnesium ion ( $\text{Mg}^{2+}$ ). AMPAR supports NMDAR activity by causing membrane depolarization after  $\text{Na}^+$  entry, consequently promoting the release of  $\text{Mg}^{2+}$  that blocks NMDAR under resting conditions. Notably, AMPAR diffuses freely in the synaptic membrane surface and their level of diffusion depends on receptor composition, for instance, receptors mainly constituted of GluA2 subunits move slower in neurons. Furthermore, diffusion movements are mediated by interactions with PSD-95, a scaffolding postsynaptic protein important to stabilize glutamate receptors located at excitatory synapses (Bats et al., 2007), allowing the receptors to anchor at the membrane surface after an increase in neural activity. In addition, the diffusion speed of AMPAR is modulated by the levels of neural activity, namely by an increase in neuronal function that causes the receptors to move more slowly (Groc et al., 2004). Of note, synaptic plasticity promotes dendritic spine growth (associated with synaptic plasticity enhancement), where changes in AMPAR and NMDAR function enhance the generation of  $\text{Na}^+$  and  $\text{K}^+$  currents, as well as  $\text{Ca}^{2+}$  transients. In fact,  $\text{Ca}^{2+}$ , constitutes an important regulator of synaptic transmission (Katz and Miledi, 1968) in particular, after an action potential, as residual  $\text{Ca}^{2+}$  at the presynaptic terminal provides a basal neurotransmitter release for synapse generation (Catterall and Few, 2008). Importantly, typical basal  $\text{Ca}^{2+}$  concentration is 50 -100 nM, although, after neuron activation, it increases 10 to 100 times, allowing the activation of various biochemical cascades which enzymes are  $\text{Ca}^{2+}$ -dependent (Borczyk, et al., 2019) that then modulate synaptic plasticity.

Synaptic plasticity is classified into two major types, short-term plasticity, and long-term plasticity. Regarding the first type, although the pre-and post-synaptic mechanisms can contribute to it, the first ones seem to be the most prevalent. In particular, presynaptic vesicle trafficking is generally considered fundamental to explain short-term plasticity. As such, vesicle depletion is used to model depression dynamics, whereas  $\text{Ca}^{2+}$ -dependent transmitter release models facilitation dynamics. The second classification, long-term plasticity refers to the long-lasting changes in synaptic activity that modify synaptic strength by either enhancing it, the LTP, or depressing it, the long-term depression (LTD). LTD is an activity weakening of neuronal synapses induced by repeated activation

of presynaptic neurons at lower frequencies of synaptic stimulation (Bear and Malenka, 1994). Slow rises in postsynaptic  $Ca^{2+}$  levels are generated, and LTD induction arises from the activation of  $Ca^{2+}$  dependent phosphatases (Lüscher and Malenka, 2012). In contrast, after a brief high-frequency synaptic stimulation and simultaneous activation of pre- and postsynaptic neurons LTP is induced. A high influx of  $Ca^{2+}$  is generated, which activates calcium/calmodulin-dependent kinase II (CaMKII) and protein kinase C (PKC), which remain active even after lowering of  $Ca^{2+}$  levels, in a process named early-LTP (Bear and Malenka, 1994). The maintenance of the process will be dependent on protein kinase M- $\zeta$  activity, which is independent of  $Ca^{2+}$  levels. Furthermore, late-phase LTP will require gene transcription and protein synthesis in the postsynaptic cells, in a process involving activation of transcription factor cAMP response element-binding protein (CREB) (Sacktor and Fenton, 2018) (**Figure 2**).

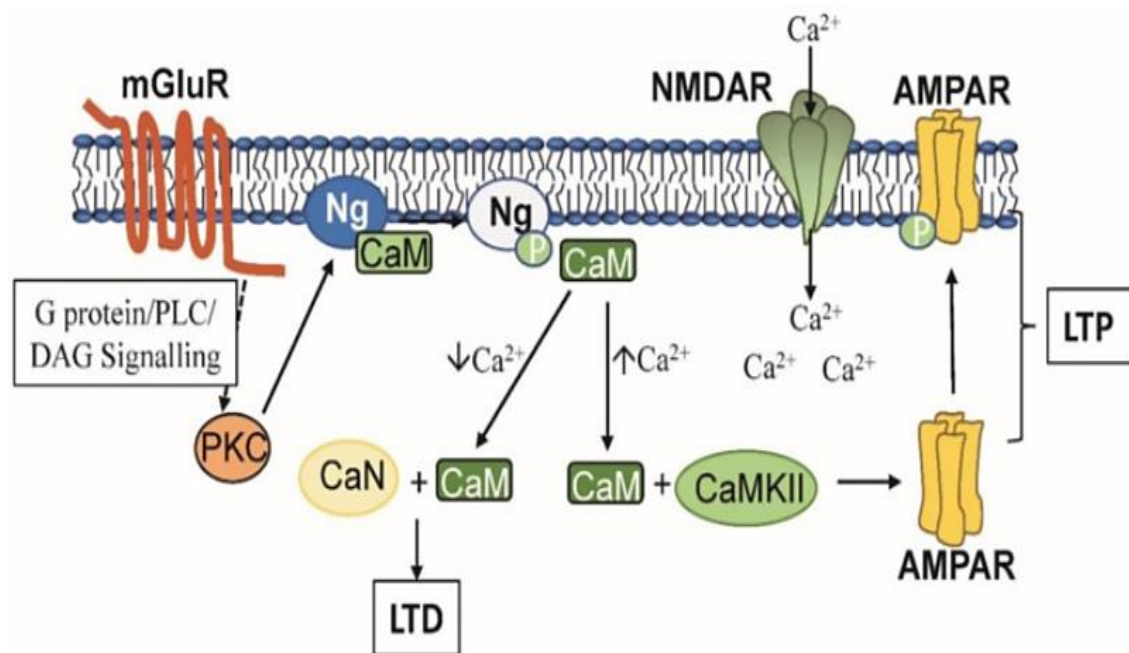


**Figure 2-Model for LTP induction.** High frequency synaptic stimulation activates NMDAR located at the postsynaptic membrane causing high  $Ca^{2+}$  influx which leads to  $Ca^{2+}$ /CaM activation and then CaMKII activation. CaMKII phosphorylates AMPARs inducing the receptor translocation and insertion in the post-synaptic membrane (the higher AMPAR number the stronger the LTP signal). Metabotropic glutamate receptors (mGluRs) mediate the molecular signaling that activates PKC which phosphorylates Neurogranin (Ng) and consequently liberates CaM enabling it to continue activate CaMKII and sustain the LTP (O'Day, 2020).

### 1.2.2 Dendritic spine changes in synaptic plasticity

Spines are one of the most important morphological specializations located in dendrites serving as storage sites for synaptic strength and helping transmit electrical signals to neuron cell body. Structurally, spines are generally composed of a small spherical head

connected to a narrow neck linked to the dendrite. The spine neck serves as a restrictor of  $\text{Ca}^{2+}$  diffusion into the neighbourhood (Ebrahimi and Okabe, 2014) being fundamental to strengthen synaptic plasticity. Notably, spine neck width is modulated by synaptic plasticity and its size increases or decreases after an LTP (Tonnesen et al., 2014). Spine structure is stabilized and supported by the cytoskeleton, composed by an organized network of F-actin filaments (Bosch and Hayashi 2012). Importantly, CaMKII in association with calcineurin regulate the activity of GTPase proteins such as Rac1, Cdc42, and RhoA which regulate the stability of actin cytoskeletal (Li et al., 2002). Cell adhesion molecules (CAMs) bind to calcineurin causing spine shrinkage, a phenomenon observed in spines that are more susceptible to neuropsychiatric and neurodegenerative diseases (Yasuda, 2017; Stein and Zito, 2019) (**Figure 3**).

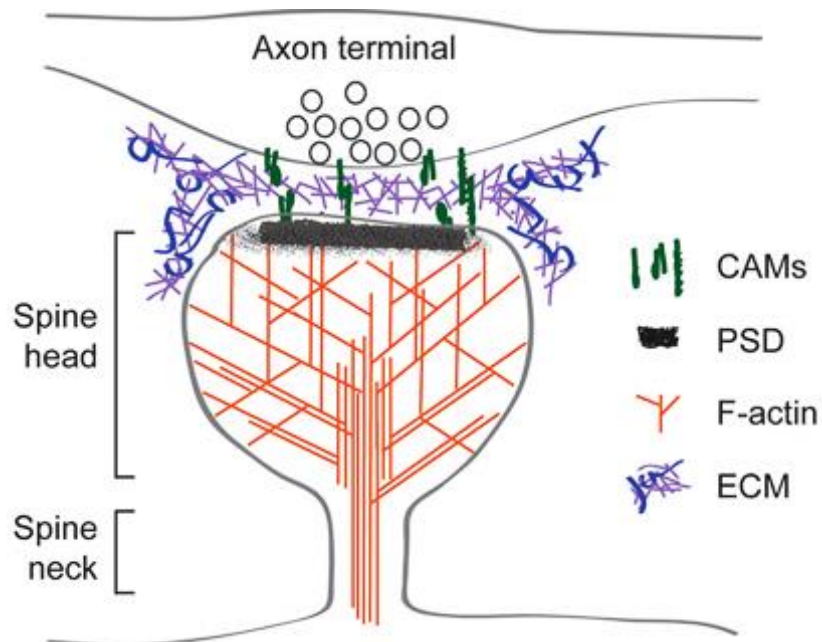


**Figure 3-Dendritic spine structure.** This membrane protrusion is composed by a head and neck and is supported by a network of F-actin. Postsynaptic CAMs which are a subset of cell adhesion proteins localized on the cell surface where they mediate interactions cell-to-cell or cell-to-extracellular matrix (ECM), are fundamental for spine structure, since they link the PSD (a protein dense specialization) and the F-actin in the spine. The majority of CAMs located at synaptic clefts belong to cadherin, integrin and neuexins families, and the immunoglobulin superfamily. Furthermore, the ECM (composed by collagen, enzymes, glycoproteins, and hydroxyapatite) through its interacting with CAMs and membrane receptors confers dynamics to dendritic spines (Levy and Koleske, 2014).

Spine architecture is variable; thus, spine neck diameters lengths may vary from 0.04  $\mu\text{m}$  up to 1  $\mu\text{m}$  and the head, when present, have a size varying from 0.5  $\mu\text{m}$  to 2  $\mu\text{m}$  (Harris and 1994). As previously described, most of excitatory synapses are in dendritic spines; typically, they present total lengths of 2-3  $\mu\text{m}$ , but can also achieve lengths up to

6-8  $\mu\text{m}$  in the case of filopodia spines (Ruszczycki, et al., 2012). Located on top of spines, the PSD region is an electron-dense region holding glutamatergic receptors. PSD complexity and configuration is correlated with AMPAR and NMDAR expression, as well as the size of the region (Ganeshina et al., 2004). A protein family that is part of PSD region is the Shank family, which modulates the structural and functional organization of dendritic spines and synapses and promotes spine maturation and selective enlargement (Sala et al., 2001). Thus, an increase in spine head size is correlated with PSD area enlargement and synaptic strengthening (Ebrahimi and Okabe, 2014).

Spines are dynamic structures dependent on actin cytoskeleton dynamism (Bonhoeffer and Yuste, 2002), thus changes in spine morphology and number (structural neuroplasticity) influence synaptic plasticity (Nakahata and Yasuda, 2018). These post-synaptic structures receive one or multiple excitatory inputs and establish contact with presynaptic terminals that are quite stable (Deng and Dunaevsky, 2005). Interestingly, an enhancement in spine turnover and spine clustering, causes the modulation of neural network function, namely an improvement in memory formation and storage (Frank et al., 2018). Indeed, spines are organized F-actin networks that undergo long-term modifications during synaptic plasticity, where actin switches from states of polymerization to depolymerization. Importantly, LTP induces an increase in spine volume as well as in PSD surface volume (Borczyk, 2019). In addition, dendritic spine remodelling is essential for the process of structural LTP (sLTP), and therefore memory consolidation (Nakahata and Yasuda, 2018). The spine long-term circuit reorganization can be divided into three stages highly dependent on the actin cytoskeleton (Bosch and Hayashi, 2012): i) after stimulation, spines undergo rapid and large volume increase, called the transient phase; ii) the sustained phase, which may take more than one hour, correspond to a decrease in spine volume, although it stabilizes at a higher level than the original one; and iii) in the final phase the spine increases its sensitivity to glutamate.

These specialized protrusions can be classified according to their shape and size, which is extremely useful in order to evaluate states of maturation and pathologies in neurons. In this sense, spines are classified into four main categories: filopodia, thin, mushroom, and stubby. Importantly, the variety in dendritic spines morphologies is correlated with synaptic strength variability (Arellano et al., 2007), and therefore memory and learning capacity. In the initial stages of brain development, dendrites do not possess spines. These structures only begin to appear when the plasma membrane of dendrites forms tentacle-like projections, forming the filopodia spines. These structures are thin, devoid of a head and generally lack a PSD region and disappear with aging, but they may still

be observed in the adult brain, although, only in specific situations such as during induction of neuroplasticity or neuronal regeneration, after brain injury (Yoshihara and Muller, 2009). Furthermore, in the initial stages, spines are highly mobile and gradually, along with the development of the organism, they are replaced by thin spines that are less dynamic than the previous ones, although they already possess a small head that enables them to receive synaptic signals (Lohmann and Kessels, 2014). Thin spines carry small or immature synapses, which allows them to be prone for synaptic strengthening and to a greater plasticity, being therefore generally called learning spines. Interestingly, their number decrease with aging (Berry and Nedivi, 2017), which may explain the decline in brain neural plasticity observed. In contrast with thin spines, mushroom spines are even more stable and less dynamic. These protrusions (also called “memory spines”) possess a larger bulbous head and a narrow neck, an architecture that allows them to hold bigger glutamatergic synapses. These synapses possess a bigger PSD region, and therefore, a bigger area of glutamatergic receptors, possessing stronger synaptic signals (Cugno et al., 2019). These glutamatergic receptors, in particular, AMPAR are more expressed in mushroom spines. Interestingly, when immature protrusions are stimulated, it might initiate morphological changes that result in the acquisition of a mature spine morphology (mushroom), namely a decrease in length (head and neck), an increase in the diameter of the head, an increase in the diameter of the neck and an increase in the diameter of the base (Mattison et al., 2014). Of note, generally, spine population in the hippocampus and neocortex of adult healthy mouse is composed by approximately 65% of thin spines and 25% of mushroom spines (Bourne and Harris, 2007). Finally, stubby spines generally do not possess a neck, being present in early development but also in adulthood, resulting mainly from mushroom spine elimination (Pchitskaya and Bezprozvanny, 2020). Interestingly, in both rat and mice slice cultures a loss of immature protrusions (filopodia and thin) and appearance of mature spines (mushroom and stubby) is observed during the second week of development (Mattison et al., 2014).

### **1.2.3 Impaired synaptic plasticity in AD**

Consistent reports have established a link between decreased synaptic plasticity and abnormalities in dendritic spines. In AD, cognitive impairment has been associated to low dendritic spine density and altered morphology (Dickstein et al., 2010). The Tg2576 mouse model showed a decrease in dendritic spine density near amyloid plaques, as a consequence of spine formation disruption, and later associated to synaptic loss (Spire-

Jones et al., 2007). In mouse primary hippocampal neuronal cultures, most of dendritic spines were highly stable under basal conditions; however, treatment with A $\beta$ O induced an increase in the number of stubby spines and a decrease in the number of mushroom spines, suggesting a higher susceptibility of mushroom spines to A $\beta$  exposure, when compared to thin spines, which did not suffer considerable changes. Notably, low concentrations of human A $\beta$  caused a shift in spine morphology from mature to immature spines (Tackenberg and Brandt, 2009). In a study aiming to evaluate the progression of spine morphology in AD, an *ex vivo* model was used based on hippocampal organotypic cultures from APP transgenic mouse model; data in this model indicated that spine morphology progressively changes from mushroom-shaped to stubby, in a process mediated by microtubules (MTs) destabilization. This effect could be recovered by MTs polymerization agents (Penazzi et al., 2016).

The mechanisms behind spine loss, synaptic failure, as well as memory loss in AD are still under debate, although two explanations stand out, one centred in the F-actin role and another centred on Ca<sup>2+</sup> modulation. In primary cortical neurons of APP/PS1 mouse model cultured for 10 days in vitro (DIV), the reduction of F-actin levels, was not correlated with significant changes in the number of spines or spine total extent but was accompanied with a slight decrease in spine head diameter when compared to WT cells (Kommaddi, et al., 2018). Importantly, at 16 DIV, reduction of F-actin levels was accompanied by a reduction in the number of spines, spine total extent, and head diameter (Kommaddi, et al., 2018). Furthermore, exposure to A $\beta$ O induced excitotoxicity, mechanism responsible for neuronal death through the over activation of NMDARs and further increase in intracellular Ca<sup>2+</sup> (Ferreira et al. 2012; Ferreira et al., 2015; Shankar et al., 2007; Sengupta Urmi et al., 2016; MacDermott et al., 1986; Rammes et al., 2017). Extra synaptic NMDARs activation seems to be particularly important to mediate A $\beta$ O neurotoxicity (Zhang et al., 2016) impairing the activity of cAMPs that bind fundamental transcription factors, as CREB, thus, shutting off important molecular pathways (Tong et al., 2001). Of note, A $\beta$  aggregates induce the formation of pores in neuronal membranes, promoting an increase in membrane conductance and a higher entry of Ca<sup>2+</sup>. Thus, the neurotoxic effects resulting from this dynamic process, taking place in the brains of patients, are loss of synaptic proteins and a decrease in neuronal viability (Sepúlveda et al., 2010; 2014). Furthermore, A $\beta$ O bind to neurites preferentially to the postsynaptic region, where the PSD-95 normally interacts with NMDAR, neuroligin (NL) (postsynaptic protein that binds to presynaptic protein) and neurexin and forms an anchorage complex. Importantly, when this complex is disrupted due to A $\beta$ O accumulation, the integrity of the synaptic contact is compromised (Dinamarca and Inestrosa, 2012). A progressive

accumulation of A $\beta$ O causes selective alterations in pre- and postsynaptic proteins, such as synaptophysin (a presynaptic protein present in synaptic vesicles) and PSD-95, causing destabilization of the spine formation/elimination equilibrium (Birnbaum and Rajendran, 2015; Shanar et al., 2007).

### **1.3. Mitochondria**

#### **1.3.1 General features**

Mitochondria are maternally inherited organelles constituted by a matrix surrounded by an inner mitochondrial membrane (IMM) separated from an outer mitochondrial membrane (OMM) by a sub-compartment called mitochondrial intermembrane space; unlike other organelles, mitochondria possess their own DNA, a circular mitochondrial DNA (mtDNA). Generally, mitochondria possess a size of 0.75-3  $\mu$ m and their diameter and length vary depending on the cell type or physiological state (Miyazono et al., 2018). Mitochondria are commonly referred to as the “powerhouse” of the cell due to their involvement in ATP production, fundamental for the maintenance of normal cell function, through the process of oxidative phosphorylation (OXPHOS). Briefly, during OXPHOS, electrons derived from reduced coenzymes (NADH and FADH<sub>2</sub>) are transferred across IMM complexes through redox reactions. The energy associated to this electron flow is used to transport protons (H<sup>+</sup>) across the IMM, from the matrix to the mitochondrial intermembrane space, producing both a pH gradient ( $\Delta$ pH) and an electrical potential difference ( $\Delta\Psi$ ) across the membrane. Thus, mitochondrial transmembrane potential ( $\Delta\Psi_m$ ) is used to define mitochondrial function. Importantly,  $\Delta\Psi_m$  achieves values around -150 to -180 mV in the matrix side of the IMM (Jonckheere, et al., 2012, Cenini and Voos, 2019). Ultimately, protons flow back to the mitochondrial matrix through ATP synthase (Complex V), generating ATP from ADP (**Figure 4**).

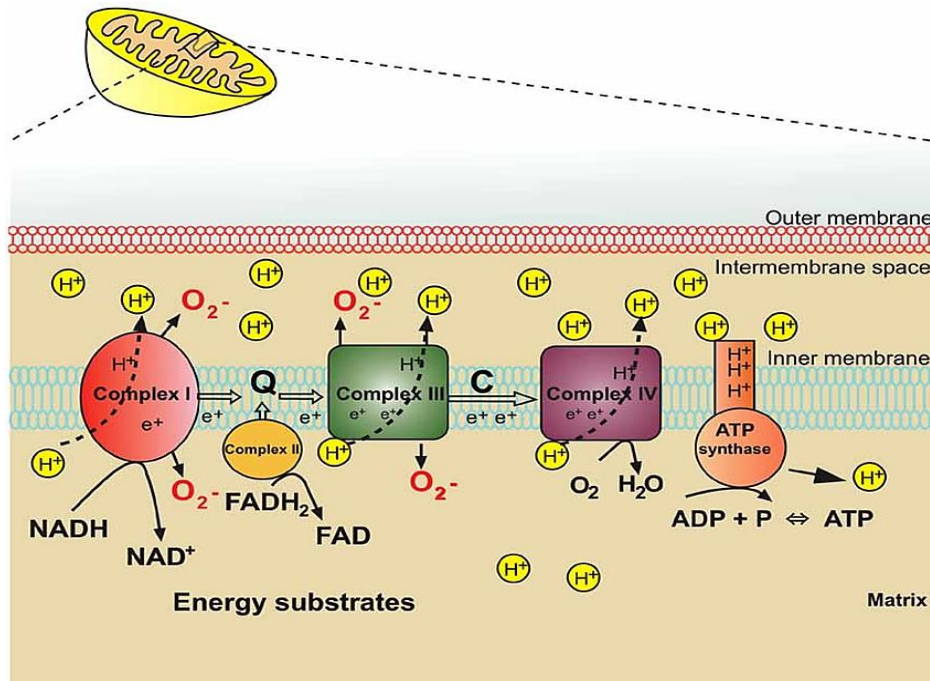


**Figure 4-ATP formation through mitochondrial OXPHOS** creates an H<sup>+</sup> gradient that is fundamental in order to generate ATP, through OXPHOS, used to sustain the synaptic activity (Andrews, 2010).

One of the fundamental roles of mitochondria is, as mentioned, to produce ATP. In this process besides mitochondrial chain complexes, the activity of mitochondrial dehydrogenases located in the matrix, is regulated by Ca<sup>2+</sup> levels, so that an increase in Ca<sup>2+</sup> levels stimulate the production of ATP (Young et al., 2008). Indeed, mitochondria are extremely sensitive to Ca<sup>2+</sup> levels, which enable them not only to decode synaptic signals, but also to regulate intracellular Ca<sup>2+</sup> content by buffering this ion when above a certain threshold (~0.5 μM) in the cytosol or establishing a close link with the ER through the mitochondrial associated membrane (MAM). Importantly, an excessive accumulation of Ca<sup>2+</sup> inside mitochondria increases IMM permeability, leading to mitochondrial depolarization and affecting ATP production. As a result, ATP levels drop and ultimately cause cell death through the opening of mitochondrial permeability transition pore (mPTP) (Webster 2012). Conversely, high ATP levels are associated to stable ΔΨ<sub>m</sub> values (Zorova et al., 2018). Moreover, strategically placed mitochondria connect neuronal depolarization to synaptic activity through the modulation of membrane potential and Ca<sup>2+</sup> oscillations at synapses (Giorgi et al. 2018).

In the CNS, mitochondria can be located at synapses, serving as energy suppliers, and regulating neurite formation, synaptic strengthening, stability, and signalling (Devine and

Kittler, 2018). Mitochondria respond preferentially to high levels of  $\text{Ca}^{2+}$  at post-synaptic sites, managing  $\text{Ca}^{2+}$  uptake into the organelle and compartmentalizing the distribution of  $\text{Ca}^{2+}$  along the neuron. Dendritic mitochondria evidence higher levels of  $\text{Ca}^{2+}$  than somatic mitochondria. The differences in  $\text{Ca}^{2+}$  compartmentalization and in  $\text{Ca}^{2+}$  levels of somatic and dendritic mitochondria may suggest that these are strategies to avoid the activation of  $\text{Ca}^{2+}$ -dependent proteases and prevent cell death (Young et al., 2008). Furthermore, there is a spatiotemporal correlation between  $\text{Ca}^{2+}$  and ATP levels. Thus, in HeLa cells expressing an ATP plasmid (GO-ATeams) and loaded with a  $\text{Ca}^{2+}$  fluorescent probe, stimulation with histamine proportionally increased both intracellular  $\text{Ca}^{2+}$  and mitochondrial ATP, indicating that the ion levels may precisely control mitochondrial ATP synthesis (Nakano et al., 2011).

In response to high metabolic demand, mitochondria travel and distribute along dendrites, axons, and synaptic terminals, supporting neuronal function (Mishra and Chan, 2016). ADP/ATP ratio levels increase along with mitochondrial movement towards synapses, reinforcing the decisive role of ATP as a signalling agent of mitochondrial movement. Interestingly, mitochondria decrease their velocity near synapses, which is associated with lower levels of ATP, as a consequence of a higher ATP demand at synapse (Mironov, 2007). Furthermore, mitochondrial morphology is continually changing along neural network depending on their location. Remarkably, presynaptic mitochondria are smaller and shorter, and most of them do not extend beyond presynaptic terminals. These mitochondria travel to places of high ATP demand and  $\text{Ca}^{2+}$  flux, participating in the homeostatic mechanism (Devine and Kittle 2018); thus, impairment of a proper supply of energy and buffering of  $\text{Ca}^{2+}$ , compromises neuronal function. In contrast, postsynaptic and dendritic mitochondria are larger and spread throughout dendrites (Delgado et al., 2019).

### **1.3.2 Mitochondrial transport and dynamics**

The long-range transport of mitochondria along axons and dendrites is accomplished through a system of MTs, in which these structures act as trails to mitochondria. Axonal MTs are uniformly polarized with positive ends pointing to axonal terminals and negative terminals pointing to cell bodies, in contrast to dendritic MTs that have mixed polarities (Lovas and Wang, 2013). The classification of the type of mitochondrial movement depends on the direction in which the organelles move. Short-range mitochondrial movement occurs mainly in dendritic spines, growth cones and synaptic buds and is

mediated by actin filaments using myosin motor proteins (Saxton and Hollenbeck, 2012). In addition, actin filaments are also used for docking organelles (Correia et al., 2016).

Two main motor proteins are involved in neurite mitochondrial movement, namely in anterograde or retrograde movement, respectively kinesins (KIFs) and dynein. Different KIF isoforms regulate anterograde movement of distinct cell cargoes. In particular, KIF-1 and KIF-3 are highly expressed in the CNS (Lin and Sheng, 2015). These motor proteins are recruited to mitochondria with the help of adaptor proteins, forming a complex required for mitochondrial movement. One of the most studied adaptor proteins is Grif-1 or Track1, which associates with Miro1, a subfamily of mitochondrial Rho GTPase located at the OMM to form a movement protein complex. Besides Track1 and Miro1, other protein isoforms can take part in the movement complex, such as Track2 and Miro2. Importantly, increasing Miro expression recruits Track adaptors into mitochondria forming the movement complex, and therefore enabling mitochondrial movement in the direction of the nerve terminal (MacAskill et al., 2009). The retrograde movement constitutes a communication strategy between the mitochondria and the nucleus, as it signals the energetic state of the organelle (Lovas and Wang, 2013). Complexes consisting of dynein and dynactin proteins mediate mitochondrial retrograde movement, although, unlike the multiple isoforms of KIFs, there is only one form of dynein. However, dynein has several components and arrangements that allow to have different functions. Dynein's cargo carrier or cargo anchor functions make dynein a highly complex and multifunctional motor protein. Notably, mitochondria with low  $\Delta\Psi_m$  tend to move retrograde, although the mechanisms involved are still poorly understood (Miller and Sheetz, 2004; Zorova et al., 2018).

Mitochondrial motility is influenced by the organelle's function and dynamics influencing their spread throughout neurons. Thus, factors as  $\Delta\Psi_m$ , ATP levels and  $Ca^{2+}$  buffering, or mitochondrial morphology modulate mitochondrial distribution. Complete mitochondrial depolarization induced by the protonophore Carbonyl cyanide m-chlorophenylhydrazone (CCCP) was shown to reduce both retrograde and anterograde movements. Interestingly, a high  $\Delta\Psi_m$  promoted mitochondrial movement towards growth cones (~90%), whereas a lower  $\Delta\Psi_m$  promoted mitochondrial movement towards the cell body (~80%) (Miller and Sheetz, 2004). ATP levels also influence mitochondrial movement, in fact, motor proteins are strongly fuelled by ATP that is produced at OXPHOS rather than glycolysis (Zala et al., 2013). In primary cultures of dentate granule cells, neuronal depolarization caused the activation of AMP-activated protein kinase (AMPK) and an increase in mitochondrial anterograde movement (Tao

and Koyama, 2014). Of note, AMPK is a regulator of the intracellular metabolic state that is sensitive to low intracellular ATP levels (Mihaylova and Shaw, 2011). Furthermore, in cultured neurons mitochondrial movement was demonstrated to be influenced by ATP depletion, suggesting that its consumption during synapse activity facilitates mitochondrial recruitment since these are places of high energetic demand (Mironov, 2007).

Ca<sup>2+</sup> distribution throughout neuronal compartments is heterogeneous and seems to be dependent on cellular ATP content. This is particularly evident at synapses and dendritic spines, where Ca<sup>2+</sup> concentration is high and the ATP content is low, suggesting that mitochondria are arrested to promote Ca<sup>2+</sup> buffer and produce ATP for neuronal function (Lovas and Wang, 2013). Thus, in addition to ATP levels, Ca<sup>2+</sup> levels also influence mitochondrial movement, playing an important role in physiological signalling. Basal levels of cytosolic Ca<sup>2+</sup> promote mitochondrial movement although, when elevated, it can block mitochondrial movement along neurons (Lovas and Wang, 2013; Verma et al., 2018). Ca<sup>2+</sup> regulates protein Miro1, which possesses two EF-hands Ca<sup>2+</sup>-binding domains, acting as a Ca<sup>2+</sup> sensor to promote mitochondrial mobility. Complexes involving the arrangement of key proteins (KIF, Tracks, and Miro) allow mitochondria to move through MTs along dendrites and axons, where mitochondrial recruitment is mediated by Ca<sup>2+</sup> (Cai and Sheng, 2009) (**Figure 5**), a mechanism that is compromised in neurodegenerative diseases.

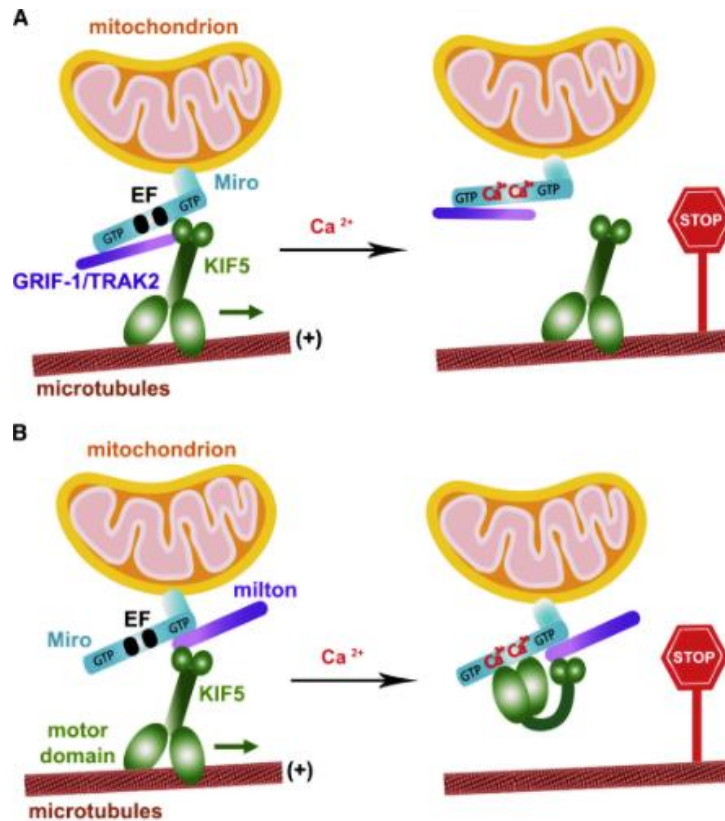


**Figure 5-Two models of Ca<sup>2+</sup> recruitment of mitochondria in a Miro adaptor-dependent manner.** In (A) Mitochondria transport is mediated by the complex formed by Miro associated with KIF-5, when Ca<sup>2+</sup> binds to the EF hands dissociates Miro from KIF-5 (B) Ca<sup>2+</sup> binds to EF-hands and promotes a direct interaction of KIF-5 domain with Miro which turns “off” KIF-5 interaction with MTs (Cai and Sheng 2009).

Interestingly, bigger mitochondria are less motile than smaller mitochondria (Miller and Sheetz, 2004). These organelles possess two states, as they either move long or short distances at a constant speed or pause and restart again although, notably, with different speeds, and may even change movement direction. Importantly, in cortical axons, hippocampal axons, and hippocampal dendrites, at all stages of maturation, only approximately 25-30% of mitochondria are motile, thus mitochondria move along neurons in an intermittent manner (“jumping” movement) with short periods of constant velocity followed by longer pauses. (Lovas and Wang, 2013; Loss and Stephenson, 2017; Vanden Berghe et al., 2004). Importantly, mitochondrial motility appears to decrease with neurons maturation, an observation reported in cortical axons mature neurons in which mitochondrial motility was significantly reduced. Interestingly, there was increased recruitment of mitochondria in presynaptic sites (an important hallmark of CNS maturation) (Lewis et al., 2016). Furthermore, mitochondrial motility patterns are distinct and dependent on the neuronal compartment. In a study in embryonic rat

hippocampal neurons performing a time-lapse imaging analysis, it was observed dendritic mitochondria exhibited more mobile and more persistent changes in direction than axonal mitochondria although, the axonal mitochondria have a longer moving length than dendritic mitochondria. (Overly and Hollenbeck, 1996). Overall, axonal mitochondria tend to possess more dynamic patterns of motility and longer run lengths, compared with dendritic mitochondria (Melkov and Abdu, 2018). Notably, in primary dentate granule cells, plasmatic membrane depolarization induces a rebalance of mitochondrial motility and an increase in anterograde axonal transport of mitochondria (Tao and Koyama, 2014). Moreover, mitochondrial velocity is a key parameter to characterize mitochondrial movement, especially to distinguish between normal and abnormal mitochondrial movement. In primary hippocampal neurons mean velocities in axons and dendrites are reported between 0.43 and 0.61  $\mu\text{m/s}$ , while in axons and dendrites of cortical neurons mean mitochondrial velocities are reported between 0.39 and 0.53  $\mu\text{m/s}$  (Niescier et al., 2016; Loss and Stephenson, 2017).

Mitochondrial dynamics consists in changes in morphology and movement. Particularly, changes in mitochondria membrane cause mitochondria either to elongate (after fusion) or shorten (fission). This dynamic process is especially important to maintain a healthy mitochondrial activity and provide the necessary number of mitochondria to places of high energetic demand. The organelles can either be organized in complex interconnected networks that represent an efficient system of energy delivering and functional individual units. In several cell lines, mitochondria appear as heterogeneous mixtures of elongated, tubular, or short vesicular forms (Karbowski and Youle, 2003). When a loss of  $\Delta\Psi\text{m}$  occurs mitochondria undergo structural changes, namely mitochondrial shrinkage along the long axis into a small spherical structure (Miyazono et al., 2018). Indeed, the formation of short and round mitochondria occurs under conditions such as mtDNA depletion or treatment with mitochondrial toxins. These shifts in mitochondrial shape result in a potential strategy to regulate mitochondrial health (Karbowski and Youle, 2003). Fission begins first with the recruitment of ER to the mitochondrial constriction site composed of several OMM-linked proteins (FIS1, MFF, MiD49, and MiD51) and then DRP1 is recruited to the surface of the mitochondrial constriction, forming a constriction ring around the mitochondria and initiating the fission process; this requires the recruiting of other proteins, namely Dyn2 and Dnm2, two GTPases responsible for ending the fragmentation process (Westermann, 2010; Cai and Tammineni, 2016; Cadete et al., 2019; Palmer et al., 2011). Impairment of mitochondrial fission may cause a reduction in the density of dendritic mitochondria and limit their distribution throughout axons, dendrites, spines, and synapses (Li et al., 2004). In

contrast, the fusion process involves mainly two GTPases: mitofusins (Mfn1 and Mfn2) located in the OMM and promoting its fusion, and optic atrophy protein 1 (OPA1), located in the IMM. This is a fundamental process to maintain mitochondrial DNA, as well as the distribution of metabolites. In this sense it is extremely important to maintain the mitochondrial population, thus a disruption of this process leads to mitochondrial heterogeneity and dysfunction (Westermann, 2010, Zhu et al., 2018). This is a two-step process, first Mfn-1 and Mfn-2 and their C-terminal coiled-coil region mediates tethering between mitochondria through homo- or heterotypic complexes established with adjacent mitochondria, promoting OMM fusion. OPA-1 at the IMM mediates the attachment and fusion of IMM. Importantly, mitochondrial fusion is induced by an increase in mitochondrial potential, ATP levels and oxygen consumption, in contrast with fission, which is induced by a decrease in these parameters (Chiong et al., 2014). Mitochondrial fusion and fission, respectively, increases and decreases the  $\Delta\Psi_m$ , which influences mitochondrial  $Ca^{2+}$  buffering that increase or decrease in a proportional manner. (Flippo and Strack, 2017). Interestingly, LTP promotes dendritic mitochondrial fission, which results from increased cytosolic  $Ca^{2+}$ , being an essential event for LTP expression (Divakaruni et al., 2018). Furthermore, lower mitochondrial  $Ca^{2+}$  buffering resulting from mitochondrial fission events and increases cytosolic  $Ca^{2+}$  which promotes dendritic spine development (Flippo and Strack, 2017).

### **1.3.3 A $\beta$ induced mitochondrial dysfunction in AD**

One of the early features in AD is mitochondrial dysfunction, which is associated to structural and functional changes such as increased ROS production and decreased ATP production. In fact, abnormal cerebral metabolic rates are observed in PET imaging, even before the observation of an impairment in cerebral functional parameters and brain atrophy (Blass, 2000). Importantly, AD patient's brains possess high levels of mitochondrial DNA (mtDNA) mutations (Wang et al., 2014). Given the fact that mtDNA encodes fundamental proteins constituting mitochondrial electron transport chain, mutations in mitochondrial genome will compromise mitochondrial function, causing a decreasing ATP production and oxygen consumption, which ultimately promote cell death (Pagliarini et al., 2008; Lu et al., 2009). Furthermore, analysis of brain tissue from patients with AD showed an abnormal activity of electron transport chain cytochrome c oxidase (COX) (or complex IV), responsible for inducing energy loss in AD (Kish et al., 1999). Mitochondrial dysfunction observed in AD is a result not only of the direct effect of A $\beta$  on mitochondria, but also of compromised  $Ca^{2+}$  homeostasis. In fact, an overload

of  $\text{Ca}^{2+}$  induced by  $\text{A}\beta$ , through the activation of ionotropic NMDAR causes mitochondrial membrane depolarization increasing oxidative stress and neurotoxicity (Alberdi et al., 2010; Perluigi et al., 2016 Hardingham, and Bading, 2003, Ferreira et al., 2015). Of note, cell susceptibility to ROS neurotoxic effects varies according to its content in superoxide dismutase (SOD) enzyme, one of the major antioxidant proteins (Guo and Du, 2017), and according to its capacity to bind  $\text{A}\beta$  peptide (Simakova, 2007). Thus, cells with a high content of SOD and a low capacity to bind  $\text{A}\beta$  are less susceptible to oxidative stress. Interestingly, high mPTP pore opening, resulting from increased intracellular  $\text{Ca}^{2+}$  and ROS levels, causes  $\Delta\Psi_m$  dissipation and reduced oxidative phosphorylation (Webster, 2012). Notably, brain tissue analysis of transgenic mice that start developing amyloid plaques at 6 months of age shows a reduced ATP content, suggesting mitochondrial dysfunction (Zhang et al., 2015). Moreover, in mice overexpressing human mutant APP,  $\text{A}\beta$  peptide can accumulate with mitochondria in the brain correlated with decreased mitochondrial activity of complexes III and mainly IV (Hansson Petersen et al. 2008) (**Figure 6**).

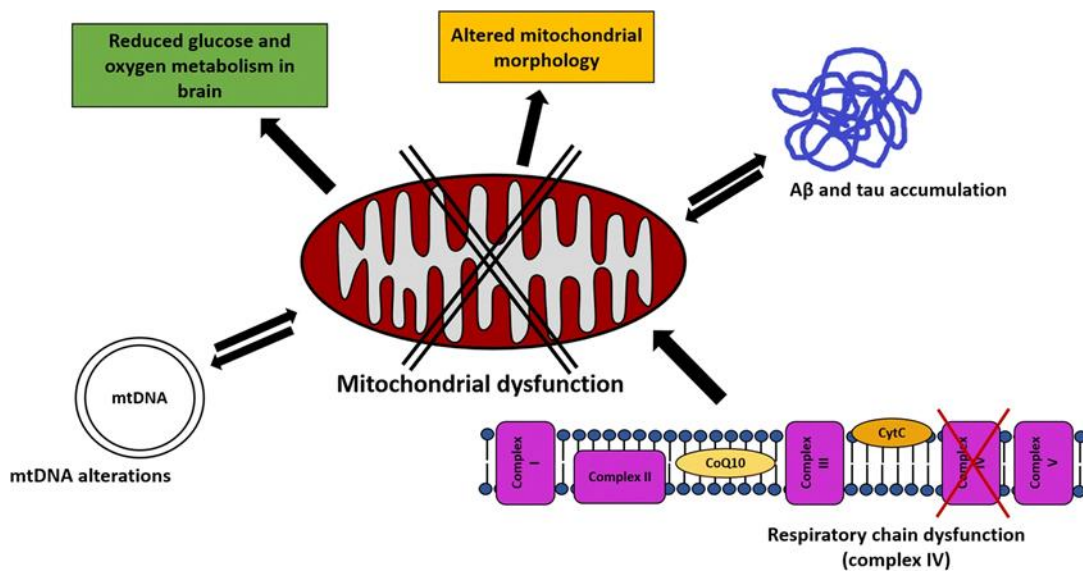


**Figure 6-Representation of main mitochondrial mechanisms potentially affected in AD onset.** Consistent reports have demonstrated a close link between mitochondrial dysfunction and the main protein hallmarks in AD,  $\text{A}\beta$  and tau. Thus, altered mitochondrial morphology, reduced glucose and oxygen consumption, impaired respiratory chain activity (complex IV) and damage mitochondrial DNA appear to be relevant triggers of AD pathogenesis (Monzio et al., 2020)

Mitochondrial dysfunction in AD is also associated to changes in mitochondrial transport. In hippocampal neurons treated with A $\beta$ O a decrease in the number of motile mitochondria, in their velocities and run length was observed (Calkins and Reddy, 2011; Rui, et al., 2006; Rui and Zheng, 2016; Kim et al., 2012). Interestingly, A $\beta$ O treatment caused higher damages in the transport of dendritic mitochondria than axonal mitochondria (Rui and Zheng, 2016). Furthermore, hyperphosphorylated Tau caused impairments in axonal transport, resulting in abnormal localization and distribution of mitochondria and consequently, axonal damage and synapse degeneration (Kopeikina et al., 2012). Both A $\beta$  and hyperphosphorylated Tau interact with DRP1 causing higher mitochondrial fragmentation and consequent synaptic deficits (Manczak and Reddy, 2012). In addition, A $\beta$ -induced abnormal mitochondrial dynamics. Thus, changes in the expression and distribution of mitochondrial fission and fusion proteins in AD brain were observed (Wang, et al., 2009). The rates at which fusion and fission occur may also dictate the dysfunctional process in neurological diseases. Indeed, mitochondrial fusion- and fission-related proteins levels were deregulated in the hippocampus of AD patients. DRP1 protein was shown to be increased, whereas fusion proteins, namely Mfn1, Mfn2 and OPA1, were downregulated (Oliver et al., 2019), thus promoting mitochondrial fission. Similar results were observed in APP transgenic mice, and data were further correlated with dendritic spine loss and neuronal dysfunction (Manczak et al., 2018). Importantly, impairment in mitochondrial fusion affects mitochondrial distribution by accumulating mitochondria in neurite branches thus preventing cargos to move towards critical neural places, such as synapses, compromising neural activity (Chen et al., 2007).

## **1.4 The tyrosine kinase protein Src**

### **1.4.1 General features**

Src protein belongs to the Src kinase family (SKF), a family of non-receptor tyrosine (Tyr) kinases formed by eleven members that are grouped into two subfamilies: 1) the Src-related group constituted by Src, Yes, Fyn, Fgr, Frk, Srm; and 2) the Lyn-related group, constituted by Lyn, Hck, Lck, Brk and Blk. SKF members are expressed ubiquitously and involved in a vast range of functions, namely cell survival, proliferation, differentiation, stress response, cell death, gene expression and neural function regulation.

Starting from the N-terminal to the C-terminal, members of SFKs share a similar domain arrangement being constituted of a Src homology 4 domain (SH4), a unique domain, SH3 domain, SH2 domain, SH1 domain (the catalytic domain) and finally, a regulatory domain. SH4 domain is a short sequencing of 15 a.a. that holds the N-terminal of SFKs and possesses a 14-carbon myristoyl group that promotes the attachment of Src kinases to cell membranes. The SH3 domain (sequence of 60 a.a.) interacts with proline rich domains from receptors and can suffer phosphorylation that will eventually modulate the interactions between Src and its targets (Winkler et al., 1993; Johnson et al., 2000; Chen et al., 2001). Between SH3 and SH4 is the unique region that is different between Src members in 50-70 a.a. The SH2 domain (sequence of 90 a.a.) is a non-catalytic segment that plays an important role in the recognition of phosphorylated Tyr segments. Both SH3 and SH2 domains participate in the regulation of SFK interactions with other proteins and in the modulation of its enzymatic activity. SH1 domain constitutes a catalytic domain that holds a Tyr-416 residue fundamental for the regulation of kinase activity (Parsons and Parsons, 2004). The regulatory domain (sequence of 15-17 a.a.) is located at the C-terminal, retaining a Tyr-527 residue that, when phosphorylated, binds intramolecularly to the SH2 domain, causing the inhibition of Src activity. This mechanism is mediated by Src-specific kinase Csk and Chk (protein kinase that negatively controls the activity of the SFK) (Boggon and Eck, 2004). Therefore, Tyr-527 phosphorylation stabilizes a closed conformation of the protein binding the SH2 and SH3 domains, suppressing the kinase activity towards its substrates, whereas phosphorylation at Tyr-416 promotes an

elevated kinase activity by stabilizing the activation loop in a manner permissive for substrate binding (**Figure 7**).

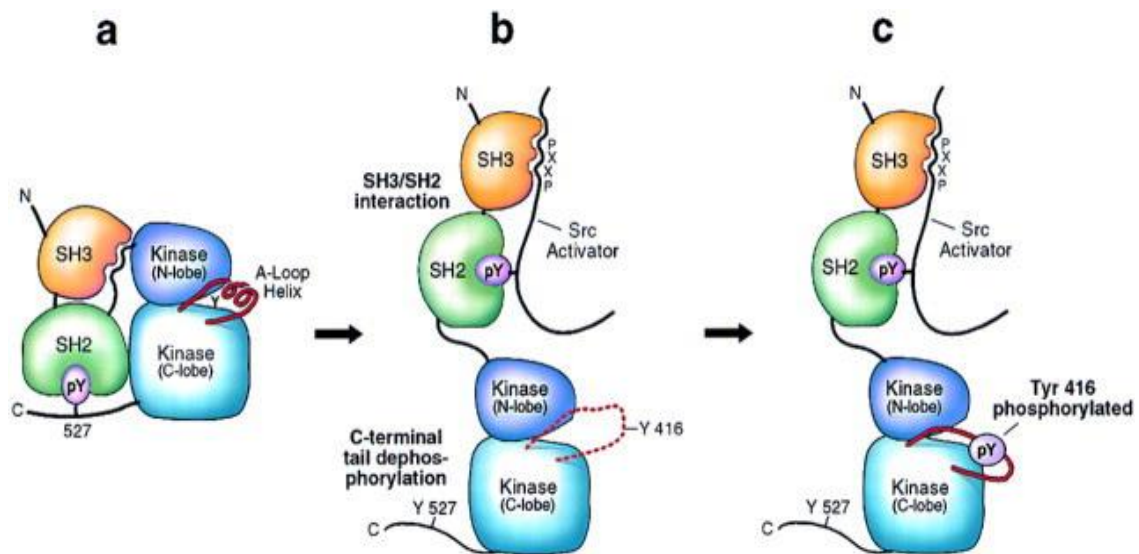


**Figure 7-c-Src activation mechanism.** In **a**) Src closed conformation is sustained through interactions of SH2 and SH3 domains and the phosphorylated C-terminal tail, in this conformation, the A loop helix that interacts with substrate binding protects from phosphorylation at Tyr-416. **b**) When C-terminal tail suffers dephosphorylation or competitive binding of ligands to optimal SH2/SH3 kinase domain, this opens disrupting A loop helix and exposing Tyr-416 to phosphorylation. **c**) After Tyr-416 phosphorylation occurs c-Src rearrangement and activation (Xu et al., 1999).

Of note, the equivalents in humans to residues Tyr-416 and Tyr-527 in mice are, respectively Tyr-418 and Tyr-530 (Fuss et al., 2008; Irby and Yeatman, 2000). Importantly, Tyr-527 is also susceptible to suffer dephosphorylation by phosphatases: PTP1B, Shp1 and Shp2 (Baker et al., 2000). Moreover, SFK activity is up regulated by ROS through the oxidation of cysteine groups on protein tyrosine kinases. These processes occur in the SH1 and SH2 domains, mainly at Cys245, Cys-487, Cys-277, and Cys-185 residues, inducing a change in the conformation of Src kinase into an open state and consequently, into its active form (Giannoni et al., 2005; Heppner et al., 2018). Notably, calmodulin (CaM) promotes Src activation since, when Src is in the closed state and when basal concentration of cytosolic  $Ca^{2+}$  is low, after a receptor-mediated signalling process, occurring the dephosphorylation of Tyr-527 by phosphatases and its activation upon  $Ca^{2+}$  free-calmodulin (apo-CaM) binding. Furthermore, Src induces phosphorylation of phospholipase  $C\gamma$  (PLC $\gamma$ ), which produces inositol-1,4,5-trisphosphate (IP3) and consequently releases  $Ca^{2+}$  from intracellular stores, increasing

its cytosolic levels and forming the  $\text{Ca}^{2+}/\text{CaM}$  complex. Notably, Src activity declines after formation and binding of the  $\text{Ca}^{2+}/\text{CaM}$  complex because it acts as a negative feedback (Anguita and Villalobo, 2017), suggesting that Src activity is more efficient in the presence of low levels of cytosolic  $\text{Ca}^{2+}$ .

#### **1.4.2 Src and mitochondria**

The SFK members can be found in numerous subcellular compartments, including mitochondria, where tyrosine phosphorylation plays a fundamental role in the regulation of mitochondrial pathways and function (Hebert-Chatelain, 2013). Five members of the SFK (Src, Fyn, Lyn, Yes and Lck) were found in the intermembrane space of mitochondria, where they modulate mitochondrial activity (Salvi et al., 2002; Ohnishi et al., 2011). Regarding Src, reports have demonstrated that the association of Src with mitochondria results from constant movements of import and export since it is not located in the mitochondria. In fact, its translocation into the organelle relies on protein adaptors namely, two anchoring proteins: Kinase Anchor Proteins 121 (AKAP121) and Downstream of tyrosine kinase 4 (Dok-4) (Livigni et al., 2006). AKAP121 is found in the IMM with Src and Lyn, where it binds to protein tyrosine phosphatase D1 (PTPD1), anchoring Src to the OMM by activating PTPD1. AKAP121 enhances COX activity,  $\Delta\Psi_m$  and ATP oxidative synthesis in a Src and PKA-dependent manner (Livigni et al., 2006).

A wide set of mitochondrial proteins suffer phosphorylation in Src-overexpressing HEK 293 cells, which suggests that Src catalyses Tyr phosphorylation of mitochondrial proteins, particularly in the COX subunits, and potentially regulates energy production (Miyazaki et al., 2003). Of note, Tyr phosphorylation in the subunit II of COX is mandatory for the activity of mitochondrial electron transport chain, whereas the phosphorylation of subunit I, in cooperation with cAMP-dependent pathway, inhibits mitochondrial enzymatic activity of complex IV (Ogura et al., 2012). In its turn, Dok-4 is involved in Src translocation into mitochondria in bovine endothelial cells. Interestingly, a decrease of Dok-4 induces an extra-mitochondrial localization of Src (Lim, et al., 2016). Src also phosphorylates NADH dehydrogenase flavoprotein 2 (NDUFV2) at Tyr193 (complex I of the respiratory chain) modulating the activity of NADH dehydrogenase, thus influences ATP production (Ogura et al., 2014). In addition, Src modulates mitochondrial metabolism in cancer disease, supporting metastasis and cell proliferation, being detected an abnormal activity of Src in metastatic biopsies and cell lines. In the

metastatic tissue, an increase in Src expression is correlated with a reduced expression of mitochondrial complexes I and IV (Hunter et al., 2020).

#### **1.4.3 Src at glutamatergic synapses**

The SFK members, namely, Src, Fyn, Lyn, Yes and Lck are expressed in the CNS in differentiated, post-mitotic neurons and astrocytes. Interestingly, the levels of Src are 15 to 20 times higher than the Src levels in fibroblasts, and its specified activity in neuronal cultures is 6 to 12 times higher than in astrocyte cultures, indicating its key role in neurons (Khanna et al., 2002).

Src kinase is a key regulator of glutamatergic receptors, especially NMDAR, which is one of the main receptors in the glutamatergic synapses. Notably, PSD-95 is critical to locate and regulate protein Tyr kinases at NMDAR (Kalia and Salter, 2004), anchoring NMDAR to the post-synaptic membrane and activating the receptors. Furthermore, NMDAR activity requires a balance between dephosphorylation (mediated by phosphatases) and phosphorylation (mediated by Tyr kinases) of NMDAR subunits. The activity of Src depends on SH2 and SH3 domains, since, when they are compromised it decreases the autophosphorylation of Src in the activation loop, affecting its kinase activity and consequently, its capacity to phosphorylate NMDAR (Groverman, et al., 2011). The GluN2A subunit of NMDAR is phosphorylated mainly in three residues: Tyr-1292, Tyr-1325, and Tyr-1387 (Yang and Leonard, 2001). Of note, Fyn and Src phosphorylate GluN2B (located in the PSD area) at Tyr-1472 residue (Nakazawa et al., 2006; Choi et al., 2011). Thus, Src kinases are up-regulators of NMDAR function by increasing single-channel gating without changing NMDAR single-channel conductance (Wang and Salter, 1994; Wang et al., 1996) (**Figure 8**).

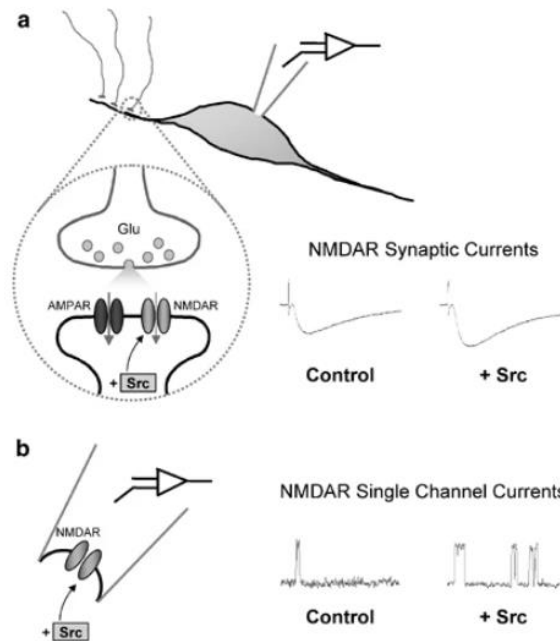


**Figure 8- Src kinase is an up regulator of NMDAR activity enhancing LTP induction.** In (a) performing the patch-clamp technique in order to evaluate NMDAR synaptic currents and after the application of recombinant Src an enhancement in NMDAR synaptic currents is observed. (b) Higher NMDAR single-channel currents and increased NMDAR channel activity are observed in the presence of Src, without affecting the conductance of NMDAR (Kalia and Salter, 2004).

Src kinases are key agents in glutamatergic synapses promoting LTP induction. The involvement of Src was first proposed by O'Dell which suggested that LTP induction in the CA1 region requires the NMDAR activity, an influx of  $Ca^{2+}$  and the activation of protein tyrosine kinases (O'Dell et al., 1991). More importantly, the activation of postsynaptic Src is responsible for the induction and the early stabilization of tetanic LTP (Huang and Hsu, 1999). The model for LTP induction proposes that a tetanic stimulation activates the cell adhesion kinase  $\beta$  (CAK $\beta$ /PYK2) and then induces Src activation, which overcomes the suppressed NMDAR function mediated by tyrosine phosphates, STEP. Furthermore,  $Ca^{2+}$  influx and  $Mg^{2+}$  decrease trigger a signalling cascade (Salter and Kalia, 2004) and an increased AMPAR mediated currents and the consequent LTP induction (Bliss and Collingridge, 1993). Thus, beyond the phosphorylation of NMDAR subunits, Src kinase also phosphorylates AMPAR, namely the GluA2 subunit at Tyr- 876 (near its C-terminal), which binds GluA2 subunit to glutamate receptor interaction protein 1 (GRIP1), a protein crucial for synaptic strengthening (Hayashi and Huganir, 2004; Yong et al., 2020). Furthermore, AMPAR is maintained at postsynaptic sites through  $\alpha$ -actinin, a critical PSD-95 anchor, which ties the AMPAR - PSD-95 complex at this

particular location in a Src-dependent manner (Matt et al., 2018; Bissen and Acker-Palmer, 2019).

#### **1.4.4 Src kinase in AD**

One of the first evidence of SFK involvement in AD was finding a more intense labelling of Fyn in AD patients' brains, when compared to healthy patients (Shirazi and Wood, 1993). Furthermore, administration of A $\beta$  to primary human and rat brain cortical cultures showed an increased Tyr phosphorylation, suggesting a possible role of Tyr kinases in A $\beta$ -mediated effects (Williamson et al., 2002). Interestingly, BACE1 activity and consequent A $\beta$  production are inhibited by SFK inhibitors and depletion of endogenous Src with RNAi, which suggests that the activity of BACE1 is regulated by Src (Zou et al., 2007). These studies suggested a regulation loop in which A $\beta$  leads to Src activation, which further increases A $\beta$  production. Also, in this sense, the generation of A $\beta$  requires the internalization of membrane-bound APP which is dependent on the activation of the adaptor protein Mint2, which is regulated by Src (Chauffy et al., 2012). SFK (Src and Fyn) are also involved in the modulation of NMDARs specially through the phosphorylation of GluN2B subunit, fundamental for synaptic plasticity, (Zhang et al., 2008; Nakazawa and Yamamoto, 2002) and are involved in mediating A $\beta$ -induced excitotoxicity, suggesting that increased Src activation may lead to increased NMDARs and further A $\beta$ -mediated excitotoxicity. A deregulation in the Src-dependent signalling pathway involving GluN2B and post-synaptic actin cytoskeleton depolymerisation was observed in the hippocampus in early stages of AD (Mota et al., 2014). Moreover, PSD-95 which is tethered to NMDAR at the synapse is phosphorylated by Src kinase at Tyr-523 residue, facilitating NMDAR-mediated currents and contributing to the overactivation of NMDARs (Du et al., 2009). Tau protein is phosphorylated by Src. Importantly, in primary human and rat brain cortical cultures treated with A $\beta$  peptide, enhanced Tyr phosphorylation of tau protein and actin cytoskeletal is observed (Sharma et al., 2007; Williamson et al., 2002). Moreover, primary murine microglia cultures exposed to A $\beta$ O show higher neuroinflammation although, after using Src/Abl inhibitor, dasatinib (Dhawan et al, 2012) this A $\beta$ -induced effect is attenuated. Furthermore, after peripherally injected with the c-Abl inhibitor imatinib, AD transgenic mice showed decreased levels of A $\beta$ O measured in the plasma and brain (Estrada et al., 2017). Similarly, inhibition of Fyn activity also showed interesting results. In mice expressing mutant human amyloid precursor protein (hAPP), and presenting higher Fyn expression correlated with cognitive deficits, A $\beta$ -induced memory impairments was neutralized after Tyr kinase

inhibition (Chin et al., 2005). Additionally, treatment of the APP<sup>swe</sup>/PS1 $\Delta$ E9 AD mouse model with the Fyn inhibitor saracatinib, remarkably improved their spatial memory (Smith et al., 2018). Thus, regulation of Src activity might constitute a promising therapeutic strategy in AD.

### **1.5 Objectives**

AD is one of the most prevalent neurodegenerative disorders worldwide, characterized by the accumulation of extracellular plaques and intracellular neurofibrillary tangles mainly composed by A $\beta$  and hyperphosphorylated Tau, respectively. Neurons are highly energy-demanding cells that rely on mitochondria. Importantly, mitochondrial dysfunction has been associated with the progression of neurodegenerative disorders (Federico et al., 2012). Thus, changes in mitochondrial dynamics and function affect Ca<sup>2+</sup> homeostasis and ATP production (Alberdi et al., 2010; Zhang et al., 2015), modulating synaptic activity and dendritic spine dynamics. In addition, the SFK is found throughout the brain and is involved in the regulation of a large variety of cellular processes, such as cell survival, presynaptic vesicles trafficking and regulation of glutamatergic receptors. More interestingly, Src was found in mitochondria (Ohnishi et al., 2011).

Previously our group showed that A $\beta$ <sub>1-42</sub> oligomers (A $\beta$ O<sub>1-42</sub>) induces mitochondrial hydrogen peroxide (H<sub>2</sub>O<sub>2</sub>) production and Src activation, which were prevented by antioxidants (Fão, 2016). In the present study we aimed to evaluate the impact of A $\beta$ O on dendritic mitochondrial function and dynamics in mature hippocampal neurons, which are highly affected in AD, and how these changes are related with modified synaptic plasticity, namely through the assessment of dendritic spine dynamics. Importantly, and considering the role of Src in AD brain, our study also aims to assess the role of Src on A $\beta$ -induced dysfunction, both in mitochondria and dendritic spines. For this purpose, the following specific objectives were pursued:

- I. **Evaluate the impact of A $\beta$ O<sub>1-42</sub> on dendritic mitochondrial function and dynamics in mature hippocampal neurons.**

Cultured hippocampal neurons exposed to A $\beta$ O suffer a reduction in the number of moving mitochondria and their velocity (Rui and Zheng, 2016). In addition, A $\beta$ O<sub>1-42</sub> induces a massive Ca<sup>2+</sup> entry into the hippocampal neurons,

promoting mitochondrial  $\text{Ca}^{2+}$  overload and cause oxidative stress and excitotoxicity (Sanz-Blasco et al., 2008), accompanied by changes in mitochondrial morphology, in particular mitochondrial fragmentation (Martorell-Riera et al., 2014). Thus, we aimed to characterize in more detail the distribution and motion of mitochondria in cultured hippocampal neurons exposed to  $\text{A}\beta_{1-42}$  (acute exposure and 24h incubation). Mitochondrial function was evaluated by determining mitochondrial  $\text{Ca}^{2+}$  oscillations, and mitochondrial dynamics was assessed through the analysis of mitochondrial movement and morphology (aspect ratio and circularity).

**II. Evaluate the correlation between mitochondrial changes and dendritic spine dynamics after exposure to  $\text{A}\beta_{1-42}$  in mature hippocampal neurons.**

We previously demonstrated that  $\text{A}\beta_{1-42}$  induces neuronal MTs disassembly in association with neurite retraction, in a process regulated by the NMDARs in mature hippocampal cells (Mota et al., 2012). Importantly, the long-range transport of mitochondria occurs along the MTs. In the CNS, mitochondria may be located at synapses, acting as energy suppliers, and regulating synaptic strengthening, stability, and signalling (Devine and Kittler, 2018). Importantly, changes in mitochondrial morphology and number within dendrites might affect the formation and maintenance of dendritic spines and potentially modulate synaptic plasticity (structural neuroplasticity) (Nakahata and Yasuda, 2018). Thus, we aimed to evaluate the morphological changes of dendritic spine structure (total length, head width, ratio, see Table1) and spine classification distribution in cultured mature hippocampal neurons exposed to  $\text{A}\beta_{1-42}$  (acute and 24h exposure) and correlate these changes with mitochondrial changes.

**III. Evaluate the role of Src on  $\text{A}\beta$ -induced mitochondrial dysfunction and postsynaptic dendritic spine morphological changes and function in hippocampal glutamatergic synapses.**

Src modulates mitochondrial activity and it is also fundamental for a proper function of NMDARs. We previously described a deregulation in the Src-dependent signalling pathway involving GluN2B and a post-synaptic actin

cytoskeleton depolymerization in the hippocampus in early stages of AD (Mota et al., 2014). Thus, this work aimed to evaluate the role of Src in A $\beta$ O–induced changes in mitochondrial dynamics and function and in synaptic plasticity using a selective Src inhibitor, SU6656.

## **CHAPTER II – MATERIALS AND METHODS**

## **2.1 Materials**

Neurobasal medium, gentamicin, B27 supplement and horse serum were purchased from GIBCO (Paisley, UK). The synthetic A $\beta$ 1-42 peptide was obtained from Bachem (Bubendorf, Switzerland). Bradford protein assay was purchased from BioRad (Hercules, CA, USA). Acrylamide, methanol, acetic acid was purchased from Thermo Fisher Scientific (Rockford, IL, USA). Other analytical grade reagents were from Sigma Chemical and Co. (St. Louis, MO, USA). pDsRed2-Mito Vector (MitoDsRed) was obtained from Clontech (catalog no: 632421), pCMV6-AC-GFP Vector (GFP) was purchased from Orgene (catalog no: PS100010) and pCMV-CEPIA3mt was obtained from Addgene (catalog no: 58219). M-cherry vector was kindly gifted by Ana Luísa Carvalho laboratory (CNC).

## **2.2 Primary Hippocampal Cultures**

Primary hippocampal neurons culture was prepared as described previously (Ambrósio et al., 2000), with some modifications. Pregnant Female Wistar rats (E17-18) were anesthetized using isoflurane and then sacrificed by cervical dislocation. Embryos were placed in isolation medium containing 120 mM NaCl, 1.2 mM KH<sub>2</sub>PO<sub>4</sub>, 5 mM KCl, 14.3 mM glucose, 10 mM HEPES, 0.1% phenol red, pH 7.3 and hippocampus were dissected out. Hippocampus were mechanically digested by up and down using a micropipette in plating medium solution containing 84 mM MEM containing 43.3 mM NaHCO<sub>3</sub>, 33 mM glucose, 1 mM sodium pyruvate, 10% inactivated horse serum, pH 7.3 and cells were plated at a density of  $4.2 \times 10^4$  cells/cm<sup>2</sup> in poly-D-lysine coated glass coverslips for two hours in plating medium. Then, plating medium was replaced by Neurobasal medium supplemented with 2% B27, 25  $\mu$ M glutamate, 0.5 mM glutamine and 0.12 mg/mL gentamicin and cells were cultured for 17 DIV in 95% air and 5% CO<sub>2</sub>. To reduce glia growth, 10  $\mu$ M of the mitotic inhibitor 5-fluoro-2'-deoxyuridine was added to the culture at 72 hours in culture. One half of the medium was changed with fresh medium without added glutamate or 5-FDU every 7 DIV. Previous data obtained in the group evidenced the presence of 1.7% of astrocytes in our cultures. All animal experiments were carried out in accordance with the guidelines of the Institutional Animal Care and Use of Committee and the European Community directive (2010/63/EU) and protocols approved by the Faculty of Medicine, University of Coimbra (ref: ORBEA\_211\_2018) and the Direção Geral de Alimentação e Veterinária (DGAV, ref: 0421/000/000/2019). All

efforts were made to minimize animal suffering and to reduce the number of animals used.

### **2.3 A $\beta$ O<sub>1-42</sub> Preparation**

A $\beta$ O<sub>s</sub> were prepared from synthetic A $\beta$ <sub>1-42</sub> peptide according to a previously described protocol (Klein, 2002). Briefly, synthetic A $\beta$  peptide was dissolved in cold 1,1,1,3,3,3-hexafluoro-2-propanol (HFIP) to a final concentration of 1 mM and aliquoted. The peptide—HFIP solutions were incubated at room temperature for 60 min, with the vial closed and then was back on ice for 5-10min. HFIP was first evaporated overnight in the hood at room temperature and then removed in a Speed Vac (Ilshin Lab. Co. Ltd., Ede, The Netherlands), and dried HFIP film was stored at -20°C. When necessary, the peptide film was resuspended to make a 5 mM solution in anhydrous dimethyl sulfoxide and then dissolved in phenol red-free Ham's F-12 medium without glutamine to a final concentration of 100  $\mu$ M, and incubated overnight at 4°C. The preparation was centrifuged at 14,000  $\times$ g for 10 min at 4°C to remove insoluble aggregates, and the supernatant containing soluble oligomers and monomers was transferred to pre-lubricated clean tubes (Costar) and stored at -20°C. Protein content was determined by using the BioRad protein assay and quantified by using a microplate reader Spectra Max Plus 384 (Molecular Devices, USA). The presence of different assembly peptide forms (monomers, oligomers and/or fibrils) in the preparation was evaluated by 4–16% non-denaturing Tris–Tricine PAGE gel electrophoresis and further staining with Coomassie blue. Typically, our preparations evidence only oligomers from 16 to 24 kDa, no fibrils and no monomers visible in the gel.

### **2.4 Cell Transfection**

Primary hippocampal neurons were transfected when still immature at 8 DIV using calcium phosphate co-precipitation protocol. Briefly, 4 coverslips were placed in a 60 mm petri dish with 4 mL of fresh Neurobasal medium supplemented with B27 plus 1 mL of cell conditioned Neurobasal medium. A solution 1 was prepared adding sequentially TE solution (in mM: 1 Tris-HCl, 1 EDTA, pH 7.3), 1  $\mu$ g of plasmid per coverslip and 2.5 mM CaCl<sub>2</sub> (in 10 mM HEPES, pH 7.2) added dropwise to a final volume of 150  $\mu$ l. Then, solution 1 was mix dropwise with an equal volume of solution 2, 2x HBS (in mM: 12 dextrose, 50 HEPES, 10 KCl, 280 NaCl and 1.5 Na<sub>2</sub>HPO<sub>4</sub>·2H<sub>2</sub>O, pH 7.2) using a

micropipette while bubbles were made in the microtube using another micropipette. The transfection solution was added to the cells dropwise and incubated for 1h30m (at 37°C, 5% CO<sub>2</sub>). Transfection medium was then removed, and precipitates dissolved using 5 ml of Stop solution containing 20 mM Hepes in Neurobasal medium (pH 6.8). Cells were washed 3 times with PBS composed by 136.9 mM NaCl, 8.10 mM Na<sub>2</sub>HPO<sub>4</sub>, 1.5 mM KH<sub>2</sub>PO<sub>4</sub>, 2.7 mM KCl, pH 7.3, and then return to their initial culture plate.

## **2.5 Live-Cell Imaging-Calcium Fluorescence**

Hippocampal neurons were co-transfected with M-cherry and CEPIA3mt plasmids, kindly gifted by Ana Luísa Carvalho's laboratory (CNC) and Matsamitsu Iino's laboratory (Japan) respectively, to fill in the cell and follow mitochondrial Ca<sup>2+</sup> flux. In fact, CEPIA (calcium-measuring organelle-entrapped protein indicators) 3mt is a mitochondrial green fluorescent with a moderately low affinity for calcium that allows to follow Ca<sup>2+</sup> levels within mitochondria by direct detection of fluorescence (Suzuki et al., 2014). Mitochondrial Ca<sup>2+</sup> was recorded for 10 min in Mg<sup>2+</sup>-free Na<sup>+</sup> medium (containing 140 mM NaCl, 5 mM KCl, 1 mM CaCl<sub>2</sub>, 1 mM MgCl<sub>2</sub>, 10 mM glucose, 10 mM Hepes, pH 7.4/NaOH) supplemented with 20 μM glycine and 30 μM serine to maximize NMDAR activation, using a 40x objective, on a Carl Zeiss Axio Observed Z1 inverted confocal microscope, using the CSU-X1M spinning disc technology (Zeiss, Jena, Germany). Parameters of acquisition were one image per 5 sec before stimulus and one image per 2 sec after stimulus. Differences of mitochondrial Ca<sup>2+</sup> levels between conditions were assessed by calculation of the fluorescence variation after 1 μM Aβ<sub>1-42</sub> stimulus, in the presence or absence of 5 μM SU6656, and after maximal mitochondrial depolarization using the formula  $\Delta F/F_0$  ratio (where  $\Delta F = F - F_0$ , F represents the calcium fluorescence after stimulus and F<sub>0</sub> the Ca<sup>2+</sup> resting fluorescence intensity) in a defined region of interest (ROI), corresponding here to a neurite. Maximal mitochondrial depolarization (mmp collapse) was achieved by adding a protonophore (0.5 μM carbonyl cyanide-4-(trifluoromethoxy) phenylhydrazone (FCCP)). Variation of fluorescence in neuritis was assessed using the Time Series Analyzer V3 plugin (software FIJI). Data were then analyzed using Excel (Microsoft, Seattle, WA, US).

## **2.6 Mitochondrial Movement Analysis**

MitoDsRed plus GFP co-transfected hippocampal neurons were washed and incubated in Na medium supplemented with 20  $\mu$ M glycine and 30  $\mu$ M serine at 37°C for mitochondrial movement studies. Neuronal projections were imaged every 2 seconds for a total of 601 frames (during 10 min), using a 63x objective with NA=1.4, on a Carl Zeiss Axio Observed Z1 inverted confocal microscope, using the CSU-X1M spinning disc technology (Zeiss, Jena, Germany). When necessary, histograms were matched to the first frame to correct fluorescence variations using Bleach Correction plugin developed by Miura and Rietdorf (2014), and time lapse-dependent x-y drift was corrected by applying the TurboReg plugin. Then, mitochondrial movement analysis was performed using the KymoAnalyzer package of macros (Newman et al., 2017) in FIJI following authors instructions in which a ROI was defined as a neurite (traced using the GFP image). Of note, the velocity of all moving mitochondria is calculated as the slope of kymograph lines. We then selected relevant parameters considering the specificity of mitochondrial movement, namely density, type of movement, percentage of time in pause, anterograde and retrograde movement, run length, segmental velocity, and switch. Briefly, to calculate segmental velocity, the macro only considered the segments of the mitochondria which were moving and, when mitochondria presented a complex movement composed by different segments, we calculated the average velocity *per* mitochondria using the information provided by the automatic analysis.

## **2.7 Morphology Analysis**

Analysis of mitochondrial morphology was performed in images of neuronal projections (MitoDSRed plus GFP) acquired using a 63x objective with NA=1.4, on a Carl Zeiss Axio Observed Z1 inverted confocal microscope using the CSU-X1M spinning disc technology (Zeiss, Jena, Germany) obtained after acquisition of mitochondrial movement. The macros AutoROI and MitoProtAnalyser for FIJI were applied to assess the following parameters *per* mitochondrion: aspect ratio and circularity. AutoROI was used to define ROIs (e.g. a neurite), whereas mitochondrial morphological parameters within the ROI were extracted using MitoProtAnalyser. Importantly, some adaptations were performed in the original code of MitoProtAnalyser considering the type of information pretended and the properties of the Z-Stacks acquired. The first correction was in the function "protpresence" where protein channel was set to 1 corresponding to the filling channel (GFP) in the Z-stack image, thus removing the protein analysis of mitochondria. Besides,

in the function 'mitos' the channel was set to 2 corresponding to mitochondria (MitoDsRed) in our Z-stack. Finally, we added a pause in the code in order to extract information (aspect ratio and circularity) per mitochondrion within a ROI instead of only obtaining an average value for the initial ROI defined. This last modification also allowed us to see the mitochondrial mask (**Figure 9**) designed by the macro, which is an important step to validate our model.

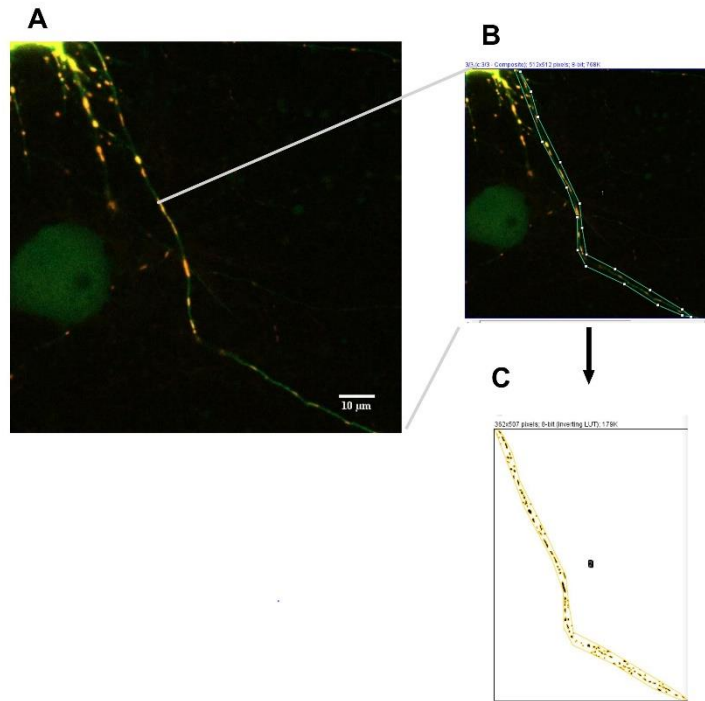


**Figure 9-Main steps of MitoProtAnalyser a macro for FIJI/imageJ.** Z-stack obtained in Spinning disk confocal microscope (**A**); ROI containing a neuronal extension with mitochondria target for morphological evaluation (**B**); Mitochondrial mask (**C**).

The morphological parameters used to analyse mitochondrial morphology were:

- Mitochondrial aspect ratio, the ratio between the major and minor axes of a fitted ellipse:

$$\text{Aspect ratio} = \frac{\text{Major Axis}}{\text{minor Axis}} \quad (1)$$

- Mitochondrial circularity, where a value of 1 indicates a perfect circle, whereas values as close to 0 indicate increasingly elongated shape mitochondria.

$$Circularity = \frac{4\pi Area}{Perimeter^2} \quad (2)$$

## **2.8 Spine Morphology Analysis**

Spine morphology analysis was performed in images of neuronal projections (GFP) acquired using a 63x objective with NA=1.4, on a Carl Zeiss Axio Observed Z1 inverted confocal microscope using the CSU-X1M spinning disc technology (Zeiss, Jena, Germany) obtained after acquisition of mitochondrial movement. Average intensity Z-projections were obtained using FIJI/ImageJ; image brightness and contrast levels were adjusted for better visualization using the Brightness and Contrast tool of the software. We then performed an image segmentation through the creation of a binarized image using the SpineJ plugin for FIJI/ImageJ and dendritic spine parameters (length and width) were measured using the segmented and straight-line selection tool of ImageJ, to measure manually the total length and width of the spines. Different classifications were obtained based on spine parameters of **Table 1**.

**Table 1-Spine classification according to the head, length and width.** The ratio between spine width and length is used to determine the classification of a spine in a set of four possible categories: Filopodia, Stubby, Thin and Mushroom (Olaya et al., 2015).

Spine type/parameter	Head	Length	Width/length ratio
		$\mu m$	
Filopodia	No	>1.2	Not applicable
Stubby	No/Yes	<1.2	If the head is present, <0.5; if no head, not applicable
Thin	Yes	>1.2	<0.5
Mushroom	Yes	Not applicable	>0.5

## **2.9 Statistical Analysis**

Data were expressed as the mean  $\pm$  SEM of the number of experiments or elements (neuritis or mitochondria) indicated in the figure legends. The normal distribution of each population was analysed and all experimental groups were considered non-parametric. Thus, comparisons among multiple groups (relative to control or to A $\beta$ O treatment) were performed by non-parametric one-way analysis of variance (ANOVA), followed by the Kruskal-Wallis Multiple Comparison post-hoc test. Mann-Whitney U-test was also performed for comparison between two populations, as described in figure legends. Significance was defined as  $p < 0.05$ .



## **CHAPTER III – RESULTS**

### **3.1 A $\beta$ O<sub>1-42</sub> alters neurite mitochondrial movement in mature hippocampal neurons – influence of Src**

Previous studies evidence that exposure to A $\beta$ O in primary hippocampal cultures decreases the number of motile mitochondria, their velocity and run length (Calkins and Reddy, 2011; Rui and Zheng, 2016), compromising the energy supply of synapses and ultimately causing their loss, a neuropathological feature observed in AD.

Src is found within mitochondria, where it participates in the modulation of its activity (Hebert-Chatelain, 2013). Moreover, Src is involved in the regulation of NMDAR (Yang and Leonard, 2001) and consequently in local Ca<sup>2+</sup> influx modulation, which *per se* regulate mitochondrial movement (Lovas and Wang, 2013).

In this context, we investigated the role of Src in A $\beta$ O-induced mitochondrial movement changes using a specific inhibitor, SU6656 (5 $\mu$ M). The effect of A $\beta$ O<sub>1-42</sub> was tested for 10 min and 24h treatment (A $\beta$ a and A $\beta$ 24h, respectively). We also assessed the involvement of NMDARs using MK-801 (10 $\mu$ M), a NMDAR non-competitive antagonist.

**Figure 10** shows the categorization of mitochondria according to its motion state using the results from the Net Cargo Population macro from the KymoAnalyzer plugin. Our data evidence no significant changes in the type of movement distribution of mitochondria between conditions (**Figure 10A**). **Fig. 10Aii** and **iii** show a trend for an increase in mitochondrial anterograde movement, associated to a decrease in the retrograde movement, following exposure to A $\beta$ O<sub>1-42</sub> for 24h.

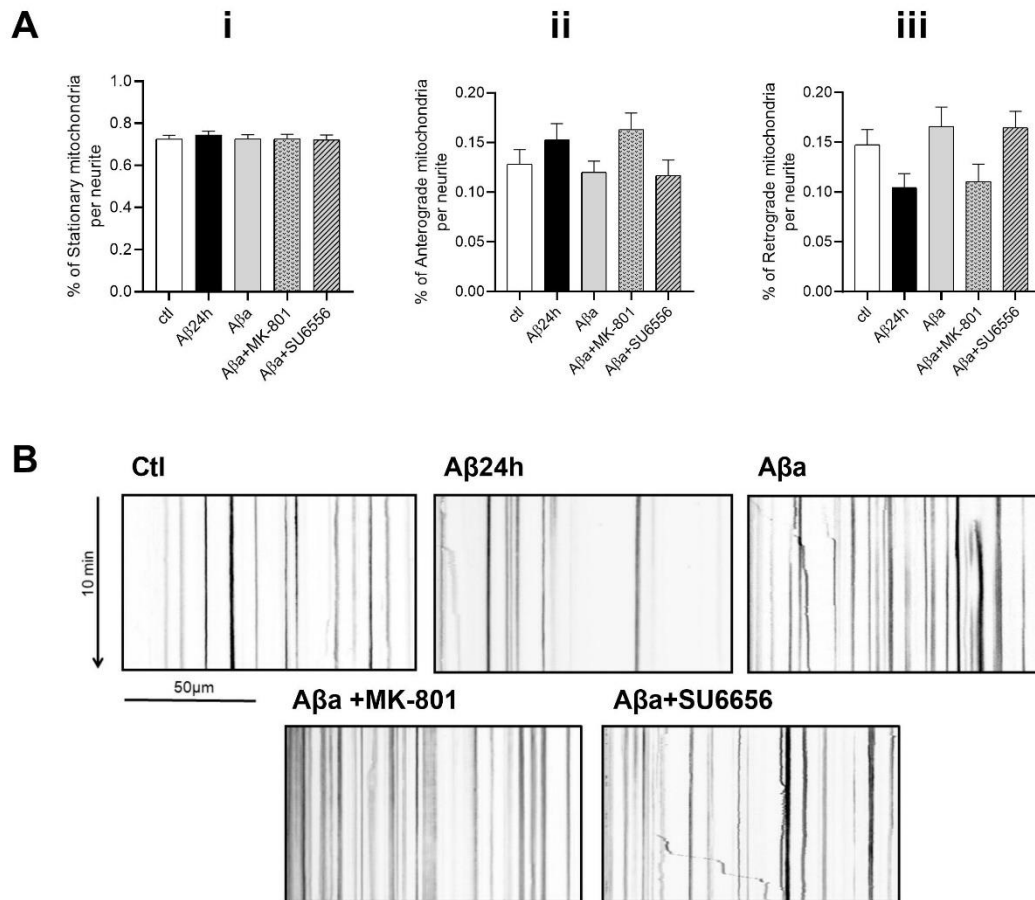


**Figure 10-Mitochondrial distribution parameters and respective kymographs following exposure to A $\beta$ O<sub>1-42</sub> in hippocampal neurons.** Mitochondrial distribution parameters were assessed in mature hippocampal neurons co-transfected with MitodsRed (red) and GFP plasmids and treated with 1  $\mu$ M A $\beta$ O, for 10 min and 24h. Neurons were pre-incubated with 10  $\mu$ M MK-801 or 5  $\mu$ M SU6656. Mitochondrial movement was recorded for 10 min using a Spinning disk confocal microscope and analyzed using the Fiji software and the KymoAnalyzer plugin that (A) categorizes mitochondria based on their directionality of movement and fraction of mitochondria moving in anterograde (ii), retrograde (iii) directions, or those that are stationary (i). (B) shows representative kymographs of MitodsRed-labeled mitochondrial transport in neurites. The kymograph was generated from a 10 min movie (301 frames, 1 frame every 2 sec). Scale bar: 50  $\mu$ m. Data are the mean  $\pm$  SEM of n=5-9 experiments, 5 to 10 dendrites per experiment.

Besides classifying particle trajectories, the Kymoanalyzer plugin also systematically calculates velocities, pauses and other movement parameters, which are depicted in **Figure 11**. **Figure 11A** shows the average run length traveled by a single mitochondrion. Although, exposure to A $\beta$  did not induce significant changes in run length for anterograde and retrograde movement (**Figure 11 Ai and ii**, respectively), data evidence a tendency for decreased run length in anterograde movement after A $\beta$  treatment. **Figure 11B**

depict the average segmental velocity of mitochondria along the experiment. Importantly, to calculate the average velocity, the plugin only takes into consideration the moments when the particle is moving during the acquisition, discarding the stationary episodes. Our data evidence no effect of  $A\beta_{O_{1-42}}$  on anterograde movement regarding the mitochondrial velocity; however, we observed a significant increase in mitochondrial velocity in retrograde movement after 10 min exposure to  $A\beta$ , which was maintained after 24h (**Figure 11 Bii**). Interestingly, pre-treatment with MK-801 (NMDAR antagonist) prevented this increase, while SU6656 exacerbated it (**Figure 11 Bii**). Data depicted in **Figure 11 C** indicate the percentage of time each mitochondrion remained stationary, in anterograde and retrograde movement. Results indicate a significant decrease in the percentage of time in which mitochondria remained stationary after 10 min exposure to  $A\beta$ , when compared to control condition, which was not maintained after 24h. This effect was not prevented neither by MK-801, nor by Src inhibition (**Figure 11 Ci**). Interestingly, concomitantly with a decrease in time spend stationary, a significant increase in the percentage of time spend in anterograde and retrograde (**Figure 11 Cii and iii**, respectively) was observed. Notably, pre-treatment with MK-801 significantly decreased  $A\beta$ -induced increase in retrograde movement (**Figure 11 Ciii**). In **D**, we assessed the average number of movements switch each mitochondrion performed during the acquisition. Results evidence a significant increase in the number of switch *per* mitochondrion after acute exposure to  $A\beta_{O_{1-42}}$  (**Figure 11 D**), which was not prevented by MK-801 or SU6656.

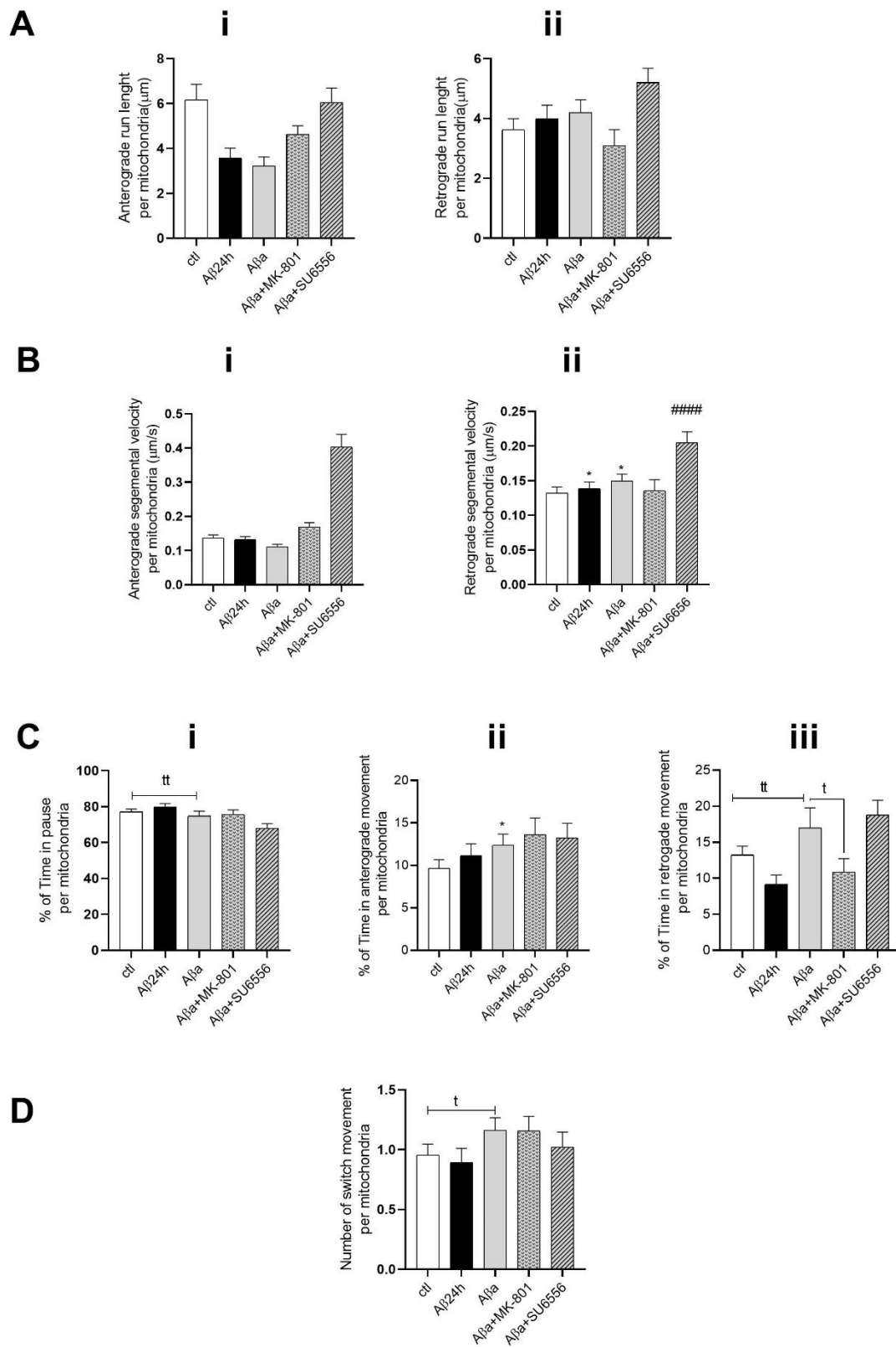


**Figure 11-Mitochondrial movement parameters in hippocampal neurons treated with AβO<sub>1-42</sub>.** Mitochondrial movement parameters were assessed in mature hippocampal neurons co-transfected with MitodsRed (red) and GFP plasmids and treated with 1 μM AβO for 10 min or 24h

versus non-treated (Control, Ctl) conditions. When indicated, neurons were pre-incubated with 10  $\mu$ M MK-801 or 5  $\mu$ M SU6656. Mitochondrial movement was recorded for 10 min using a spinning disk confocal microscope and analyzed using the Fiji software and the KymoAnalyzer plugin. Mitochondrial run length corresponds to the distance traveled per mitochondrion in a neurite (A) in anterograde movement (i) and retrograde movement (ii). Segmental velocity (B) is calculated from combined segments in moving anterograde mitochondria and (i) retrograde mitochondria (ii). The percentage of time in motion (C) describes the percentage of time in which a particle is in anterograde motion (i), pausing (ii) or retrograde motion (iii), throughout the period of imaging. Mitochondria switch corresponds to the number of changes in movement type per mitochondria during the acquisition (D). Movie of mitochondrial movement was generated during 10 min acquisition at the rate of 1 frame every 2 sec (301 frames total). Data are the mean  $\pm$  SEM of n=9 experiments, considering 5 to 10 dendrites per experiments. Statistical analysis: (A) ###p<0.01 versus A $\beta$ , #p<0.05 versus A $\beta$  and \$p<0.05 A $\beta$ +MK-801 versus A $\beta$ +SU6656 (Kruskal-Wallis, followed by Dunn's test); (B) ##p <0.01 versus A $\beta$ , ####p<0.0001 and \$\$\$p<0.0001 A $\beta$ +MK-801 versus A $\beta$ +SU6656 (Kruskal-Wallis) (C) \*p<0.05 versus control (Ctl) (Kruskal-Wallis, followed by Dunn's test), ## p<0.01 versus A $\beta$ , tt p<0.01 versus Ctl (Mann-Whitney test) and tp<0.05 versus A $\beta$  (Mann-Whitney) (D) tp<0.05 versus Ctl (Mann-Witney) and #p<0.05 versus A $\beta$  (Kruskal – Wallis followed by Dunn's test).

### **3.2 A $\beta$ O<sub>1-42</sub> impact on neurite mitochondrial morphology in a Src dependent manner**

Considering the effects of A $\beta$ O<sub>1-42</sub> on mitochondrial function previously observed by the group (Fão, 2016; Ferreira et al., 2015) and the impact of A $\beta$  on mitochondrial dynamics (Wang, et al., 2009) herein, we analysed the effect of A $\beta$ O<sub>1-42</sub> on mitochondrial morphology-associated parameters as well as the role of NMDARs and Src kinase. Results depicted in **Figure 12B** evidence that A $\beta$ O<sub>1-42</sub> do not affect mitochondria density, neither after 10 min, nor after 24h of exposure. Interestingly, results evidence a significant decrease in mitochondrial aspect ratio (**Figure 12C**) and increase in mitochondrial circularity (**Figure 12 D**) after 10 min exposure to A $\beta$ O<sub>1-42</sub> which is maintained after 24h. These results suggest a decrease in length and in mitochondrial shape complexity probably correlated with increased fragmented organelle (Miyazono et al., 2018). Importantly, pre-treatment with SU6656 and with MK-801 significantly reverted A $\beta$ O<sub>1-42</sub> effect, suggesting that A $\beta$ -induced mitochondrial fragmentation occurs in a Src- and NMDAR-dependent manner.

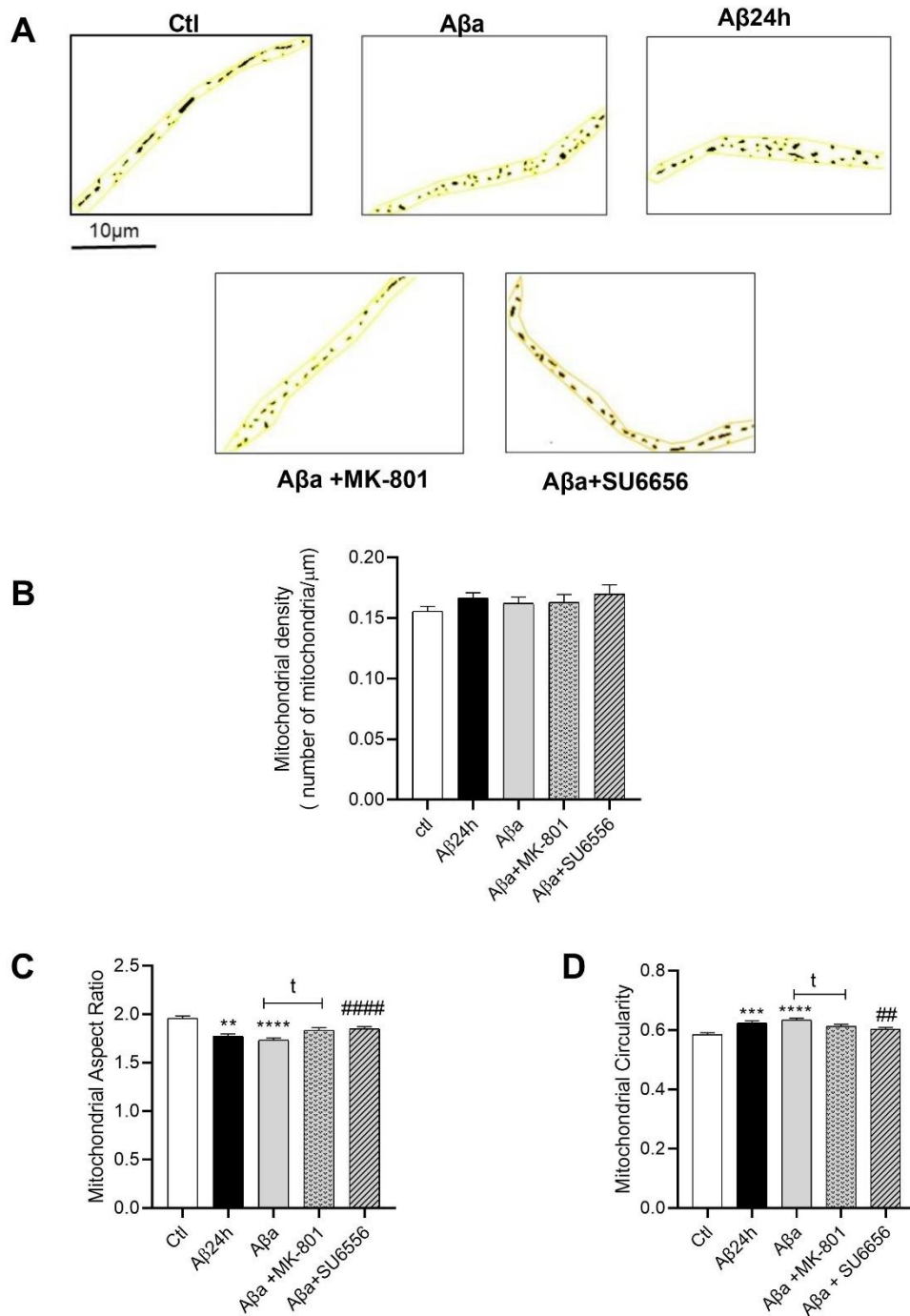


**Figure 12-Mitochondrial morphology evaluation in mature hippocampal neurons exposed to Aβ<sub>1-42</sub>.** Mature hippocampal neurons co-transfected with MitodsRed (red) and GFP plasmids were treated with 1 μM Aβ<sub>1-42</sub> for 10 min and 24h and, when indicated, the involvement of NMDARs and Src kinase were assessed using 10 μM MK-801 and 5 μM SU6656, respectively. Images of neuritic mitochondria were acquired using a spinning disk confocal microscope, and mitochondrial morphology parameters were assessed. **(A)** Representative masks of mitochondria obtained using macros AutoROI and MitoProtAnalyser for FIJI/ImageJ (Scale bar: 10 μm). **(B)** Mitochondrial

density (average number of mitochondria per  $\mu\text{m}$  and per neurite). **(C)** Aspect Ratio and **(D)** Circularity. Data are the mean  $\pm$  SEM of  $n=5$  experiments, considering 5 to 10 dendrites per experiment. Statistical analysis: (C)  $**p<0.01$ ,  $***p<0.001$  and  $****p<0.0001$  versus Ctl,  $##p<0.01$ , and  $####p<0.0001$  versus  $\text{A}\beta$  (Kruskal – Wallis followed by Dunn's test) and  $^{\dagger}p<0.05$  versus  $\text{A}\beta$  (Mann-Witney test).

### **3.3. $\text{A}\beta\text{O}_{1-42}$ -induce decrease mitochondrial $\text{Ca}^{2+}$ retention in hippocampal neurites**

$\text{Ca}^{2+}$  is an important enhancer of synaptic transmission and a key regulator of mitochondrial function. Importantly,  $\text{A}\beta$ -induced oxidative stress and  $\text{Ca}^{2+}$  rise lead to neurons apoptosis (Sanz-Blasco et al., 2008). Furthermore, Src can be found in neuronal mitochondria controlling its activity (Hebert-Chatelain, 2013). Thus, considering the close relationship between  $\text{Ca}^{2+}$  homeostasis and mitochondrial function we examined the effect of  $\text{A}\beta\text{O}_{1-42}$  on mitochondrial  $\text{Ca}^{2+}$  levels and whether Src modulation could influence this effect in mature hippocampal neurons. Mitochondrial  $\text{Ca}^{2+}$  variations were measured using the CEPIA3mt plasmid as described in Material and Methods.

Acute treatment with  $\text{A}\beta\text{O}_{1-42}$  (1  $\mu\text{M}$ ) induced a transient increase in mitochondrial  $\text{Ca}^{2+}$  levels (**Figure 13 Ai and Bii**). Importantly, our preliminary results suggest that this  $\text{Ca}^{2+}$  rise might be diminished following inhibition of Src kinase (**Figure 13 Ai**). To evaluate the mitochondrial  $\text{Ca}^{2+}$  accumulation under control, after an immediate exposition to  $1\text{A}\beta\text{O}_{1-42}$  in the presence or absence of pre-incubated 5  $\mu\text{M}$  SU6656 ( $t=10\text{min}$ ), we induced mitochondrial complete depolarization using the mitochondrial uncoupler FCCP. Results depicted in **Figure 13 Aii** evidence that although  $\text{A}\beta\text{O}$  induce mitochondrial  $\text{Ca}^{2+}$  influx, the total amount of mitochondrial  $\text{Ca}^{2+}$  accumulated was significantly lower than under control/untreated conditions; these data suggest that the mitochondrial depolarization induced by  $\text{A}\beta\text{O}_{1-42}$  under the same experimental conditions (Fão, 2016) might impair mitochondrial ability to retain  $\text{Ca}^{2+}$ . Indeed, a time-dependent mitochondrial  $\text{Ca}^{2+}$  release was observed following exposure to  $\text{A}\beta\text{O}_{1-42}$  (**Figure Bii**). Preliminary data do not evidence any role of Src in the regulation of  $\text{A}\beta\text{O}_{1-42}$ -induced mitochondrial  $\text{Ca}^{2+}$  uptake (**Figure 13 Aii**).

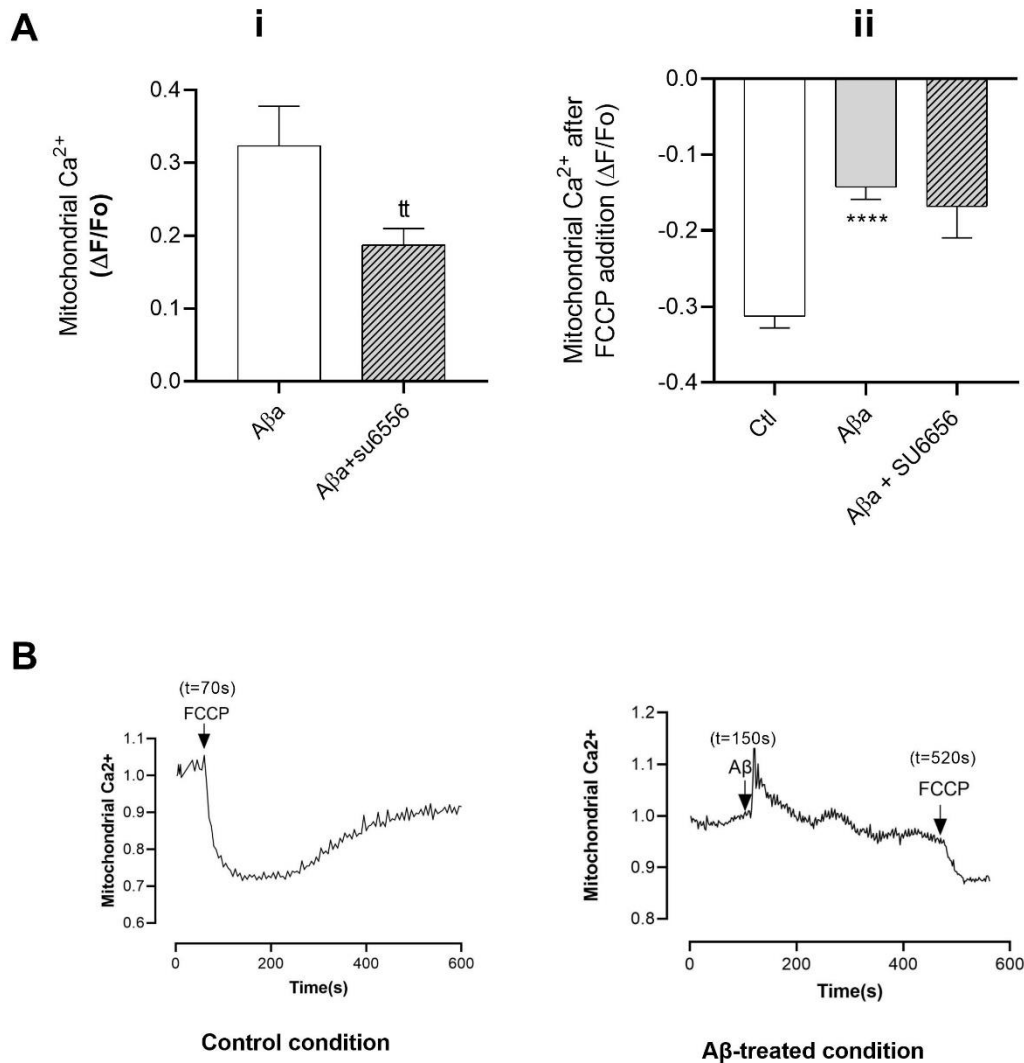


**Figure 13-Mitochondrial Ca<sup>2+</sup> levels assessed using CEPIA3mt plasmid in mature hippocampal neurons treated with Aβ<sub>1-42</sub>.** Ca<sup>2+</sup> variations were assessed in mature hippocampal neurons co-transfect with CEPIA3mt and M-cherry plasmids. CEPIA3mt fluorescence was followed using a spinning disk confocal microscope. The immediate effect of 1 μM Aβ<sub>1-42</sub> (Aβ<sub>a</sub>) was evaluated in the absence or presence of 5 μM SU6656, and mitochondrial Ca<sup>2+</sup> content assessed after complete mitochondrial depolarization using FCCP (2 μM). Image acquisition was performed every 5 seconds during the acquisition of basal fluorescence and every 2 seconds after addition of stimuli. **(A)** Data were plotted as ΔF/F<sub>0</sub> (where ΔF= F-F<sub>0</sub>, F represents the calcium fluorescence after stimulus, and F<sub>0</sub> the Ca<sup>2+</sup> resting fluorescence intensity). **(B)** Representative graphics of CEPIA3mt fluorescence variation along time, normalized to basal (F/F<sub>0</sub>). Condition of no treatment (Ctl, control) and the application of 0.5 μM FCCP (t=70 s); application of 1 μM Aβ<sub>a</sub> (t=150 s) and 0.5 μM FCCP (t=520 s); Data were analysed per mitochondrion and are the mean ± SEM of n=5 experiments for Ctl condition, n=3 experiments for Aβ<sub>a</sub> condition and n=1 experiments for Aβ<sub>a</sub>+SU6656 condition, considering 5 to 10 dendrites per experiment. Statistical analysis: **(A)** <sup>††</sup>p<0.01 versus Ctl (Mann-Witney test), <sup>\*\*\*\*</sup>p<0.0001 versus Ct (Kruskal – Wallis followed by Dunn's test).

### **3.4 A $\beta$ O<sub>1-42</sub> seem to induce a fast increase in mushroom spine content in hippocampal dendrites dependent on Src**

Dendritic spines are organized structures of F-actin that undergo modifications during synaptic plasticity; indeed, spine volume increases after LTP induction (Borczyk, 2019). Consistent reports have established a link between decreased synaptic plasticity and abnormalities in dendritic spines; as such, spine morphology seems to underlie impaired synaptic plasticity observed in AD (Dickstein et al., 2010).

We previously evidence a deregulation in Src-dependent signalling pathway involving GluN2B subunits, concomitantly with postsynaptic actin cytoskeleton depolymerisation in the hippocampus of young 3xTg-AD mice (Mota et al., 2014). Thus, in this work, we performed a preliminary spine morphology analysis in dendrites of hippocampal neurons treated with A $\beta$ O<sub>1-42</sub>, for 10 min (acute exposure) or 24h (prolonged exposure) and evaluated the involvement of Src. Data demonstrated that A $\beta$ O acutely (after 10 min exposure) induced a significant reduction in the length of spines that was accentuated after 24h (**Figure 14 Bi**). This effect seems to be significantly counteracted by the inhibition of Src kinase with SU6656 (**Figure 14 Bi**). Although the analysis of spine width did not evidence significant differences between any of the experimental conditions tested (**Figure 14 Bii**), the replotting of width and length data into the ratio width/length (**Figure 14 Biii**) evidenced a significant increase in hippocampal neurons treated with A $\beta$ O for 10 min which was promoted over time and was significantly prevented by SU6656. This ratio was then used to classify spines: thin, stubby and mushroom (see Materials and methods) (**Figure 14 C**), to assess spine population's distribution. Preliminary data suggest that A $\beta$ O treatment (10 min and 24h) induces an increase in mushroom and stubby spines, while the percentage of thin spines is decreased (**Figure 14 C**). These results suggest that A $\beta$  may trigger spine maturation (mushroom spines) in an initial phase increasing the number of stubby spines that generally results from the degradation of mushroom spines (Popugaeva et al., 2015). Interestingly, data suggest that Src inhibition does not affect spine maturation but may prevent their degradation (**Figure 14C**).

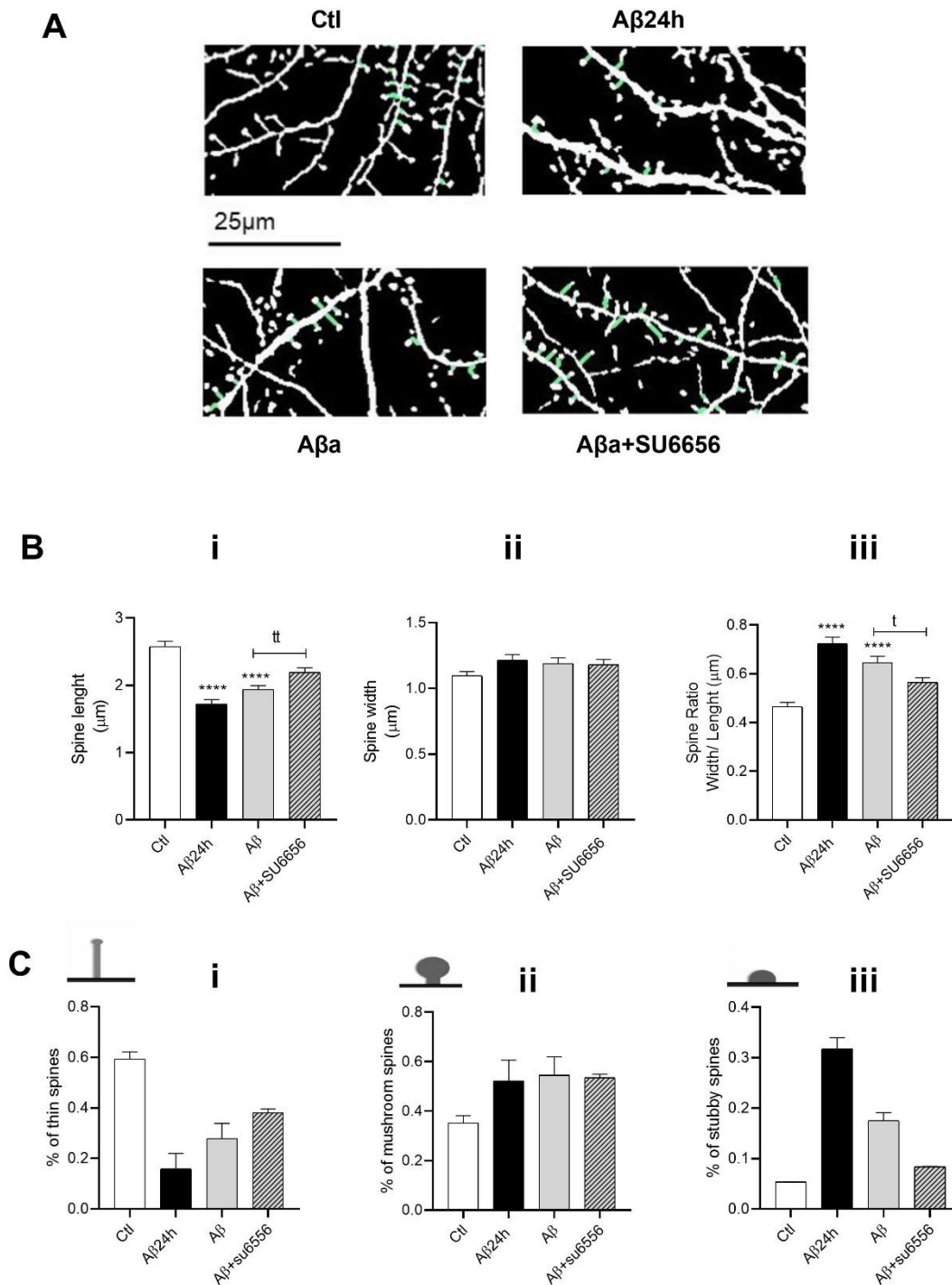


**Figure 14-Dendritic spines morphology in mature hippocampal neurons treated with Aβ<sub>1-42</sub>.** Using the images obtained from the analysis of mitochondrial movement, a binarize image from a Z-stack composed image was created. Spine parameters, namely total spine length and width, were manually measured using the straight- and segmented-line tool from FIDJI/imageJ in hippocampal neurons treated with 1 μM Aβ for 10 min (acute exposition) or 24h (prolonged exposition). The involvement of Src kinase was assessed using SU6656 (5 μM). **(A)** Representative images (binarize images) from dendritic spines (scale bar: 25 μm). **(B)** Spine Length (i), Spine Width (ii) and Spine Ratio (iii). **(C)** Dendritic spines distribution according to their classification: thin, mushroom, and stubby. Data are the mean ± SEM of n=2 considering an

average of 100 spines per n. Statistical Analysis: **(B)** \*\*\*\* $p < 0.0001$  versus Ctl, #### $p < 0.0001$  versus A $\beta$  (Kruskal – Wallis followed by Dunn's test), <sup>††</sup> $p < 0.01$  versus A $\beta$ O (Mann-Whitney test), <sup>†</sup> $p < 0.05$  versus A $\beta$ O (Mann-Whitney test) **(C)**.

## **CHAPTER IV – DISCUSSION AND CONCLUSIONS**

#### **4.1 Discussion**

A $\beta$  exposure was previously shown to induce impairments in mitochondrial motility and function that may precede the synaptic disturbances observed in AD (Trushina et al., 2012; Cai and Tammineni, 2017). Du and co-authors observed that low concentrations of A $\beta$  (0.2  $\mu$ M) in hippocampal culture neurons from transgenic mice overexpressing human APP interfered with mitochondrial trafficking, reducing the number of moving mitochondria (Du et al., 2010). Rui et al. reported that 20  $\mu$ M A $\beta_{25-35}$  caused a significant reduction in the percentage of moving mitochondria in hippocampal neurons already after 10 min treatment which became more pronounced after 30 min treatment (Rui et al., 2006). Same results were observed following treatment with 2  $\mu$ M and 20  $\mu$ M A $\beta_{1-42}$  (monomers) for 30 min (Rui et al., 2006). Later, Rui et al. showed a significant reduction in the percentage of moving mitochondria and their speed which was more pronounced in dendritic than axonal mitochondria in hippocampal neurons treated with 0.04-1  $\mu$ M A $\beta_{1-42}$  for 30 min (Rui et al., 2016). Mitochondrial movement is also affected by 24h exposure to A $\beta$ O. In fact, A $\beta$ O 2  $\mu$ M for 24h, induced a significant reduction in both directions in mitochondrial motility and velocity in hippocampal neurons (Kim et al., 2012) while 20  $\mu$ M A $\beta_{25-35}$  induced mitochondrial transport impairments in primary hippocampal neurons, affecting particularly the anterograde movement (Calkins and Reddy, 2011). In our study, we observed changes in neurite mitochondrial motility in primary mature hippocampal neurons treated with A $\beta$ O $_{1-42}$  using a detailed analysis of mitochondrial movement parameters. We evidenced an immediate effect of A $\beta$ O $_{1-42}$  (after 10 min) on mitochondrial motility, significantly reducing the percentage of time spent as stationary, and concomitantly increasing the time spent in anterograde and retrograde movements, as well as an increase in the number of switch movement *per* mitochondrion, suggesting that A $\beta$  acute treatment promotes mitochondrial movement. Interestingly, changes in mitochondria direction between synaptic and non-synaptic sites are caused by alterations in synaptic activity (Chang et al., 2006) and we previously demonstrated that A $\beta$ O $_{1-42}$  leads to the immediate activation of NMDARs (Ferreira et al., 2012, 2015). Interestingly, A $\beta$ O acute-induced retrograde movement was shown to be dependent on NMDAR activation. Thus, NMDARs activation by A $\beta$ O $_{1-42}$  may regulate synaptic plasticity, by modifying mitochondrial movement. On the other hand, A $\beta$ O $_{1-42}$  for 24 h seems to induce a decrease in the retrograde movement although mitochondrial velocity in this direction was significantly higher, without affecting anterograde movement. Anterograde movement reflects a higher deliver and exchange of

mitochondrial components (Schwarz, 2013), while retrograde movement is particularly important to repair damaged mitochondria and sustain fundamental proteins to maintain mitochondrial function and neuronal activity (Mandal et al., 2020). We have recently shown that A $\beta$ O<sub>1-42</sub> for 24 h induce significant mitochondrial impairment and cell death by apoptosis (Mota et al., unpublished data). Thus, the decrease in the number of mitochondria moving backwards to the soma (retrograde transport) might indicate an impairment in mitochondria repair and an accumulation in neurites and synapses of damaged mitochondria after prolonged exposure to A $\beta$ O. SU6656, a Src inhibitor, did not prevent the effects caused by acute A $\beta$ O<sub>1-42</sub>; instead, in the presence of A $\beta$ , SU6656 seems to increase mitochondrial velocity. Thus, our mitochondrial movement data does not seem to point out a crucial role for Src kinase(s) on A $\beta$ -induced changes in organelle motility; however, Src might be implicated in mitochondrial movement modulation, although further experiments are needed.

A $\beta$ -induced oxidative stress has been described to promote an imbalance between mitochondrial fusion and fission by increasing mitochondrial fission (fragmentation) through the activation of Drp1 protein (Wu et al., 2011; Ruiz et al., 2018; Nakamura et al., 2010). Our results evidence increased mitochondrial fragmentation after 24h exposure to A $\beta$ O<sub>1-42</sub>, as indicated by the increase in circularity and decrease in aspect ratio, which is in accordance with literature (Manczak and Reddy, 2012; Reddy, 2014). Interestingly, mitochondrial fragmentation seems to start already after 10 min treatment. Initial mitochondrial fragmentation seems to occur within minutes, being a transient state that can be restored by the decrease in intra-mitochondrial Ca<sup>2+</sup> (Hom et al., 2007). Paula-Lima and colleagues previously demonstrated that 1  $\mu$ M A $\beta$ O for 24h generates prolonged Ca<sup>2+</sup> signal and induced mitochondrial fragmentation, which could be prevented MK-801 pre-incubation for 30 min (Paula-Lima et al., 2011). In the present study, we show that both NMDARs and Src mediate mitochondrial fragmentation induced by immediate exposure to acute A $\beta$ O<sub>1-42</sub>. Indeed, results suggest that Src kinase regulate mitochondrial morphology rather than mitochondrial movement. Altogether, these observations are particularly important when considering the identification of selective cellular targets for pharmacological intervention acting in early stages of AD pathogenesis, since abnormal changes in mitochondrial morphology are on the basis of mitochondrial dysfunction, which ultimately compromise neuronal function. Previously, Wang and co-authors evidenced that inhibition of mitochondrial fission in a mouse model of AD (CRND8) improve mitochondrial function *in vitro* and *in vivo*, improved synaptic function and prevented cognitive deficits (Wang et al., 2017).

Mitochondria are  $\text{Ca}^{2+}$  reservoirs and buffer agents that have the capacity to manage transient changes in  $\text{Ca}^{2+}$  levels and particularly  $\text{Ca}^{2+}$  overload, associated with neurodegenerative diseases (Celsi et al., 2009). Acute treatment of cortical and hippocampal neurons with 20  $\mu\text{M}$   $\text{A}\beta_{25-35}$  and 500 nM  $\text{A}\beta_{1-42}$  caused a large increase in mitochondrial  $\text{Ca}^{2+}$  (Sanz-Blasco et al., 2008). Concordantly, our very preliminary evaluation of mitochondrial  $\text{Ca}^{2+}$  levels in mature hippocampal neurites using a  $\text{Ca}^{2+}$ -sensitive fluorescent sensor evidenced that acute treatment with 1  $\mu\text{M}$   $\text{A}\beta_{1-42}$  promotes increased intra-mitochondrial  $\text{Ca}^{2+}$  levels. Interestingly, inhibition of Src kinase activity seems to prevent immediate  $\text{A}\beta$ -induced  $\text{Ca}^{2+}$  flux. High  $\text{Ca}^{2+}$  influx into mitochondria through voltage-dependent anion channel (VDAC, also known as mitochondrial porin, located at the OMM) mitochondrial calcium uniporter (MCU, at the IMM) induces rapid mitochondrial fission that is dependent on DRP1 (Han et al., 2008). Our data evidence increased mitochondrial fragmentation concomitantly with increased mitochondrial  $\text{Ca}^{2+}$  flux and both appear to be prevented by Src inhibition, suggesting that Src modulation may prevent mitochondrial fragmentation through the regulation of mitochondrial  $\text{Ca}^{2+}$  influx. Importantly, Mukherjee and colleagues have demonstrated a correlation between higher  $\text{Ca}^{2+}$  levels induced by oxidative stress and mitochondrial depolarization (Mukherjee et al., 2002) and lower  $\Delta\Psi_m$  promotes increased mitochondrial retrograde movement (Miller and Sheetz, 2004). Thus, increased mitochondrial retrograde movement observed in this work might be related with increased mitochondrial  $\text{Ca}^{2+}$  levels and decreased  $\Delta\Psi_m$ . Of note, we observed an increase in  $\text{Ca}^{2+}$  influx, but not in its retention, evident in the decreased time dependent  $\text{Ca}^{2+}$  outflow, which may be associated to loss of  $\Delta\Psi_m$ . More experiments will be required in mature hippocampal neurites to better define the modifications in  $\text{A}\beta$ -induced mitochondrial  $\text{Ca}^{2+}$  changes.

Dendritic spines hold most of excitatory synapses in the CNS and synaptic strength is expressed by structural changes in dendritic spines, where abnormal modifications underlie the synaptic loss occurring in AD. In  $\text{APP}_{\text{SDL}}$  transgenic mice-derived hippocampal neurons, Pennazzi and co-authors found a reduction in spine length, although no differences in spine head volume were found (Pennazzi et al., 2016). Concordantly, our analysis of spine width does not evidence significant differences between conditions; however, we observed an immediate decrease in spine length after  $\text{A}\beta_{1-42}$  treatment that is maintained after 24h. LTP induces an increased spine width and reduction of length, consistent with spine maturation (Keifer et al., 2015). Importantly, the ratio between spine width and length was significantly increased by  $\text{A}\beta_{1-42}$  in our conditions, suggesting a spine enlargement. These results are in accordance with the study by Koppensteiner and colleagues who demonstrated that

short A $\beta$ O<sub>1-42</sub> exposition induces synaptic enhancement in hippocampal neurons, while longer exposures (12h-24h) reduce synaptic plasticity (Koppensteiner et al., 2016). Spine shrinkage requires NMDARs activity and Ca<sup>2+</sup> influx that further lead to the activation of calcium-dependent phosphatases and consequent spine actin cytoskeleton modulation (Stein et al., 2015; Zhou et al., 2004). Acute treatment with a low concentration of A $\beta$  (100 nM) can already induce F-actin stabilization in spines and compromise synaptic transmission (Rush et al., 2018). Herein, we evidence that spine shrinkage is significantly prevented by the inhibition of Src kinase, suggesting that spine shrinkage occurs in a Src-dependent manner. Wider spines are more responsive to local Ca<sup>2+</sup> influx in contrast with smaller spines which are more flexible and can rapidly become enlarged or suffer shrinkage, after activation (Bourne and Harris, 2007). In APP mouse organotypic hippocampal slice cultures A $\beta$  was shown to promote a shift from mushroom to stubby spines through a mechanism involving NMDAR, calcineurin, and GSK-3 $\beta$  activation (Tackenberg and Brandt, 2009). In organotypic hippocampal slices 1  $\mu$ M A $\beta$ O increased stubby spines number mainly as the result of mushroom spine elimination (Ortiz-Sanz et al., 2020). Our preliminary data (n=2) suggest a slight tendency to increase mushroom and stubby spines population following A $\beta$ O treatment. Moreover, the percentage of stubby spines after 24h A $\beta$ O exposure seems to be higher than after 10 min. Thus, results suggest that in one hand, A $\beta$  could potentiate spine maturity and therefore increase the probability of holding a synapse (Yuste and Bonhoeffer, 2001), and on the other hand, the prolonged exposure to A $\beta$  can cause a possible degradation of the more matured mushroom spines.

## **4.2 Conclusions**

In conclusion, this study provides evidence of an immediate A $\beta$ O-induced effects in mitochondrial function and dynamics and their impact on synaptic plasticity. In fact, acute treatment with A $\beta$ O<sub>1-42</sub> seems to promote mitochondrial movement, as well as potentiate dendritic spine maturation. On the other hand, prolonged treatment with A $\beta$ O<sub>1-42</sub> decreases retrograde movement, which may be in accordance with impaired mitochondrial repair and an accumulation of damaged mitochondria in neurites and synapses, leading to a possible degradation of more matured spines. Moreover, A $\beta$ O immediately induces mitochondrial fragmentation, concomitantly with increased mitochondrial Ca<sup>2+</sup> influx. Interestingly, while Src inhibition does not prevent A $\beta$ O-

induced changes in mitochondrial movement, it prevents mitochondrial fragmentation and increased  $\text{Ca}^{2+}$  influx, suggesting that Src acts on mitochondrial morphology and function, rather than on mitochondrial movement. Furthermore, inhibition of Src kinase also significantly prevents the  $\text{A}\beta\text{O}$ -induced spine shrinkage, suggesting that it occurs in a Src-dependent manner. In this sense, these observations evidence a therapeutic potential of Src at an early stage of AD development and even during its progression. Further experiments are needed to deepen the impact of specific mitochondrial or cytosolic Src in the modulation of  $\text{A}\beta\text{O}$ -induced neuronal dysfunctional pathways.

## **REFERENCES**

- Alberdi, E., Sánchez-Gómez, M. V., Cavaliere, F., Pérez-Samartín, A., Zugaza, J. L., Trullas, R., Domercq, M., & Matute, C. (2010). Amyloid beta oligomers induce Ca<sup>2+</sup> dysregulation and neuronal death through activation of ionotropic glutamate receptors. *Cell calcium*, 47(3), 264–272. <https://doi.org/10.1016/j.ceca.2009.12.010>
- Andreasen, N., Vanmechelen, E., Van de Voorde, A., Davidsson, P., Hesse, C., Tarvonen, S., Råihä, I., Sourander, L., Winblad, B., & Blennow, K. (1998). Cerebrospinal fluid tau protein as a biochemical marker for Alzheimer's disease: a community based follow up study. *Journal of neurology, neurosurgery, and psychiatry*, 64(3), 298–305. <https://doi.org/10.1136/jnnp.64.3.298>
- Andrews Z. B. (2010). Uncoupling protein-2 and the potential link between metabolism and longevity. *Current aging science*, 3(2), 102–112. <https://doi.org/10.2174/1874609811003020102>
- Arikkath J. (2012). Molecular mechanisms of dendrite morphogenesis. *Frontiers in cellular neuroscience*, 6, 61. <https://doi.org/10.3389/fncel.2012.00061>
- Bateman, R. J., Xiong, C., Benzinger, T. L., Fagan, A. M., Goate, A., Fox, N. C., Marcus, D. S., Cairns, N. J., Xie, X., Blazey, T. M., Holtzman, D. M., Santacruz, A., Buckles, V., Oliver, A., Moulder, K., Aisen, P. S., Ghetti, B., Klunk, W. E., McDade, E., Martins, R. N., ... Dominantly Inherited Alzheimer Network (2012). Clinical and biomarker changes in dominantly inherited Alzheimer's disease. *The New England journal of medicine*, 367(9), 795–804. <https://doi.org/10.1056/NEJMoa1202753>
- Bats, C., Groc, L., & Choquet, D. (2007). The interaction between Stargazin and PSD-95 regulates AMPA receptor surface trafficking. *Neuron*, 53(5), 719–734. <https://doi.org/10.1016/j.neuron.2007.01.030>
- Bear, M. F., & Malenka, R. C. (1994). Synaptic plasticity: LTP and LTD. *Current opinion in neurobiology*, 4(3), 389–399. [https://doi.org/10.1016/0959-4388\(94\)90101-5](https://doi.org/10.1016/0959-4388(94)90101-5)
- Beck, S. J., Guo, L., Phensy, A., Tian, J., Wang, L., Tandon, N., Gauba, E., Lu, L., Pascual, J. M., Kroener, S., & Du, H. (2016). Deregulation of mitochondrial F1FO-ATP synthase via OSCP in Alzheimer's disease. *Nature communications*, 7, 11483. <https://doi.org/10.1038/ncomms11483>
- Benarroch E. E. (2018). Glutamatergic synaptic plasticity and dysfunction in Alzheimer disease: Emerging mechanisms. *Neurology*, 91(3), 125–132. <https://doi.org/10.1212/WNL.0000000000005807>
- Berger A. (2003). How does it work? Positron emission tomography. *BMJ (Clinical research ed.)*, 326(7404), 1449. <https://doi.org/10.1136/bmj.326.7404.1449>
- Berry, K. P., & Nedivi, E. (2017). Spine Dynamics: Are They All the Same?. *Neuron*, 96(1), 43–55. <https://doi.org/10.1016/j.neuron.2017.08.008>
- Bissen, D., Foss, F., & Acker-Palmer, A. (2019). AMPA receptors and their minions: auxiliary proteins in AMPA receptor trafficking. *Cellular and molecular life sciences : CMLS*, 76(11), 2133–2169. <https://doi.org/10.1007/s00018-019-03068-7>
- Bjerke, M., & Engelborghs, S. (2018). Cerebrospinal Fluid Biomarkers for Early and Differential Alzheimer's Disease Diagnosis. *Journal of Alzheimer's disease : JAD*, 62(3), 1199–1209. <https://doi.org/10.3233/JAD-170680>

- Blennow, K., de Leon, M. J., & Zetterberg, H. (2006). Alzheimer's disease. *Lancet* (London, England), 368(9533), 387–403. [https://doi.org/10.1016/S0140-6736\(06\)69113-7](https://doi.org/10.1016/S0140-6736(06)69113-7)
- Bliss, T. V., & Collingridge, G. L. (1993). A synaptic model of memory: long-term potentiation in the hippocampus. *Nature*, 361(6407), 31–39. <https://doi.org/10.1038/361031a0>
- Boggon, T. J., & Eck, M. J. (2004). Structure and regulation of Src family kinases. *Oncogene*, 23(48), 7918–7927. <https://doi.org/10.1038/sj.onc.1208081>
- Boisvert, M. M., Erikson, G. A., Shokhirev, M. N., & Allen, N. J. (2018). The Aging Astrocyte Transcriptome from Multiple Regions of the Mouse Brain. *Cell reports*, 22(1), 269–285. <https://doi.org/10.1016/j.celrep.2017.12.039>
- Bonhoeffer, T., and R. Yuste. 2002. Spine motility. Phenomenology, mechanisms, and function. *Neuron*. 35:1019–1027. [http://dx.doi.org/10.1016/S0896-6273\(02\)00906-6](http://dx.doi.org/10.1016/S0896-6273(02)00906-6)
- Borczyk, M., Śliwińska, M.A., Caly, A. et al. Neuronal plasticity affects correlation between the size of dendritic spine and its postsynaptic density. *Sci Rep* 9, 1693 (2019). <https://doi.org/10.1038/s41598-018-38412-7>
- Bosch, M., & Hayashi, Y. (2012). Structural plasticity of dendritic spines. *Current opinion in neurobiology*, 22(3), 383–388. <https://doi.org/10.1016/j.conb.2011.09.002>
- Bosch, M., & Hayashi, Y. (2012). Structural plasticity of dendritic spines. *Current opinion in neurobiology*, 22(3), 383–388. <https://doi.org/10.1016/j.conb.2011.09.002>
- Buchbinder B. R. (2016). Functional magnetic resonance imaging. *Handbook of clinical neurology*, 135, 61–92. <https://doi.org/10.1016/B978-0-444-53485-9.00004-0>
- Bourne, J., & Harris, K. M. (2007). Do thin spines learn to be mushroom spines that remember?. *Current opinion in neurobiology*, 17(3), 381–386. <https://doi.org/10.1016/j.conb.2007.04.009>
- Brooks, C., Wei, Q., Feng, L., Dong, G., Tao, Y., Mei, L., Xie, Z. J., & Dong, Z. (2007). Bak regulates mitochondrial morphology and pathology during apoptosis by interacting with mitofusins. *Proceedings of the National Academy of Sciences of the United States of America*, 104(28), 11649–11654. <https://doi.org/10.1073/pnas.0703976104>
- Brown, M. R., Sullivan, P. G., & Geddes, J. W. (2006). Synaptic mitochondria are more susceptible to Ca<sup>2+</sup> overload than nonsynaptic mitochondria. *The Journal of biological chemistry*, 281(17), 11658–11668. <https://doi.org/10.1074/jbc.M510303200>
- Cadete, V., Vasam, G., Menzies, K. J., & Burrelle, Y. (2019). Mitochondrial quality control in the cardiac system: An integrative view. *Biochimica et biophysica acta. Molecular basis of disease*, 1865(4), 782–796. <https://doi.org/10.1016/j.bbadis.2018.11.018>
- Cai, Q., & Sheng, Z. H. (2009). Moving or stopping mitochondria: Miro as a traffic cop by sensing calcium. *Neuron*, 61(4), 493–496. <https://doi.org/10.1016/j.neuron.2009.02.003>
- Cai, Q., & Tammineni, P. (2016). Alterations in Mitochondrial Quality Control in Alzheimer's Disease. *Frontiers in cellular neuroscience*, 10, 24. <https://doi.org/10.3389/fncel.2016.00024>
- Cai, Q., & Tammineni, P. (2017). Mitochondrial Aspects of Synaptic Dysfunction in Alzheimer's Disease. *Journal of Alzheimer's disease : JAD*, 57(4), 1087–1103. <https://doi.org/10.3233/JAD-160726>
- Calkins, M. J., & Reddy, P. H. (2011). Amyloid beta impairs mitochondrial anterograde transport and degenerates synapses in Alzheimer's disease neurons. *Biochimica et biophysica acta*, 1812(4), 507–513. <https://doi.org/10.1016/j.bbadis.2011.01.007>

Callahan, L. M., Vaules, W. A., & Coleman, P. D. (2002). Progressive reduction of synaptophysin message in single neurons in Alzheimer disease. *Journal of neuropathology and experimental neurology*, 61(5), 384–395. <https://doi.org/10.1093/jnen/61.5.384>

Calvo-Rodriguez, M., Hernando-Perez, E., Nuñez, L., & Villalobos, C. (2019). Amyloid  $\beta$  Oligomers Increase ER-Mitochondria  $Ca^{2+}$  Cross Talk in Young Hippocampal Neurons and Exacerbate Aging-Induced Intracellular  $Ca^{2+}$  Remodeling. *Frontiers in cellular neuroscience*, 13, 22. <https://doi.org/10.3389/fncel.2019.00022>

Catterall, W. A., & Few, A. P. (2008). Calcium channel regulation and presynaptic plasticity. *Neuron*, 59(6), 882–901. <https://doi.org/10.1016/j.neuron.2008.09.005>

Celsi, F., Pizzo, P., Brini, M., Leo, S., Fotino, C., Pinton, P., & Rizzuto, R. (2009). Mitochondria, calcium and cell death: a deadly triad in neurodegeneration. *Biochimica et biophysica acta*, 1787(5), 335–344. <https://doi.org/10.1016/j.bbabi.2009.02.021>

Cenini, G., & Voos, W. (2019). Mitochondria as Potential Targets in Alzheimer Disease Therapy: An Update. *Frontiers in pharmacology*, 10, 902. <https://doi.org/10.3389/fphar.2019.00902>

Chauffy, J., Sullivan, S. E., & Ho, A. (2012). Intracellular amyloid precursor protein sorting and amyloid- $\beta$  secretion are regulated by Src-mediated phosphorylation of Mint2. *The Journal of neuroscience : the official journal of the Society for Neuroscience*, 32(28), 9613–9625. <https://doi.org/10.1523/JNEUROSCI.0602-12.2012>

Chen, G. F., Xu, T. H., Yan, Y., Zhou, Y. R., Jiang, Y., Melcher, K., & Xu, H. E. (2017). Amyloid beta: structure, biology and structure-based therapeutic development. *Acta pharmacologica Sinica*, 38(9), 1205–1235. <https://doi.org/10.1038/aps.2017.28>

Chin, J., Palop, J. J., Puoliväli, J., Massaro, C., Bien-Ly, N., Gerstein, H., Scarsce-Levie, K., Masliah, E., & Mucke, L. (2005). Fyn kinase induces synaptic and cognitive impairments in a transgenic mouse model of Alzheimer's disease. *The Journal of neuroscience : the official journal of the Society for Neuroscience*, 25(42), 9694–9703. <https://doi.org/10.1523/JNEUROSCI.2980-05.2005>

Chiong, M., Cartes-Saavedra, B., Norambuena-Soto, I., Mondaca-Ruff, D., Morales, P. E., García-Miguel, M., & Mellado, R. (2014). Mitochondrial metabolism and the control of vascular smooth muscle cell proliferation. *Frontiers in cell and developmental biology*, 2, 72. <https://doi.org/10.3389/fcell.2014.00072>

Choi, U. B., Xiao, S., Wollmuth, L. P., & Bowen, M. E. (2011). Effect of Src kinase phosphorylation on disordered C-terminal domain of N-methyl-D-aspartic acid (NMDA) receptor subunit GluN2B protein. *The Journal of biological chemistry*, 286(34), 29904–29912. <https://doi.org/10.1074/jbc.M111.258897>

Citron, M., Diehl, T. S., Gordon, G., Biere, A. L., Seubert, P., & Selkoe, D. J. (1996). Evidence that the 42- and 40-amino acid forms of amyloid beta protein are generated from the beta-amyloid precursor protein by different protease activities. *Proceedings of the National Academy of Sciences of the United States of America*, 93(23), 13170–13175. <https://doi.org/10.1073/pnas.93.23.13170>

Cohen, A. D., & Klunk, W. E. (2014). Early detection of Alzheimer's disease using PiB and FDG PET. *Neurobiology of disease*, 72 Pt A, 117–122. <https://doi.org/10.1016/j.nbd.2014.05.001>

Cohen, A. D., Rabinovici, G. D., Mathis, C. A., Jagust, W. J., Klunk, W. E., & Ikonomic, M. D. (2012). Using Pittsburgh Compound B for in vivo PET imaging of fibrillar amyloid-beta. *Advances in pharmacology (San Diego, Calif.)*, 64, 27–81. <https://doi.org/10.1016/B978-0-12-394816-8.00002-7>

Collingridge, G. (1987). The role of NMDA receptors in learning and memory. *Nature*, 330(6149), 604–605. doi:10.1038/330604a0

Correia, S. C., Perry, G., & Moreira, P. I. (2016). Mitochondrial traffic jams in Alzheimer's disease - pinpointing the roadblocks. *Biochimica et biophysica acta*, 1862(10), 1909–1917. <https://doi.org/10.1016/j.bbadis.2016.07.010>

Coskun PE, Beal MF, Wallace DC. Alzheimer's brains harbor somatic mtDNA control-region mutations that suppress mitochondrial transcription and replication. *Proc Natl Acad Sci U S A*. 2004;101:10726–10731.

Cras, P., Kawai, M., Lowery, D., Gonzalez-DeWhitt, P., Greenberg, B., & Perry, G. (1991). Senile plaque neurites in Alzheimer disease accumulate amyloid precursor protein. *Proceedings of the National Academy of Sciences of the United States of America*, 88(17), 7552–7556. <https://doi.org/10.1073/pnas.88.17.7552>

Crous-Bou, M., Minguillón, C., Gramunt, N., & Molinuevo, J. L. (2017). Alzheimer's disease prevention: from risk factors to early intervention. *Alzheimer's research & therapy*, 9(1), 71. <https://doi.org/10.1186/s13195-017-0297-z>

Cugno, A., Bartol, T. M., Sejnowski, T. J., Iyengar, R., & Rangamani, P. (2019). Geometric principles of second messenger dynamics in dendritic spines. *Scientific reports*, 9(1), 11676. <https://doi.org/10.1038/s41598-019-48028-0>

Delgado, T., Petralia, R. S., Freeman, D. W., Sedlacek, M., Wang, Y. X., Brenowitz, S. D., Sheu, S. H., Gu, J. W., Kapogiannis, D., Mattson, M. P., & Yao, P. J. (2019). Comparing 3D ultrastructure of presynaptic and postsynaptic mitochondria. *Biology open*, 8(8), bio044834. <https://doi.org/10.1242/bio.044834>

Deng, J., & Dunaevsky, A. (2005). Dynamics of dendritic spines and their afferent terminals: spines are more motile than presynaptic boutons. *Developmental biology*, 277(2), 366–377. <https://doi.org/10.1016/j.ydbio.2004.09.028>

Destaing, O., Sanjay, A., Itzstein, C., Horne, W. C., Toomre, D., De Camilli, P., & Baron, R. (2008). The tyrosine kinase activity of c-Src regulates actin dynamics and organization of podosomes in osteoclasts. *Molecular biology of the cell*, 19(1), 394–404. <https://doi.org/10.1091/mbc.e07-03-0227>

Devine, M. J., & Kittler, J. T. (2018). Mitochondria at the neuronal presynapse in health and disease. *Nature reviews. Neuroscience*, 19(2), 63–80. <https://doi.org/10.1038/nrn.2017.170>

Dhawan, G., Floden, A. M., & Combs, C. K. (2012). Amyloid- $\beta$  oligomers stimulate microglia through a tyrosine kinase dependent mechanism. *Neurobiology of aging*, 33(10), 2247–2261. <https://doi.org/10.1016/j.neurobiolaging.2011.10.027>

Dickstein, D. L., Weaver, C. M., Luebke, J. I., & Hof, P. R. (2013). Dendritic spine changes associated with normal aging. *Neuroscience*, 251, 21–32. <https://doi.org/10.1016/j.neuroscience.2012.09.077>

Dinamarca, M. C., Ríos, J. A., & Inestrosa, N. C. (2012). Postsynaptic Receptors for Amyloid- $\beta$  Oligomers as Mediators of Neuronal Damage in Alzheimer's Disease. *Frontiers in physiology*, 3, 464. <https://doi.org/10.3389/fphys.2012.00464>.

Divakaruni, S. S., Van Dyke, A. M., Chandra, R., LeGates, T. A., Contreras, M., Dharmasri, P. A., Higgs, H. N., Lobo, M. K., Thompson, S. M., & Blanpied, T. A. (2018). Long-Term Potentiation Requires a Rapid Burst of Dendritic Mitochondrial Fission during Induction. *Neuron*, 100(4), 860–875.e7. <https://doi.org/10.1016/j.neuron.2018.09.025>

Du, C. P., Gao, J., Tai, J. M., Liu, Y., Qi, J., Wang, W., & Hou, X. Y. (2009). Increased tyrosine phosphorylation of PSD-95 by Src family kinases after brain ischaemia. *The Biochemical journal*, 417(1), 277–285. <https://doi.org/10.1042/BJ20080004>

Du, H., Guo, L., Yan, S., Sosunov, A. A., McKhann, G. M., & Yan, S. S. (2010). Early deficits in synaptic mitochondria in an Alzheimer's disease mouse model. *Proceedings of the National Academy of Sciences of the United States of America*, 107(43), 18670–18675. <https://doi.org/10.1073/pnas.1006586107>

Du, X., Wang, X., & Geng, M. (2018). Alzheimer's disease hypothesis and related therapies. *Translational neurodegeneration*, 7, 2. <https://doi.org/10.1186/s40035-018-0107-y>

Duan, A. R., Jonasson, E. M., Alberico, E. O., Li, C., Scripture, J. P., Miller, R. A., Alber, M. S., & Goodson, H. V. (2017). Interactions between Tau and Different Conformations of Tubulin: Implications for Tau Function and Mechanism. *Journal of molecular biology*, 429(9), 1424–1438. <https://doi.org/10.1016/j.jmb.2017.03.018>

Ebrahimi, S., & Okabe, S. (2014). Structural dynamics of dendritic spines: molecular composition, geometry and functional regulation. *Biochimica et biophysica acta*, 1838(10), 2391–2398. <https://doi.org/10.1016/j.bbame.2014.06.002>

Estrada, L. D., Chamorro, D., Yañez, M. J., Gonzalez, M., Leal, N., von Bernhardi, R., Dulcey, A. E., Marugan, J., Ferrer, M., Soto, C., Zanlungo, S., Inestrosa, N. C., & Alvarez, A. R. (2016). Reduction of Blood Amyloid- $\beta$  Oligomers in Alzheimer's Disease Transgenic Mice by c-Abl Kinase Inhibition. *Journal of Alzheimer's disease : JAD*, 54(3), 1193–1205. <https://doi.org/10.3233/JAD-151087>

Fão, L. V. R. (2016). Amyloid-beta peptide-evoked Src signaling and redox changes in hippocampal cells (Master's thesis).

Federico, A., Cardaioli, E., Da Pozzo, P., Formichi, P., Gallus, G. N., & Radi, E. (2012). Mitochondria, oxidative stress and neurodegeneration. *Journal of the neurological sciences*, 322(1-2), 254–262. <https://doi.org/10.1016/j.jns.2012.05.030>

Fernandez, C. G., Hamby, M. E., McReynolds, M. L., & Ray, W. J. (2019). The Role of APOE4 in Disrupting the Homeostatic Functions of Astrocytes and Microglia in Aging and Alzheimer's Disease. *Frontiers in aging neuroscience*, 11, 14. <https://doi.org/10.3389/fnagi.2019.00014>

Ferreira, I. L., Bajouco, L. M., Mota, S. I., Auberson, Y. P., Oliveira, C. R., & Rego, A. C. (2012). Amyloid beta peptide 1-42 disturbs intracellular calcium homeostasis through activation of GluN2B-containing N-methyl-d-aspartate receptors in cortical cultures. *Cell calcium*, 51(2), 95–106. <https://doi.org/10.1016/j.ceca.2011.11.008>

Ferreira, I. L., Ferreira, E., Schmidt, J., Cardoso, J. M., Pereira, C. M., Carvalho, A. L., Oliveira, C. R., & Rego, A. C. (2015). A $\beta$  and NMDAR activation cause mitochondrial dysfunction involving ER calcium release. *Neurobiology of aging*, 36(2), 680–692. <https://doi.org/10.1016/j.neurobiolaging.2014.09.006>

Flannery, P. J., & Trushina, E. (2019). Mitochondrial dynamics and transport in Alzheimer's disease. *Molecular and cellular neurosciences*, 98, 109–120. <https://doi.org/10.1016/j.mcn.2019.06.009>

Flippo, K. H., & Strack, S. (2017). Mitochondrial dynamics in neuronal injury, development and plasticity. *Journal of cell science*, 130(4), 671–681. <https://doi.org/10.1242/jcs.171017>

Frank, A.C., Huang, S., Zhou, M. et al. Hotspots of dendritic spine turnover facilitate clustered spine addition and learning and memory. *Nat Commun* 9, 422 (2018). <https://doi.org/10.1038/s41467-017-02751-2>

Franzmeier, N., Neitzel, J., Rubinski, A. et al. Functional brain architecture is associated with the rate of tau accumulation in Alzheimer's disease. *Nat Commun* **11**, 347 (2020). <https://doi.org/10.1038/s41467-019-14159-1>

Fuss, H., Dubitzky, W., Downes, C. S., & Kurth, M. J. (2008). SRC family kinases and receptors: analysis of three activation mechanisms by dynamic systems modeling. *Biophysical journal*, *94*(6), 1995–2006. <https://doi.org/10.1529/biophysj.107.115022>

Giannoni, E., Buricchi, F., Raugei, G., Ramponi, G., & Chiarugi, P. (2005). Intracellular reactive oxygen species activate Src tyrosine kinase during cell adhesion and anchorage-dependent cell growth. *Molecular and cellular biology*, *25*(15), 6391–6403. <https://doi.org/10.1128/MCB.25.15.6391-6403.2005>

Giau, V. V., Bagyinszky, E., Yang, Y. S., Youn, Y. C., An, S., & Kim, S. Y. (2019). Genetic analyses of early-onset Alzheimer's disease using next generation sequencing. *Scientific reports*, *9*(1), 8368. <https://doi.org/10.1038/s41598-019-44848-2>

Giorgi, C., Marchi, S., & Pinton, P. (2018). The machineries, regulation and cellular functions of mitochondrial calcium. *Nature reviews. Molecular cell biology*, *19*(11), 713–730. <https://doi.org/10.1038/s41580-018-0052-8>

Gipson, C. D., & Olive, M. F. (2017). Structural and functional plasticity of dendritic spines - root or result of behavior?. *Genes, brain, and behavior*, *16*(1), 101–117. <https://doi.org/10.1111/gbb.12324>

Goedert M. (2015). NEURODEGENERATION. Alzheimer's and Parkinson's diseases: The prion concept in relation to assembled A $\beta$ , tau, and  $\alpha$ -synuclein. *Science (New York, N.Y.)*, *349*(6248), 1255555. <https://doi.org/10.1126/science.1255555>

Gold, C. A., & Budson, A. E. (2008). Memory loss in Alzheimer's disease: implications for development of therapeutics. *Expert review of neurotherapeutics*, *8*(12), 1879–1891. <https://doi.org/10.1586/14737175.8.12.1879>

Groc, L., Heine, M., Cognet, L., Brickley, K., Stephenson, F. A., Lounis, B., & Choquet, D. (2004). Differential activity-dependent regulation of the lateral mobilities of AMPA and NMDA receptors. *Nature neuroscience*, *7*(7), 695–696. <https://doi.org/10.1038/nn1270>

Groveman, B. R., Xue, S., Marin, V., Xu, J., Ali, M. K., Bienkiewicz, E. A., & Yu, X. M. (2011). Roles of the SH2 and SH3 domains in the regulation of neuronal Src kinase functions. *The FEBS journal*, *278*(4), 643–653. <https://doi.org/10.1111/j.1742-4658.2010.07985.x>

Gu, L., & Guo, Z. (2013). Alzheimer's A $\beta$ 42 and A $\beta$ 40 peptides form interlaced amyloid fibrils. *Journal of neurochemistry*, *126*(3), 305–311. <https://doi.org/10.1111/jnc.12202>

Guo, L., Tian, J., & Du, H. (2017). Mitochondrial Dysfunction and Synaptic Transmission Failure in Alzheimer's Disease. *Journal of Alzheimer's disease : JAD*, *57*(4), 1071–1086. <https://doi.org/10.3233/JAD-160702>

Han, X. J., Lu, Y. F., Li, S. A., Kaitsuka, T., Sato, Y., Tomizawa, K., Nairn, A. C., Takei, K., Matsui, H., & Matsushita, M. (2008). CaM kinase I  $\alpha$ -induced phosphorylation of Drp1 regulates mitochondrial morphology. *The Journal of cell biology*, *182*(3), 573–585. <https://doi.org/10.1083/jcb.200802164>

Hardingham, G. E., & Bading, H. (2003). The Yin and Yang of NMDA receptor signalling. *Trends in neurosciences*, *26*(2), 81–89. [https://doi.org/10.1016/S0166-2236\(02\)00040-1](https://doi.org/10.1016/S0166-2236(02)00040-1)

Hardy, J. A., & Higgins, G. A. (1992). Alzheimer's disease: the amyloid cascade hypothesis. *Science (New York, N.Y.)*, *256*(5054), 184–185. <https://doi.org/10.1126/science.1566067>

Harper, J. D., Wong, S. S., Lieber, C. M., & Lansbury, P. T., Jr (1999). Assembly of Abeta amyloid protofibrils: an in vitro model for a possible early event in Alzheimer's disease. *Biochemistry*, 38(28), 8972–8980. <https://doi.org/10.1021/bi9904149> Hebert LE, Beckett LA, Scherr PA, Evans DA. Annual incidence of Alzheimer disease in the United States projected to the years 2000 through 2050. *Alzheimer Dis Assoc Disord* 2001;15(4):169-73.

Harris, K. M., & Kater, S. B. (1994). Dendritic spines: cellular specializations imparting both stability and flexibility to synaptic function. *Annual review of neuroscience*, 17, 341–371. <https://doi.org/10.1146/annurev.ne.17.030194.002013>

Hayashi, T., & Huganir, R. L. (2004). Tyrosine phosphorylation and regulation of the AMPA receptor by SRC family tyrosine kinases. *The Journal of neuroscience : the official journal of the Society for Neuroscience*, 24(27), 6152–6160. <https://doi.org/10.1523/JNEUROSCI.0799-04.2004>

Hebert, L. E., Weuve, J., Scherr, P. A., & Evans, D. A. (2013). Alzheimer disease in the United States (2010-2050) estimated using the 2010 census. *Neurology*, 80(19), 1778–1783. <https://doi.org/10.1212/WNL.0b013e31828726f5>

Hepner, D.E., Dustin, C.M., Liao, C. et al. Direct cysteine sulfenylation drives activation of the Src kinase. *Nat Commun* 9, 4522 (2018). <https://doi.org/10.1038/s41467-018-06790-1>

Holtzman, D. M., Herz, J., & Bu, G. (2012). Apolipoprotein E and apolipoprotein E receptors: normal biology and roles in Alzheimer disease. *Cold Spring Harbor perspectives in medicine*, 2(3), a006312. <https://doi.org/10.1101/cshperspect.a006312>

Hom, J. R., Gewandter, J. S., Michael, L., Sheu, S. S., & Yoon, Y. (2007). Thapsigargin induces biphasic fragmentation of mitochondria through calcium-mediated mitochondrial fission and apoptosis. *Journal of cellular physiology*, 212(2), 498–508. <https://doi.org/10.1002/jcp.21051>

Hou, Y., Dan, X., Babbar, M. et al. Ageing as a risk factor for neurodegenerative disease. *Nat Rev Neurol* 15, 565–581 (2019). <https://doi.org/10.1038/s41582-019-0244-7>

Huang, C. C., & Hsu, K. S. (1999). Protein tyrosine kinase is required for the induction of long-term potentiation in the rat hippocampus. *The Journal of physiology*, 520 Pt 3(Pt 3), 783–796. <https://doi.org/10.1111/j.1469-7793.1999.00783.x>

Hunter, C. A., Koc, H., & Koc, E. C. (2020). c-Src kinase impairs the expression of mitochondrial OXPHOS complexes in liver cancer. *Cellular signalling*, 72, 109651. <https://doi.org/10.1016/j.cellsig.2020.109651>

Iaccarino, L., Tammewar, G., Ayakta, N., Baker, S. L., Bejanin, A., Boxer, A. L., Gorno-Tempini, M. L., Janabi, M., Kramer, J. H., Lazaris, A., Lockhart, S. N., Miller, B. L., Miller, Z. A., O'Neil, J. P., Ossenkoppele, R., Rosen, H. J., Schonhaut, D. R., Jagust, W. J., & Rabinovici, G. D. (2017). Local and distant relationships between amyloid, tau and neurodegeneration in Alzheimer's Disease. *NeuroImage. Clinical*, 17, 452–464. <https://doi.org/10.1016/j.nicl.2017.09.016>

Irby, R. B., & Yeatman, T. J. (2000). Role of Src expression and activation in human cancer. *Oncogene*, 19(49), 5636–5642. <https://doi.org/10.1038/sj.onc.1203912>

Janicki, S. C., & Schupf, N. (2010). Hormonal influences on cognition and risk for Alzheimer's disease. *Current neurology and neuroscience reports*, 10(5), 359–366. <https://doi.org/10.1007/s11910-010-0122-6>

Jeong, W., Lee, H., Cho, S., & Seo, J. (2019). ApoE4-Induced Cholesterol Dysregulation and Its Brain Cell Type-Specific Implications in the Pathogenesis of Alzheimer's Disease. *Molecules and cells*, 42(11), 739–746. <https://doi.org/10.14348/molcells.2019.0200>

Jeong, Y. J., Yoon, H. J., & Kang, D. Y. (2017). Assessment of change in glucose metabolism in white matter of amyloid-positive patients with Alzheimer disease using F-18 FDG PET. *Medicine*, 96(48), e9042. <https://doi.org/10.1097/MD.00000000000009042>

Jonckheere AI, Smeitink JA, Rodenburg RJ. Mitochondrial ATP synthase: architecture, function and pathology. *Journal of Inherited Metabolic Disease*. 2011;35(2):211-225.

Kalia, L. V., Gingrich, J. R., & Salter, M. W. (2004). Src in synaptic transmission and plasticity. *Oncogene*, 23(48), 8007–8016. <https://doi.org/10.1038/sj.onc.1208158>

Karbowski, M., & Youle, R. J. (2003). Dynamics of mitochondrial morphology in healthy cells and during apoptosis. *Cell death and differentiation*, 10(8), 870–880. <https://doi.org/10.1038/sj.cdd.4401260>

Katz, B., & Miledi, R. (1968). The role of calcium in neuromuscular facilitation. *The Journal of physiology*, 195(2), 481–492. <https://doi.org/10.1113/jphysiol.1968.sp008469>

Keifer, O. P., Jr, Hurt, R. C., Gutman, D. A., Keilholz, S. D., Gourley, S. L., & Ressler, K. J. (2015). Voxel-based morphometry predicts shifts in dendritic spine density and morphology with auditory fear conditioning. *Nature communications*, 6, 7582. <https://doi.org/10.1038/ncomms8582>

Khanna, S., Venojarvi, M., Roy, S., & Sen, C. K. (2002). Glutamate-induced c-Src activation in neuronal cells. *Methods in enzymology*, 352, 191–198. [https://doi.org/10.1016/s0076-6879\(02\)52019-x](https://doi.org/10.1016/s0076-6879(02)52019-x)

Kim, C., Choi, H., Jung, E. S., Lee, W., Oh, S., Jeon, N. L., & Mook-Jung, I. (2012). HDAC6 inhibitor blocks amyloid beta-induced impairment of mitochondrial transport in hippocampal neurons. *PloS one*, 7(8), e42983. <https://doi.org/10.1371/journal.pone.0042983>

Kim, K., Kim, M., Kim, D.W. et al. Clinically accurate diagnosis of Alzheimer's disease via multiplexed sensing of core biomarkers in human plasma. *Nat Commun* 11, 119 (2020). <https://doi.org/10.1038/s41467-019-13901-z>

Kish, S. J., Mastrogiacono, F., Guttman, M., Furukawa, Y., Taanman, J. W., Dozić, S., Pandolfo, M., Lamarche, J., DiStefano, L., & Chang, L. J. (1999). Decreased brain protein levels of cytochrome oxidase subunits in Alzheimer's disease and in hereditary spinocerebellar ataxia disorders: a nonspecific change?. *Journal of neurochemistry*, 72(2), 700–707. <https://doi.org/10.1046/j.1471-4159.1999.0720700.x>

Kommaddi, R. P., Das, D., Karunakaran, S., Nanguneri, S., Bapat, D., Ray, A., Shaw, E., Bennett, D. A., Nair, D., & Ravindranath, V. (2018). A $\beta$  mediates F-actin disassembly in dendritic spines leading to cognitive deficits in Alzheimer's disease. *The Journal of neuroscience : the official journal of the Society for Neuroscience*, 38(5), 1085–1099. <https://doi.org/10.1523/JNEUROSCI.2127-17.2017>

Koppensteiner, P., Trinchese, F., Fà, M., Puzzo, D., Gulisano, W., Yan, S., Poussin, A., Liu, S., Orozco, I., Dale, E., Teich, A. F., Palmeri, A., Ninan, I., Boehm, S., & Arancio, O. (2016). Time-dependent reversal of synaptic plasticity induced by physiological concentrations of oligomeric A $\beta$ 42: an early index of Alzheimer's disease. *Scientific reports*, 6, 32553. <https://doi.org/10.1038/srep32553>

Korade, Z., & Kenworthy, A. K. (2008). Lipid rafts, cholesterol, and the brain. *Neuropharmacology*, 55(8), 1265–1273. <https://doi.org/10.1016/j.neuropharm.2008.02.019>

Kuchibhotla, K. V., Goldman, S. T., Lattarulo, C. R., Wu, H. Y., Hyman, B. T., & Bacskai, B. J. (2008). Abeta plaques lead to aberrant regulation of calcium homeostasis in vivo resulting in structural and functional disruption of neuronal networks. *Neuron*, 59(2), 214–225. <https://doi.org/10.1016/j.neuron.2008.06.008>

Kulkarni, V. A., & Firestein, B. L. (2012). The dendritic tree and brain disorders. *Molecular and cellular neurosciences*, 50(1), 10–20. <https://doi.org/10.1016/j.mcn.2012.03.005>

Kwak, S.S., Washicosky, K.J., Brand, E. et al. Amyloid- $\beta$ 42/40 ratio drives tau pathology in 3D human neural cell culture models of Alzheimer's disease. *Nat Commun* 11, 1377 (2020). <https://doi.org/10.1038/s41467-020-15120-3>

Lacor, P. N., Buniel, M. C., Chang, L., Fernandez, S. J., Gong, Y., Viola, K. L., Lambert, M. P., Velasco, P. T., Bigio, E. H., Finch, C. E., Krafft, G. A., & Klein, W. L. (2004). Synaptic targeting by Alzheimer's-related amyloid beta oligomers. *The Journal of neuroscience : the official journal of the Society for Neuroscience*, 24(45), 10191–10200. <https://doi.org/10.1523/JNEUROSCI.3432-04.2004>

Laforce, R., Jr, Soucy, J. P., Sellami, L., Dallaire-Théroux, C., Brunet, F., Bergeron, D., Miller, B. L., & Ossenkoppele, R. (2018). Molecular imaging in dementia: Past, present, and future. *Alzheimer's & dementia : the journal of the Alzheimer's Association*, 14(11), 1522–1552. <https://doi.org/10.1016/j.jalz.2018.06.2855>

Lambert, M. P., Barlow, A. K., Chromy, B. A., Edwards, C., Freed, R., Liosatos, M., Morgan, T. E., Rozovsky, I., Trommer, B., Viola, K. L., Wals, P., Zhang, C., Finch, C. E., Krafft, G. A., & Klein, W. L. (1998). Diffusible, nonfibrillar ligands derived from A $\beta$ 1-42 are potent central nervous system neurotoxins. *Proceedings of the National Academy of Sciences of the United States of America*, 95(11), 6448–6453. <https://doi.org/10.1073/pnas.95.11.6448>

Larson, M. E., & Lesné, S. E. (2012). Soluble A $\beta$  oligomer production and toxicity. *Journal of neurochemistry*, 120 Suppl 1(Suppl 1), 125–139. <https://doi.org/10.1111/j.1471-4159.2011.07478.x>

Laurent, C., Buée, L., & Blum, D. (2018). Tau and neuroinflammation: What impact for Alzheimer's Disease and Tauopathies?. *Biomedical journal*, 41(1), 21–33. <https://doi.org/10.1016/j.bj.2018.01.003>

Lee G. (2005). Tau and src family tyrosine kinases. *Biochimica et biophysica acta*, 1739(2-3), 323–330. <https://doi.org/10.1016/j.bbadis.2004.09.002>

Lee, G., Newman, S. T., Gard, D. L., Band, H., & Panchamoorthy, G. (1998). Tau interacts with src-family non-receptor tyrosine kinases. *Journal of cell science*, 111 ( Pt 21), 3167–3177.

Levy, A. D., Omar, M. H., & Koleske, A. J. (2014). Extracellular matrix control of dendritic spine and synapse structure and plasticity in adulthood. *Frontiers in neuroanatomy*, 8, 116. <https://doi.org/10.3389/fnana.2014.00116>

Lewis, T. L., Jr, Turi, G. F., Kwon, S. K., Losonczy, A., & Polleux, F. (2016). Progressive Decrease of Mitochondrial Motility during Maturation of Cortical Axons In Vitro and In Vivo. *Current biology : CB*, 26(19), 2602–2608. <https://doi.org/10.1016/j.cub.2016.07.064>

Li, Chuanzhou and Götz, Jürgen. 'Pyk2 Is a Novel Tau Tyrosine Kinase That Is Regulated by the Tyrosine Kinase Fyn'. 1 Jan. 2018 : 205 – 221.

Li, Z., Aizenman, C. D., & Cline, H. T. (2002). Regulation of rho GTPases by crosstalk and neuronal activity in vivo. *Neuron*, 33(5), 741–750. [https://doi.org/10.1016/s0896-6273\(02\)00621-9](https://doi.org/10.1016/s0896-6273(02)00621-9)

Lim, S., Smith, K. R., Lim, S. T., Tian, R., Lu, J., & Tan, M. (2016). Regulation of mitochondrial functions by protein phosphorylation and dephosphorylation. *Cell & bioscience*, 6, 25. <https://doi.org/10.1186/s13578-016-0089-3>

Lin, M. Y., & Sheng, Z. H. (2015). Regulation of mitochondrial transport in neurons. *Experimental cell research*, 334(1), 35–44. <https://doi.org/10.1016/j.yexcr.2015.01.004>

Liu, X., Jiao, B., & Shen, L. (2018). The Epigenetics of Alzheimer's Disease: Factors and Therapeutic Implications. *Frontiers in genetics*, 9, 579. <https://doi.org/10.3389/fgene.2018.00579>

Livigni, A., Scorziello, A., Agnese, S., Adornetto, A., Carlucci, A., Garbi, C., Castaldo, I., Annunziato, L., Avvedimento, E. V., & Feliciello, A. (2006). Mitochondrial AKAP121 links cAMP and src signaling to oxidative metabolism. *Molecular biology of the cell*, 17(1), 263–271. <https://doi.org/10.1091/mbc.e05-09-0827>

Lohmann, C., & Kessels, H. W. (2014). The developmental stages of synaptic plasticity. *The Journal of physiology*, 592(1), 13–31. <https://doi.org/10.1113/jphysiol.2012.235119>

Loss, O., & Stephenson, F. A. (2017). Developmental changes in trak-mediated mitochondrial transport in neurons. *Molecular and cellular neurosciences*, 80, 134–147. <https://doi.org/10.1016/j.mcn.2017.03.006>

Lovas, J. R., & Wang, X. (2013). The meaning of mitochondrial movement to a neuron's life. *Biochimica et biophysica acta*, 1833(1), 184–194. <https://doi.org/10.1016/j.bbamcr.2012.04.007>

Lovas, S., Zhang, Y., Yu, J., & Lyubchenko, Y. L. (2013). Molecular mechanisms of misfolding and aggregation of A $\beta$ (13-23). *The journal of physical chemistry. B*, 117(20), 6175–6186. <https://doi.org/10.1021/jp402938p>

Lu, J., Sharma, L. K., & Bai, Y. (2009). Implications of mitochondrial DNA mutations and mitochondrial dysfunction in tumorigenesis. *Cell research*, 19(7), 802–815. <https://doi.org/10.1038/cr.2009.69>

Lüscher, C., & Malenka, R. C. (2012). NMDA receptor-dependent long-term potentiation and long-term depression (LTP/LTD). *Cold Spring Harbor perspectives in biology*, 4(6), a005710. <https://doi.org/10.1101/cshperspect.a005710>

M., Sheppard, P. W., Everall, I., & Anderton, B. H. (2002). Rapid tyrosine phosphorylation of neuronal proteins including tau and focal adhesion kinase in response to amyloid-beta peptide exposure: involvement of Src family protein kinases. *The Journal of neuroscience : the official journal of the Society for Neuroscience*, 22(1), 10–20. <https://doi.org/10.1523/JNEUROSCI.22-01-00010.2002>

MacAskill, A. F., Brickley, K., Stephenson, F. A., & Kittler, J. T. (2009). GTPase dependent recruitment of Grif-1 by Miro1 regulates mitochondrial trafficking in hippocampal neurons. *Molecular and cellular neurosciences*, 40(3), 301–312. <https://doi.org/10.1016/j.mcn.2008.10.016>

MacDermott, A. B., Mayer, M. L., Westbrook, G. L., Smith, S. J., & Barker, J. L. (1986). NMDA-receptor activation increases cytoplasmic calcium concentration in cultured spinal cord neurones. *Nature*, 321(6069), 519–522. <https://doi.org/10.1038/321519a0>

Mahley R. W. (1988). Apolipoprotein E: cholesterol transport protein with expanding role in cell biology. *Science (New York, N.Y.)*, 240(4852), 622–630. <https://doi.org/10.1126/science.3283935>

Manczak M, Kandimalla R, Yin X, Reddy PH. Hippocampal mutant APP and amyloid beta-induced cognitive decline, dendritic spine loss, defective autophagy, mitophagy and mitochondrial abnormalities in a mouse model of Alzheimer's disease. *Hum Mol Genet*. 2018;27(8):1332–1342. doi:10.1093/hmg/ddy042

Mandal, A., Wong, H. C., Pinter, K., Mosqueda, N., Beirl, A., Lomash, R. M., Won, S., Kindt, K. S., & Drerup, C. M. (2020). Retrograde mitochondrial transport is essential for organelle distribution and health in zebrafish neurons. *The Journal of neuroscience : the official journal of the Society for Neuroscience*, JN-RM-1316-20. Advance online publication. <https://doi.org/10.1523/JNEUROSCI.1316-20.2020>

Mao, P., & Reddy, P. H. (2011). Aging and amyloid beta-induced oxidative DNA damage and mitochondrial dysfunction in Alzheimer's disease: implications for early intervention and

therapeutics. *Biochimica et biophysica acta*, 1812(11), 1359–1370. <https://doi.org/10.1016/j.bbadis.2011.08.005>

Martorell-Riera, A., Segarra-Mondejar, M., Muñoz, J. P., Ginet, V., Olloquequi, J., Pérez-Clausell, J., Palacín, M., Reina, M., Puyal, J., Zorzano, A., & Soriano, F. X. (2014). Mfn2 downregulation in excitotoxicity causes mitochondrial dysfunction and delayed neuronal death. *The EMBO journal*, 33(20), 2388–2407. <https://doi.org/10.15252/embj.201488327>

Matt, L., Kim, K., Hergarden, A. C., Patriarchi, T., Malik, Z. A., Park, D. K., Chowdhury, D., Buonarati, O. R., Henderson, P. B., Gökçek Saraç, Ç., Zhang, Y., Mohapatra, D., Horne, M. C., Ames, J. B., & Hell, J. W. (2018).  $\alpha$ -Actinin Anchors PSD-95 at Postsynaptic Sites. *Neuron*, 97(5), 1094–1109.e9. <https://doi.org/10.1016/j.neuron.2018.01.036>

Mattison, H. A., Popovkina, D., Kao, J. P., & Thompson, S. M. (2014). The role of glutamate in the morphological and physiological development of dendritic spines. *The European journal of neuroscience*, 39(11), 1761–1770. <https://doi.org/10.1111/ejn.12536>

Mattson M. P. (2000). Apoptosis in neurodegenerative disorders. *Nature reviews. Molecular cell biology*, 1(2), 120–129. <https://doi.org/10.1038/35040009>

Meckler, X., & Checler, F. (2016). Presenilin 1 and Presenilin 2 Target  $\gamma$ -Secretase Complexes to Distinct Cellular Compartments. *The Journal of biological chemistry*, 291(24), 12821–12837. <https://doi.org/10.1074/jbc.M115.708297>

Melkov, A., & Abdu, U. (2018). Regulation of long-distance transport of mitochondria along microtubules. *Cellular and molecular life sciences : CMLS*, 75(2), 163–176. <https://doi.org/10.1007/s00018-017-2590-1>

Mihaylova, M. M., & Shaw, R. J. (2011). The AMPK signalling pathway coordinates cell growth, autophagy and metabolism. *Nature cell biology*, 13(9), 1016–1023. <https://doi.org/10.1038/ncb2329>

Miller, K. E., & Sheetz, M. P. (2004). Axonal mitochondrial transport and potential are correlated. *Journal of cell science*, 117(Pt 13), 2791–2804. <https://doi.org/10.1242/jcs.01130>

Mills, K. M., Brocardo, M. G., & Henderson, B. R. (2016). APC binds the Miro/Milton motor complex to stimulate transport of mitochondria to the plasma membrane. *Molecular biology of the cell*, 27(3), 466–482. <https://doi.org/10.1091/mbc.E15-09-0632>

Mironov S. L. (2007). ADP regulates movements of mitochondria in neurons. *Biophysical journal*, 92(8), 2944–2952. <https://doi.org/10.1529/biophysj.106.092981>

Mishra, P., & Chan, D. C. (2016). Metabolic regulation of mitochondrial dynamics. *The Journal of cell biology*, 212(4), 379–387. <https://doi.org/10.1083/jcb.201511036>

Smit-Rigter L, Rajendran R, Silva CA, Spierenburg L, Groeneweg F, Ruimschotel EM, van Versendaal D, van der Togt C, Eysel UT, Heimel JA, Lohmann C, Levelt CN. Mitochondrial Dynamics in Visual Cortex Are Limited In Vivo and Not Affected by Axonal Structural Plasticity. *Curr Biol*. 2016 Oct 10; 26(19):2609-2616.

Miura, K., Rueden, C., Hiner, M., Schindelin, J., & Rietdorf, J. (2014). ImageJ Plugin CorrectBleach V2. 0.2. V2. 0.2 ed.

Miyazaki, T., Neff, L., Tanaka, S., Horne, W. C., & Baron, R. (2003). Regulation of cytochrome c oxidase activity by c-Src in osteoclasts. *The Journal of cell biology*, 160(5), 709–718. <https://doi.org/10.1083/jcb.200209098>

Miyazono, Y., Hirashima, S., Ishihara, N., Kusukawa, J., Nakamura, K. I., & Ohta, K. (2018). Uncoupled mitochondria quickly shorten along their long axis to form indented spheroids, instead of rings, in a fission-independent manner. *Scientific reports*, 8(1), 350. <https://doi.org/10.1038/s41598-017-18582-6>

Monzio Compagnoni, G., Di Fonzo, A., Corti, S., Comi, G. P., Bresolin, N., & Masliah, E. (2020). The Role of Mitochondria in Neurodegenerative Diseases: the Lesson from Alzheimer's Disease and Parkinson's Disease. *Molecular neurobiology*, 57(7), 2959–2980. <https://doi.org/10.1007/s12035-020-01926-1>

Mota, S. I., Ferreira, I. L., Pereira, C., Oliveira, C. R., & Rego, A. C. (2012). Amyloid-beta peptide 1-42 causes microtubule deregulation through N-methyl-D-aspartate receptors in mature hippocampal cultures. *Current Alzheimer research*, 9(7), 844–856. <https://doi.org/10.2174/156720512802455322>

Mota, S. I., Ferreira, I. L., Valero, J., Ferreira, E., Carvalho, A. L., Oliveira, C. R., & Rego, A. C. (2014). Impaired Src signaling and post-synaptic actin polymerization in Alzheimer's disease mice hippocampus—linking NMDA receptors and the reelin pathway. *Experimental neurology*, 261, 698–709. <https://doi.org/10.1016/j.expneurol.2014.07.023>

Mukherjee, S. B., Das, M., Sudhandiran, G., & Shaha, C. (2002). Increase in cytosolic Ca<sup>2+</sup> levels through the activation of non-selective cation channels induced by oxidative stress causes mitochondrial depolarization leading to apoptosis-like death in *Leishmania donovani* promastigotes. *Journal of Biological Chemistry*, 277(27), 24717–24727

Nakahata, Y., & Yasuda, R. (2018). Plasticity of Spine Structure: Local Signaling, Translation and Cytoskeletal Reorganization. *Frontiers in synaptic neuroscience*, 10, 29. <https://doi.org/10.3389/fnsyn.2018.00029>

Nakamura, K., Okamura, H., Nagata, K., Komatsu, T., & Tamura, T. (1993). Purification of a factor which provides a costimulatory signal for gamma interferon production. *Infection and immunity*, 61(1), 64–70.

Nakamura, T., Cieplak, P., Cho, D. H., Godzik, A., & Lipton, S. A. (2010). S-nitrosylation of Drp1 links excessive mitochondrial fission to neuronal injury in neurodegeneration. *Mitochondrion*, 10(5), 573–578. <https://doi.org/10.1016/j.mito.2010.04.007>

Nakano, M., Imamura, H., Nagai, T., & Noji, H. (2011). Ca<sup>2+</sup> regulation of mitochondrial ATP synthesis visualized at the single cell level. *ACS chemical biology*, 6(7), 709–715. <https://doi.org/10.1021/cb100313n>

Nakazawa, T., Komai, S., Watabe, A. M., Kiyama, Y., Fukaya, M., Arima-Yoshida, F., Horai, R., Sudo, K., Ebine, K., Delawary, M., Goto, J., Umemori, H., Tezuka, T., Iwakura, Y., Watanabe, M., Yamamoto, T., & Manabe, T. (2006). NR2B tyrosine phosphorylation modulates fear learning as well as amygdaloid synaptic plasticity. *The EMBO journal*, 25(12), 2867–2877. <https://doi.org/10.1038/sj.emboj.7601156>

Nakazawa, T., Tezuka, T., & Yamamoto, T. (2002). *Nihon shinkei seishin yakurigaku zasshi = Japanese journal of psychopharmacology*, 22(5), 165–167.

Neginskaya, M. A., Solesio, M. E., Berezhnaya, E. V., Amodeo, G. F., Mnatsakanyan, N., Jonas, E. A., & Pavlov, E. V. (2019). ATP Synthase C-Subunit-Deficient Mitochondria Have a Small Cyclosporine A-Sensitive Channel, but Lack the Permeability Transition Pore. *Cell reports*, 26(1), 11–17.e2. <https://doi.org/10.1016/j.celrep.2018.12.033>

Nelson DL, Cox MM. *Lehninger Principles of biochemistry*. 5th Ed. New York: WH Freeman and Company; 2008.

Jackson JG, O'Donnell JC, Takano H, Coulter DA, Robinson MB. Neuronal activity and glutamate uptake decrease mitochondrial mobility in astrocytes and position mitochondria near glutamate transporters. *J Neurosci*. 2014 Jan 29; 34(5):1613-24.

Niemantsverdriet, E., Ottoy, J., Somers, C., De Roeck, E., Struyfs, H., Soetewey, F., Verhaeghe, J., Van den Bossche, T., Van Mossevelde, S., Goeman, J., De Deyn, P. P., Mariën, P., Versijpt, J., Slegers, K., Van Broeckhoven, C., Wyffels, L., Albert, A., Ceysens, S., Stroobants, S., Staelens, S., ... Engelborghs, S. (2017). The Cerebrospinal Fluid A $\beta$ 1-42/A $\beta$ 1-40 Ratio Improves Concordance with Amyloid-PET for Diagnosing Alzheimer's Disease in a Clinical Setting. *Journal of Alzheimer's disease : JAD*, 60(2), 561–576. <https://doi.org/10.3233/JAD-170327>

Niescier, R. F., Kwak, S. K., Joo, S. H., Chang, K. T., & Min, K. T. (2016). Dynamics of Mitochondrial Transport in Axons. *Frontiers in cellular neuroscience*, 10, 123. <https://doi.org/10.3389/fncel.2016.00123>

O'Brien, R. J., & Wong, P. C. (2011). Amyloid precursor protein processing and Alzheimer's disease. *Annual review of neuroscience*, 34, 185–204. <https://doi.org/10.1146/annurev-neuro-061010-113613>

O'Day D. H. (2020). Calmodulin Binding Proteins and Alzheimer's Disease: Biomarkers, Regulatory Enzymes and Receptors That Are Regulated by Calmodulin. *International journal of molecular sciences*, 21(19), 7344. <https://doi.org/10.3390/ijms21197344>

O'Dell, T. J., Kandel, E. R., & Grant, S. G. (1991). Long-term potentiation in the hippocampus is blocked by tyrosine kinase inhibitors. *Nature*, 353(6344), 558–560. <https://doi.org/10.1038/353558a0>

Oettinghaus, B., Schulz, J. M., Restelli, L. M., Licci, M., Savoia, C., Schmidt, A., Schmitt, K., Grimm, A., Morè, L., Hench, J., Tolnay, M., Eckert, A., D'Adamo, P., Franken, P., Ishihara, N., Mihara, K., Bischofberger, J., Scorrano, L., & Frank, S. (2016). Synaptic dysfunction, memory deficits and hippocampal atrophy due to ablation of mitochondrial fission in adult forebrain neurons. *Cell death and differentiation*, 23(1), 18–28. <https://doi.org/10.1038/cdd.2015.39>

Ogura, M., Yamaki, J., Homma, M. K., & Homma, Y. (2012). Mitochondrial c-Src regulates cell survival through phosphorylation of respiratory chain components. *The Biochemical journal*, 447(2), 281–289. <https://doi.org/10.1042/BJ20120509>

Ogura, M., Yamaki, J., Homma, M. K., & Homma, Y. (2014). Phosphorylation of flotillin-1 by mitochondrial c-Src is required to prevent the production of reactive oxygen species. *FEBS letters*, 588(17), 2837–2843. <https://doi.org/10.1016/j.febslet.2014.06.044>

Olaya Llano, Sergey Smirnov, Shetal Soni, Andrey Golubtsov, Isabelle Guillemin, Pirta Hotulainen, Igor Medina, Hans Gerd Nothwang, Claudio Rivera, Anastasia Ludwig; KCC2 regulates actin dynamics in dendritic spines via interaction with  $\beta$ -PIX. *J Cell Biol* 8 June 2015; 209 (5): 671–686. doi: <https://doi.org/10.1083/jcb.201411008>

Oliver D, Reddy PH. Dynamics of Dynamin-Related Protein 1 in Alzheimer's disease and Other Neurodegenerative Diseases. *Cells*. 2019;8(9):961. Published 2019 Aug 23. doi:10.3390/cells8090961

Onyango, I. G., Khan, S. M., & Bennett, J. P., Jr (2017). Mitochondria in the pathophysiology of Alzheimer's and Parkinson's diseases. *Frontiers in bioscience (Landmark edition)*, 22, 854–872. <https://doi.org/10.2741/4521>

Overly, C. C., Rieff, H. I., & Hollenbeck, P. J. (1996). Organelle motility and metabolism in axons vs dendrites of cultured hippocampal neurons. *Journal of cell science*, 109 ( Pt 5), 971–980

Padmanabhan, P., Martínez-Mármol, R., Xia, D., Götz, J., & Meunier, F. A. (2019). Frontotemporal dementia mutant Tau promotes aberrant Fyn nanoclustering in hippocampal dendritic spines. *eLife*, 8, e45040. <https://doi.org/10.7554/eLife.45040>

Pagliarini, D. J., Calvo, S. E., Chang, B., Sheth, S. A., Vafai, S. B., Ong, S. E., Walford, G. A., Sugiana, C., Boneh, A., Chen, W. K., Hill, D. E., Vidal, M., Evans, J. G., Thorburn, D. R., Carr, S. A., & Mootha, V. K. (2008). A mitochondrial protein compendium elucidates complex I disease biology. *Cell*, 134(1), 112–123. <https://doi.org/10.1016/j.cell.2008.06.016>

Palmer, C. S., Osellame, L. D., Laine, D., Koutsopoulos, O. S., Frazier, A. E., & Ryan, M. T. (2011). MiD49 and MiD51, new components of the mitochondrial fission machinery. *EMBO reports*, 12(6), 565–573. <https://doi.org/10.1038/embor.2011.54>

Parsons, S. J., & Parsons, J. T. (2004). Src family kinases, key regulators of signal transduction. *Oncogene*, 23(48), 7906–7909. <https://doi.org/10.1038/sj.onc.1208160>

Paula-Lima, A. C., Adasme, T., SanMartín, C., Sebollela, A., Hetz, C., Carrasco, M. A., Ferreira, S. T., & Hidalgo, C. (2011). Amyloid  $\beta$ -peptide oligomers stimulate RyR-mediated  $\text{Ca}^{2+}$  release inducing mitochondrial fragmentation in hippocampal neurons and prevent RyR-mediated dendritic spine remodeling produced by BDNF. *Antioxidants & redox signaling*, 14(7), 1209–1223. <https://doi.org/10.1089/ars.2010.3287>

Pchitskaya, E., & Bezprozvanny, I. (2020). Dendritic Spines Shape Analysis-Classification or Clusterization? Perspective. *Frontiers in synaptic neuroscience*, 12, 31. <https://doi.org/10.3389/fnsyn.2020.00031>

Penazzi, L., Tackenberg, C., Ghorri, A., Golovyashkina, N., Niewidok, B., Selle, K., Ballatore, C., Smith, A. B., 3rd, Bakota, L., & Brandt, R. (2016).  $\text{A}\beta$ -mediated spine changes in the hippocampus are microtubule-dependent and can be reversed by a subnanomolar concentration of the microtubule-stabilizing agent epothilone D. *Neuropharmacology*, 105, 84–95. <https://doi.org/10.1016/j.neuropharm.2016.01.002>

Perez Ortiz, J. M., & Swerdlow, R. H. (2019). Mitochondrial dysfunction in Alzheimer's disease: Role in pathogenesis and novel therapeutic opportunities. *British journal of pharmacology*, 176(18), 3489–3507. <https://doi.org/10.1111/bph.14585>

Perluigi, M., Barone, E., Di Domenico, F., & Butterfield, D. A. (2016). Aberrant protein phosphorylation in Alzheimer disease brain disturbs pro-survival and cell death pathways. *Biochimica et biophysica acta*, 1862(10), 1871–1882. <https://doi.org/10.1016/j.bbadis.2016.07.005>

Pham, E., Crews, L., Ubhi, K., Hansen, L., Adame, A., Cartier, A., Salmon, D., Galasko, D., Michael, S., Savas, J. N., Yates, J. R., Glabe, C., & Masliah, E. (2010)

Pinky, N. F., Wilkie, C. M., Barnes, J. R., & Parsons, M. P. (2018). Region- and Activity-Dependent Regulation of Extracellular Glutamate. *The Journal of neuroscience : the official journal of the Society for Neuroscience*, 38(23), 5351–5366. <https://doi.org/10.1523/JNEUROSCI.3213-17.2018>

Popugaeva, E., Pchitskaya, E., Speshilova, A., Alexandrov, S., Zhang, H., Vlasova, O., & Bezprozvanny, I. (2015). STIM2 protects hippocampal mushroom spines from amyloid synaptotoxicity. *Molecular neurodegeneration*, 10, 37. <https://doi.org/10.1186/s13024-015-0034-7>

R. D. (2017). Application of calibrated fMRI in Alzheimer's disease. *NeuroImage. Clinical*, 15, 348–358. <https://doi.org/10.1016/j.nicl.2017.05.009>

Rammes, G., Mattusch, C., Wulff, M., Seeser, F., Kreuzer, M., Zhu, K., Deussing, J. M., Herms, J., & Parsons, C. G. (2017). Involvement of GluN2B subunit containing N-methyl-d-aspartate

(NMDA) receptors in mediating the acute and chronic synaptotoxic effects of oligomeric amyloid-beta ( $A\beta$ ) in murine models of Alzheimer's disease (AD). *Neuropharmacology*, 123, 100–115. <https://doi.org/10.1016/j.neuropharm.2017.02.003>

Rangaraju, V., Lauterbach, M., & Schuman, E. M. (2019). Spatially Stable Mitochondrial Compartments Fuel Local Translation during Plasticity. *Cell*, 176(1-2), 73–84.e15. <https://doi.org/10.1016/j.cell.2018.12.013>

Reddy P. H. (2014). Inhibitors of mitochondrial fission as a therapeutic strategy for diseases with oxidative stress and mitochondrial dysfunction. *Journal of Alzheimer's disease : JAD*, 40(2), 245–256. <https://doi.org/10.3233/JAD-132060>

Reddy, P. H., & Oliver, D. M. (2019). Amyloid Beta and Phosphorylated Tau-Induced Defective Autophagy and Mitophagy in Alzheimer's Disease. *Cells*, 8(5), 488. <https://doi.org/10.3390/cells8050488>

Ross, J. L., Shuman, H., Holzbaur, E. L., & Goldman, Y. E. (2008). Kinesin and dynein-dynactin at intersecting microtubules: motor density affects dynein function. *Biophysical journal*, 94(8), 3115–3125. <https://doi.org/10.1529/biophysj.107.120014>

Rui, Y., & Zheng, J. Q. (2016). Amyloid  $\beta$  oligomers elicit mitochondrial transport defects and fragmentation in a time-dependent and pathway-specific manner. *Molecular brain*, 9(1), 79. <https://doi.org/10.1186/s13041-016-0261-z>

Rui, Y., Tiwari, P., Xie, Z., & Zheng, J. Q. (2006). Acute impairment of mitochondrial trafficking by beta-amyloid peptides in hippocampal neurons. *The Journal of neuroscience : the official journal of the Society for Neuroscience*, 26(41), 10480–10487. <https://doi.org/10.1523/JNEUROSCI.3231-06.2006>

Ruiz, A., Alberdi, E., & Matute, C. (2018). Mitochondrial Division Inhibitor 1 (mdivi-1) Protects Neurons against Excitotoxicity through the Modulation of Mitochondrial Function and Intracellular  $Ca^{2+}$  Signaling. *Frontiers in molecular neuroscience*, 11, 3. <https://doi.org/10.3389/fnmol.2018.00003>

Rush, T., Martinez-Hernandez, J., Dollmeyer, M., Frandemiche, M. L., Borel, E., Boisseau, S., Jacquier-Sarlin, M., & Buisson, A. (2018). Synaptotoxicity in Alzheimer's Disease Involved a Dysregulation of Actin Cytoskeleton Dynamics through Cofilin 1 Phosphorylation. *The Journal of neuroscience : the official journal of the Society for Neuroscience*, 38(48), 10349–10361. <https://doi.org/10.1523/JNEUROSCI.1409-18.2018>

Ruszczycski, B., Szepesi, Z., Wilczynski, G. M., Bijata, M., Kalita, K., Kaczmarek, L., & Włodarczyk, J. (2012). Sampling issues in quantitative analysis of dendritic spines morphology. *BMC bioinformatics*, 13, 213. <https://doi.org/10.1186/1471-2105-13-213>

S. Ramón y Cajal. *La Textura del Sistema Nerviosa del Hombre y los Vertebrados*. Moya, Madrid (1904)

S.J. Parsons, J.T. Parsons Src family kinases, key regulators of signal transduction *Oncogene*, 23 (2004), pp. 7906-7909

Sacktor, T. C., & Fenton, A. A. (2018). What does LTP tell us about the roles of CaMKII and PKM $\zeta$  in memory?. *Molecular brain*, 11(1), 77. <https://doi.org/10.1186/s13041-018-0420-5>

Safieh, M., Korczyn, A. D., & Michaelson, D. M. (2019). ApoE4: an emerging therapeutic target for Alzheimer's disease. *BMC medicine*, 17(1), 64. <https://doi.org/10.1186/s12916-019-1299-4>

Sala, C., Piëch, V., Wilson, N. R., Passafaro, M., Liu, G., & Sheng, M. (2001). Regulation of dendritic spine morphology and synaptic function by Shank and Homer. *Neuron*, 31(1), 115–130. [https://doi.org/10.1016/s0896-6273\(01\)00339-7](https://doi.org/10.1016/s0896-6273(01)00339-7)

Salter, M. W., & Kalia, L. V. (2004). Src kinases: a hub for NMDA receptor regulation. *Nature reviews. Neuroscience*, 5(4), 317–328. <https://doi.org/10.1038/nrn1368>

Salvi, M., Brunati, A. M., Bordin, L., La Rocca, N., Clari, G., & Toninello, A. (2002). Characterization and location of Src-dependent tyrosine phosphorylation in rat brain mitochondria. *Biochimica et biophysica acta*, 1589(2), 181–195. [https://doi.org/10.1016/s0167-4889\(02\)00174-x](https://doi.org/10.1016/s0167-4889(02)00174-x)

Sanjari Moghaddam, H., & Aarabi, M. H. (2018). A $\beta$ -Mediated Dysregulation of F-Actin Nanoarchitecture Leads to Loss of Dendritic Spines and Alzheimer's Disease-Related Cognitive Impairments. *The Journal of neuroscience : the official journal of the Society for Neuroscience*, 38(26), 5840–5842. <https://doi.org/10.1523/JNEUROSCI.0844-18.2018>

Sanz-Blasco, S., Valero, R. A., Rodríguez-Crespo, I., Villalobos, C., & Núñez, L. (2008). Mitochondrial Ca<sup>2+</sup> overload underlies Abeta oligomers neurotoxicity providing an unexpected mechanism of neuroprotection by NSAIDs. *PLoS one*, 3(7), e2718. <https://doi.org/10.1371/journal.pone.0002718>

Saxton, W. M., & Hollenbeck, P. J. (2012). The axonal transport of mitochondria. *Journal of cell science*, 125(Pt 9), 2095–2104. <https://doi.org/10.1242/jcs.053850>

Schwarz T. L. (2013). Mitochondrial trafficking in neurons. *Cold Spring Harbor perspectives in biology*, 5(6), a011304. <https://doi.org/10.1101/cshperspect.a011304>

Selkoe D. J. (2000). Toward a comprehensive theory for Alzheimer's disease. Hypothesis: Alzheimer's disease is caused by the cerebral accumulation and cytotoxicity of amyloid beta-protein. *Annals of the New York Academy of Sciences*, 924, 17–25. <https://doi.org/10.1111/j.1749-6632.2000.tb05554.x>

Selkoe D. J. (2001). Alzheimer's disease: genes, proteins, and therapy. *Physiological reviews*, 81(2), 741–766. <https://doi.org/10.1152/physrev.2001.81.2.741>

Selkoe, D. J., & Hardy, J. (2016). The amyloid hypothesis of Alzheimer's disease at 25 years. *EMBO molecular medicine*, 8(6), 595–608. <https://doi.org/10.15252/emmm.201606210>

Sengupta, U., Nilson, A. N., & Kayed, R. (2016). The Role of Amyloid- $\beta$  Oligomers in Toxicity, Propagation, and Immunotherapy. *EBioMedicine*, 6, 42–49. <https://doi.org/10.1016/j.ebiom.2016.03.035>

Sepúlveda, F. J., Fierro, H., Fernandez, E., Castillo, C., Peoples, R. W., Opazo, C., & Aguayo, L. G. (2014). Nature of the neurotoxic membrane actions of amyloid- $\beta$  on hippocampal neurons in Alzheimer's disease. *Neurobiology of aging*, 35(3), 472–481. <https://doi.org/10.1016/j.neurobiolaging.2013.08.035>

Sepúlveda, F. J., Parodi, J., Peoples, R. W., Opazo, C., & Aguayo, L. G. (2010). Synaptotoxicity of Alzheimer beta amyloid can be explained by its membrane perforating property. *PLoS one*, 5(7), e11820. <https://doi.org/10.1371/journal.pone.0011820>

Shafiei, S. S., Guerrero-Muñoz, M. J., & Castillo-Carranza, D. L. (2017). Tau Oligomers: Cytotoxicity, Propagation, and Mitochondrial Damage. *Frontiers in aging neuroscience*, 9, 83. <https://doi.org/10.3389/fnagi.2017.00083>

Shankar, G. M., Bloodgood, B. L., Townsend, M., Walsh, D. M., Selkoe, D. J., & Sabatini, B. L. (2007). Natural oligomers of the Alzheimer amyloid-beta protein induce reversible synapse loss by modulating an NMDA-type glutamate receptor-dependent signaling pathway. *The Journal of neuroscience : the official journal of the Society for Neuroscience*, 27(11), 2866–2875. <https://doi.org/10.1523/JNEUROSCI.4970-06.2007>

Sharma, V. M., Litersky, J. M., Bhaskar, K., & Lee, G. (2007). Tau impacts on growth-factor-stimulated actin remodeling. *Journal of cell science*, 120(Pt 5), 748–757. <https://doi.org/10.1242/jcs.03378>

Shirazi, S. K., & Wood, J. G. (1993). The protein tyrosine kinase, fyn, in Alzheimer's disease pathology. *Neuroreport*, 4(4), 435–437. <https://doi.org/10.1097/00001756-199304000-00024>

Simakova O, Arispe NJ. The cell-selective neurotoxicity of the Alzheimer's Aβ peptide is determined by surface phosphatidylserine and cytosolic ATP levels. Membrane binding is required for Aβ toxicity. *The Journal of Neuroscience : the Official Journal of the Society for Neuroscience*. 2007 Dec;27(50):13719-13729. DOI: 10.1523/JNEUROSCI.3006-07.2007.

Sisodia S. S. (1992). Beta-amyloid precursor protein cleavage by a membrane-bound protease. *Proceedings of the National Academy of Sciences of the United States of America*, 89(13), 6075–6079. <https://doi.org/10.1073/pnas.89.13.6075>

Smith, L. M., Zhu, R., & Strittmatter, S. M. (2018). Disease-modifying benefit of Fyn blockade persists after washout in mouse Alzheimer's model. *Neuropharmacology*, 130, 54–61. <https://doi.org/10.1016/j.neuropharm.2017.11.042>

Song, Z., Insel, P. S., Buckley, S., Yohannes, S., Mezher, A., Simonson, A., Wilkins, S., Tosun, D., Mueller, S., Kramer, J. H., Miller, B. L., & Weiner, M. W. (2015). Brain amyloid-β burden is associated with disruption of intrinsic functional connectivity within the medial temporal lobe in cognitively normal elderly. *The Journal of neuroscience : the official journal of the Society for Neuroscience*, 35(7), 3240–3247. <https://doi.org/10.1523/JNEUROSCI.2092-14.2015>

Spies, P. E., Verbeek, M. M., van Groen, T., & Claassen, J. A. (2012). Reviewing reasons for the decreased CSF Aβ42 concentration in Alzheimer disease. *Frontiers in bioscience (Landmark edition)*, 17, 2024–2034. <https://doi.org/10.2741/4035>

Spires-Jones, T. L., Meyer-Luehmann, M., Osetek, J. D., Jones, P. B., Stern, E. A., Bacskai, B. J., & Hyman, B. T. (2007). Impaired spine stability underlies plaque-related spine loss in an Alzheimer's disease mouse model. *The American journal of pathology*, 171(4), 1304–1311. <https://doi.org/10.2353/ajpath.2007.070055>

Stein, I. S., & Zito, K. (2019). Dendritic Spine Elimination: Molecular Mechanisms and Implications. *The Neuroscientist : a review journal bringing neurobiology, neurology and psychiatry*, 25(1), 27–47. <https://doi.org/10.1177/1073858418769644>

Stein, I. S., Gray, J. A., & Zito, K. (2015). Non-Ionotropic NMDA Receptor Signaling Drives Activity-Induced Dendritic Spine Shrinkage. *The Journal of neuroscience : the official journal of the Society for Neuroscience*, 35(35), 12303–12308. <https://doi.org/10.1523/JNEUROSCI.4289-14.2015>

Stocker, H., Möllers, T., Perna, L. et al. The genetic risk of Alzheimer's disease beyond APOE ε4: systematic review of Alzheimer's genetic risk scores. *Transl Psychiatry* 8, 166 (2018). <https://doi.org/10.1038/s41398-018-0221-8>

Sun, G., Ramdas, L., Wang, W., Vinci, J., McMurray, J., & Budde, R. J. (2002). Effect of autophosphorylation on the catalytic and regulatory properties of protein tyrosine kinase Src. *Archives of biochemistry and biophysics*, 397(1), 11–17. <https://doi.org/10.1006/abbi.2001.2627>

Suzuki, J., Kanemaru, K., Ishii, K., Ohkura, M., Okubo, Y., & Iino, M. (2014). Imaging intracellular Ca<sup>2+</sup> at subcellular resolution using CEPIA. *Nature communications*, 5, 4153. <https://doi.org/10.1038/ncomms5153>

Tackenberg, C., & Brandt, R. (2009). Divergent pathways mediate spine alterations and cell death induced by amyloid-beta, wild-type tau, and R406W tau. *The Journal of neuroscience : the official journal of the Society for Neuroscience*, 29(46), 14439–14450.

Tackenberg, C., Ghori, A., & Brandt, R. (2009). Thin, stubby or mushroom: spine pathology in Alzheimer's disease. *Current Alzheimer research*, 6(3), 261–268. <https://doi.org/10.2174/156720509788486554>

Tampellini D. (2015). Synaptic activity and Alzheimer's disease: a critical update. *Frontiers in neuroscience*, 9, 423. <https://doi.org/10.3389/fnins.2015.00423>

Tanaka, A., & Youle, R. J. (2008). A chemical inhibitor of DRP1 uncouples mitochondrial fission and apoptosis. *Molecular cell*, 29(4), 409–410. <https://doi.org/10.1016/j.molcel.2008.02.005>

Tao, K., Matsuki, N., & Koyama, R. (2014). AMP-activated protein kinase mediates activity-dependent axon branching by recruiting mitochondria to axon. *Developmental neurobiology*, 74(6), 557–573. <https://doi.org/10.1002/dneu.22149>

Tapiola, T., Alafuzoff, I., Herukka, S. K., Parkkinen, L., Hartikainen, P., Soininen, H., & Pirttilä, T. (2009). Cerebrospinal fluid {beta}-amyloid 42 and tau proteins as biomarkers of Alzheimer-type pathologic changes in the brain. *Archives of neurology*, 66(3), 382–389. <https://doi.org/10.1001/archneurol.2008.596>

Tiwari, S., Atluri, V., Kaushik, A., Yndart, A., & Nair, M. (2019). Alzheimer's disease: pathogenesis, diagnostics, and therapeutics. *International journal of nanomedicine*, 14, 5541–5554. <https://doi.org/10.2147/IJN.S200490>

Tong, L., Thornton, P. L., Balazs, R., & Cotman, C. W. (2001). Beta -amyloid-(1-42) impairs activity-dependent cAMP-response element-binding protein signaling in neurons at concentrations in which cell survival is not compromised. *The Journal of biological chemistry*, 276(20), 17301–17306. <https://doi.org/10.1074/jbc.M010450200>

Trushina, E., Nemutlu, E., Zhang, S., Christensen, T., Camp, J., Mesa, J., Siddiqui, A., Tamura, Y., Sesaki, H., Wengenack, T. M., Dzeja, P. P., & Poduslo, J. F. (2012). Defects in mitochondrial dynamics and metabolomic signatures of evolving energetic stress in mouse models of familial Alzheimer's disease. *PLoS one*, 7(2), e32737. <https://doi.org/10.1371/journal.pone.0032737>

Tycko R. (2003). Insights into the amyloid folding problem from solid-state NMR. *Biochemistry*, 42(11), 3151–3159. <https://doi.org/10.1021/bi027378p>

Vanden Berghe, P., Hennig, G. W., & Smith, T. K. (2004). Characteristics of intermittent mitochondrial transport in guinea pig enteric nerve fibers. *American journal of physiology. Gastrointestinal and liver physiology*, 286(4), G671–G682. <https://doi.org/10.1152/ajpgi.00283.2003>

Verma, M., Vats, A., & Taneja, V. (2015). Toxic species in amyloid disorders: Oligomers or mature fibrils. *Annals of Indian Academy of Neurology*, 18(2), 138–145. <https://doi.org/10.4103/0972-2327.144284>

Villemagne, V. L., Burnham, S., Bourgeat, P., Brown, B., Ellis, K. A., Salvado, O., Szoëke, C., Macaulay, S. L., Martins, R., Maruff, P., Ames, D., Rowe, C. C., Masters, C. L., & Australian Imaging Biomarkers and Lifestyle (AIBL) Research Group (2013). Amyloid  $\beta$  deposition, neurodegeneration, and cognitive decline in sporadic Alzheimer's disease: a prospective cohort study. *The Lancet. Neurology*, 12(4), 357–367. [https://doi.org/10.1016/S1474-4422\(13\)70044-9](https://doi.org/10.1016/S1474-4422(13)70044-9)

Wang, H. W., Pasternak, J. F., Kuo, H., Ristic, H., Lambert, M. P., Chromy, B., Viola, K. L., Klein, W. L., Stine, W. B., Krafft, G. A., & Trommer, B. L. (2002). Soluble oligomers of beta amyloid (1-42) inhibit long-term potentiation but not long-term depression in rat dentate gyrus. *Brain research*, 924(2), 133–140. [https://doi.org/10.1016/s0006-8993\(01\)03058-x](https://doi.org/10.1016/s0006-8993(01)03058-x)

Wang, W., Yin, J., Ma, X., Zhao, F., Siedlak, S. L., Wang, Z., Torres, S., Fujioka, H., Xu, Y., Perry, G., & Zhu, X. (2017). Inhibition of mitochondrial fragmentation protects against Alzheimer's disease in rodent model. *Human molecular genetics*, 26(21), 4118–4131. <https://doi.org/10.1093/hmg/ddx299>

Wang, X., Su, B., Lee, H. G., Li, X., Perry, G., Smith, M. A., & Zhu, X. (2009). Impaired balance of mitochondrial fission and fusion in Alzheimer's disease. *The Journal of neuroscience : the official journal of the Society for Neuroscience*, 29(28), 9090–9103. <https://doi.org/10.1523/JNEUROSCI.1357-09.2009>

Wang, X., Wang, W., Li, L., Perry, G., Lee, H. G., & Zhu, X. (2014). Oxidative stress and mitochondrial dysfunction in Alzheimer's disease. *Biochimica et biophysica acta*, 1842(8), 1240–1247. <https://doi.org/10.1016/j.bbadis.2013.10.015>

Wang, Y. T., & Salter, M. W. (1994). Regulation of NMDA receptors by tyrosine kinases and phosphatases. *Nature*, 369(6477), 233–235. <https://doi.org/10.1038/369233a0>

Wang, Y. T., Yu, X. M., & Salter, M. W. (1996). Ca<sup>2+</sup>-independent reduction of N-methyl-D-aspartate channel activity by protein tyrosine phosphatase. *Proceedings of the National Academy of Sciences of the United States of America*, 93(4), 1721–1725. <https://doi.org/10.1073/pnas.93.4.1721>

Wang, Y., Wu, F., Pan, H., Zheng, W., Feng, C., Wang, Y., Deng, Z., Wang, L., Luo, J., & Chen, S. (2016). Lost region in amyloid precursor protein (APP) through TALEN-mediated genome editing alters mitochondrial morphology. *Scientific reports*, 6, 22244. <https://doi.org/10.1038/srep22244>

Webster K. A. (2012). Mitochondrial membrane permeabilization and cell death during myocardial infarction: roles of calcium and reactive oxygen species. *Future cardiology*, 8(6), 863–884. <https://doi.org/10.2217/fca.12.58>

Wegiel, J., Kuchna, I., Nowicki, K. et al. Intraneuronal A $\beta$  immunoreactivity is not a predictor of brain amyloidosis- $\beta$  or neurofibrillary degeneration. *Acta Neuropathol* 113, 389–402 (2007). <https://doi.org/10.1007/s00401-006-0191-4>

Weller RO, Carare RO, Boche D. Amyloid: vascular and parenchymal. In: Reference Module in Neuroscience and Biobehavioral Psychology. (2017). doi: 10.1016/B978-0-12-809324-5.02590-6

Westermann B. (2010). Mitochondrial fusion and fission in cell life and death. *Nature reviews. Molecular cell biology*, 11(12), 872–884. <https://doi.org/10.1038/nrm3013>

Williamson, R., Scales, T., Clark, B. R., Gibb, G., Reynolds, C. H., Kellie, S., Bird, I. N., Varndell, I. M., Sheppard, P. W., Everall, I., & Anderton, B. H. (2002). Rapid tyrosine phosphorylation of neuronal proteins including tau and focal adhesion kinase in response to amyloid-beta peptide exposure: involvement of Src family protein kinases. *The Journal of neuroscience : the official journal of the Society for Neuroscience*, 22(1), 10–20. <https://doi.org/10.1523/JNEUROSCI.22-01-00010.2002>

Wu, J. W., Breydo, L., Isas, J. M., Lee, J., Kuznetsov, Y. G., Langen, R., & Glabe, C. (2010). Fibrillar oligomers nucleate the oligomerization of monomeric amyloid beta but do not seed fibril formation. *The Journal of biological chemistry*, 285(9), 6071–6079. <https://doi.org/10.1074/jbc.M109.069542>

Wu, S., Zhou, F., Zhang, Z., & Xing, D. (2011). Mitochondrial oxidative stress causes mitochondrial fragmentation via differential modulation of mitochondrial fission-fusion proteins. *The FEBS journal*, 278(6), 941–954. <https://doi.org/10.1111/j.1742-4658.2011.08010.x>

Xu, W., Doshi, A., Lei, M., Eck, M. J., & Harrison, S. C. (1999). Crystal structures of c-Src reveal features of its autoinhibitory mechanism. *Molecular cell*, 3(5), 629–638. [https://doi.org/10.1016/s1097-2765\(00\)80356-1](https://doi.org/10.1016/s1097-2765(00)80356-1)

Xu, Z., Horwich, A. L., & Sigler, P. B. (1997). The crystal structure of the asymmetric GroEL-GroES-(ADP)<sub>7</sub> chaperonin complex. *Nature*, 388(6644), 741–750.

<https://doi.org/10.1038/41944> Yadav, S. S., & Miller, W. T. (2007). Cooperative activation of Src family kinases by SH3 and SH2 ligands. *Cancer letters*, 257(1), 116–123. <https://doi.org/10.1016/j.canlet.2007.07.012>

Yan, X., Zhang, B., Lu, W. et al. Increased Src Family Kinase Activity Disrupts Excitatory Synaptic Transmission and Impairs Remote Fear Memory in Forebrain Shp2-Deficient Mice. *Mol Neurobiol* 54, 7235–7250 (2017). <https://doi.org/10.1007/s12035-016-0222-7>

Yang, M., & Leonard, J. P. (2001). Identification of mouse NMDA receptor subunit NR2A C-terminal tyrosine sites phosphorylated by coexpression with v-Src. *Journal of neurochemistry*, 77(2), 580–588. <https://doi.org/10.1046/j.1471-4159.2001.00255.x>

Yasuda R. (2017). Biophysics of Biochemical Signaling in Dendritic Spines: Implications in Synaptic Plasticity. *Biophysical journal*, 113(10), 2152–2159. <https://doi.org/10.1016/j.bpj.2017.07.029>

Yeatman, T. A renaissance for SRC. *Nat Rev Cancer* 4, 470–480 (2004). <https://doi.org/10.1038/nrc1366>

Yong, A., Tan, H. L., Zhu, Q., Bygrave, A. M., Johnson, R. C., & Huganir, R. L. (2020). Tyrosine phosphorylation of the AMPA receptor subunit GluA2 gates homeostatic synaptic plasticity. *Proceedings of the National Academy of Sciences of the United States of America*, 117(9), 4948–4958. <https://doi.org/10.1073/pnas.1918436117>

Yoshihara, Y., De Roo, M., & Muller, D. (2009). Dendritic spine formation and stabilization. *Current opinion in neurobiology*, 19(2), 146–153. <https://doi.org/10.1016/j.conb.2009.05.013>

Young, K. W., Bampton, E. T., Pinòn, L., Bano, D., & Nicotera, P. (2008). Mitochondrial Ca<sup>2+</sup> signalling in hippocampal neurons. *Cell calcium*, 43(3), 296–306. <https://doi.org/10.1016/j.ceca.2007.06.007> Yuan Xiang, P., Janc, O., Grochowska, K. M., Kreutz, M. R., & Reymann, K. G. (2016). Dopamine agonists rescue A $\beta$ -induced LTP impairment by Src-family tyrosine kinases. *Neurobiology of aging*, 40, 98–102. <https://doi.org/10.1016/j.neurobiolaging.2016.01.008>

Yuste, R., & Bonhoeffer, T. (2001). Morphological changes in dendritic spines associated with long-term synaptic plasticity. *Annual review of neuroscience*, 24, 1071–1089. <https://doi.org/10.1146/annurev.neuro.24.1.1071>

Zala, D., Hinckelmann, M. V., Yu, H., Lyra da Cunha, M. M., Liot, G., Cordelières, F. P., Marco, S., & Saudou, F. (2013). Vesicular glycolysis provides on-board energy for fast axonal transport. *Cell*, 152(3), 479–491. <https://doi.org/10.1016/j.cell.2012.12.029>

Zhang, C., Rissman, R. A., & Feng, J. (2015). Characterization of ATP alternations in an Alzheimer's disease transgenic mouse model. *Journal of Alzheimer's disease: JAD*, 44(2), 375–378. <https://doi.org/10.3233/JAD-141890>

Zhang, F. F., Cardarelli, R., Carroll, J., Zhang, S., Fulda, K. G., Gonzalez, K., Vishwanatha, J. K., Morabia, A., & Santella, R. M. (2011). Physical activity and global genomic DNA methylation in a cancer-free population. *Epigenetics*, 6(3), 293–299. <https://doi.org/10.4161/epi.6.3.14378>

Zhang, S., Edelmann, L., Liu, J., Crandall, J. E., & Morabito, M. A. (2008). Cdk5 regulates the phosphorylation of tyrosine 1472 NR2B and the surface expression of NMDA receptors. *The Journal of neuroscience : the official journal of the Society for Neuroscience*, 28(2), 415–424. <https://doi.org/10.1523/JNEUROSCI.1900-07.2008>

Zhang, Y., Li, P., Feng, J., Wu, M. (2016). Dysfunction of NMDA receptors in Alzheimer's disease. *Neurol Sci*, 37(7), 1039–1047. doi:10.1007/s10072-016-2546-5

Zhou, Q., Homma, K. J., & Poo, M. M. (2004). Shrinkage of dendritic spines associated with long-term depression of hippocampal synapses. *Neuron*, 44(5), 749–757. <https://doi.org/10.1016/j.neuron.2004.11.011>

Zhu, T., Chen, J. L., Wang, Q., Shao, W., & Qi, B. (2018). Modulation of Mitochondrial Dynamics in Neurodegenerative Diseases: An Insight Into Prion Diseases. *Frontiers in aging neuroscience*, 10, 336. <https://doi.org/10.3389/fnagi.2018.00336>

Zorova, L. D., Popkov, V. A., Plotnikov, E. Y., Silachev, D. N., Pevzner, I. B., Jankauskas, S. S., Babenko, V. A., Zorov, S. D., Balakireva, A. V., Juhaszova, M., Sollott, S. J., & Zorov, D. B. (2018). Mitochondrial membrane potential. *Analytical biochemistry*, 552, 50–59. <https://doi.org/10.1016/j.ab.2017.07.009>

Zou, L., Wang, Z., Shen, L., Bao, G. B., Wang, T., Kang, J. H., & Pei, G. (2007). Receptor tyrosine kinases positively regulate BACE activity and Amyloid-beta production through enhancing BACE internalization. *Cell research*, 17(5), 389–401. <https://doi.org/10.1038/cr.2007.5>

Zündorf, G., & Reiser, G. (2011). Calcium dysregulation and homeostasis of neural calcium in the molecular mechanisms of neurodegenerative diseases provide multiple targets for neuroprotection. *Antioxidants & redox signaling*, 14(7), 1275–1288. <https://doi.org/10.1089/ars.2010.3359>